

Improving the penetration resistance of textiles using novel hot and cold processing lamination techniques

Improving the penetration resistance of textiles using novel hot and cold processing lamination techniques

By PANASHE MUDZI

B.Eng.(Swansea University, Swansea, Wales, UK)

A Thesis Submitted to the School of Graduate Studies in Partial Fulfilment of the Requirements
for the Degree of Master of Applied Science in Mechanical Engineering

McMaster University © Copyright by Panashe Mudzi, August 2021

McMaster University M.A.Sc (2021) Hamilton, Ontario (Mechanical Engineering)

TITLE: IMPROVING THE PENETRATION RESISTANCE
OF TEXTILES USING NOVEL HOT AND COLD
PROCESSING LAMINATION TECHNIQUES

AUTHOR: Panashe Mudzi, B.Eng.

SUPERVISOR: Dr. P.R. Selvaganapathy
Dr. C.Y. Ching

NUMBER OF PAGES: 114

Abstract

In this study, novel lamination techniques are introduced for the coating of fabrics in order to enhance their ballistic/needle penetration resistance properties. Pressure sensitive adhesive (PSA) was used to create flexible ballistic composite panels with ultra-high molecular weight polyethylene (UHMWPE) fabric. An increase in processing pressure from 0.1 to 8 MPa significantly improved the ballistic performance against 9 mm FMJ ammunition of UHMWPE composite. The number of layers required to stop the bullet were reduced from 45 to 22 layers after lamination without a significant increase in stiffness. The backface signature (BFS) was reduced from 19.2 mm for the 45 layer neat samples to 11.7 mm for the 25 layer laminated samples pressed at 8 MPa.

The second lamination technique used patterned thermoplastic hot film to create flexible UHMWPE composite laminates. Hexagonal patterns were cut through a heat transfer vinyl carrier sheet using a vinyl cutter and was used as a mask between the UHMWPE fabric and hot film during heat treatment in order to have the fabric coated only on those regions. The patterns had a nominal diameter of 27.9 mm with a 1 mm gap between each region. A significant improvement in the ballistic performance of UHMWPE fabric is observed after coating each individual layer with patterned hot film and 25 layers of laminated fabric were sufficient to stop a .357 magnum FMJ ammunition compared to unlaminated neat fabric which required 45 layers to stop the bullet. Patterning of the hot film did not negatively affect the ballistic performance of the composite laminates whilst increasing their flexibility in relation to using plain hot film with no patterning involved. It resulted in a 21% increase in bending angle of the 25 layer samples

and 9.5% reduction in bending length of the single plies which both relate to greater flexibility because a higher bending angle and lower bending length correlates to more flexibility.

The same technique of patterning of hot film is used in the lamination of woven cotton fabric to enhance needle penetration resistance properties whilst maintaining the flexibility. Patterns used in this study were either hexagonal or a combination of hexagons and triangles and the nominal diameter ranged from 2.6-13.5 mm. The lamination significantly improved the 25G hypodermic needle penetration resistance of the fabric. By increasing the number of laminated fabric plies from 1 to 2, the needle resistance force increased by up to 150%. However, in comparison to just one layer, the flexibility decreased by about 12% to 26% for two and three layers, respectively. It was observed that reducing the sizes of the patterns improved the flexibility of the samples by up to 30% without compromising the needle penetration resistance.

Keywords: Backface signature; Ballistic; Penetration; Ultra-high molecular weight polyethylene (UHMWPE), body armor.

Acknowledgments

Frist of all, I want to thank God for giving the strength and knowledge to complete this work during the COVID-19 pandemic.

I would like to express my deep and sincere gratitude to my supervisors Dr. Ravi Selvaganapathy and Dr Chan Ching for giving me the opportunity to complete my studies under their supervision and the priceless guidance throughout the 2 years of my masters degree. Thank you for assisting me to cope with the ‘new normal’ in Canada during the pandemic. Your guidance has gone a long way and allowed me to improve my experimental skills and technical knowledge.

Special thanks to Dariush Firouzi for your guidance and assistance with helping me understand the concepts of ballistic performances. My thanks to Rong Wu for helping me with carrying out experiments. My thanks to Nicole Mclean for helping me find this research opportunity and for always being there to assist me when I faced some issues. My Thanks to the Mechanical Engineering staff, Mark Mackenzie, Michael Lee, Ron Lodewyks, and Troy Farncombe.

I thank my fellow labmates in Center for Advanced Micro-Electro-Fluidics laboratory: Dr. Jain Nidhi, Alireza Shahin-Shamsabadi, Fathalla Mohamed, Shadi Shahriari, Sreekant Damodara, Vinay patel, Islam Helaza, Neda Saraei, Sneha Shanbhag and Aydin Jalali. A very special thanks. They are very supportive colleagues and provides great motivation and conversations.

Table of contents

Abstract.....	iv
Acknowledgments.....	vi
List of figures.....	ix
List of Tables	xii
Chapter 1: Introduction	1
1.1 Scope and organization of this thesis	3
1.2 Contribution.....	5
Chapter 2: Literature Review	6
2.1 Background	6
2.2 Ballistic and Puncture penetration mechanisms	7
2.2.1 Ballistic impact mechanisms	7
2.2.2 Puncture, stab, and needle resistance mechanisms.....	10
2.3 Fabric coating.....	11
Chapter 3: Use of pressure sensitive adhesives to create flexible ballistic composite laminates from UHMWPE fabric	17
ABSTRACT.....	18
3.1. Introduction	19
3.2. Materials and Methods.....	22
3.2.1 Preparation of ballistic target samples	22
3.2.2 Ballistic testing	23
3.2.3 Bending stiffness and adhesive bond strength testing.....	25
3.2.4 CT-scan analysis	26
3.3. Results and Discussion	27
3.3.1 Effects of processing pressure on properties of composite laminates.....	27
3.3.2 Failure and deformation analysis of target samples.....	31
3.4. Conclusions	43
3.5 Acknowledgements.....	44
3.6 Funding sources	44
3.7 Compliance with ethical standards.....	45
3.8 Appendix	45
3.9 References	48
Chapter 4: Use of patterned thermoplastic hot film to create flexible ballistic composite laminates from UHMWPE fabric	53

Abstract.....	54
4.1 Introduction	55
4.2. Materials and Methods.....	60
4.2.1 Preparation of patterned hot film	60
4.2.2 Preparation of ballistic target samples	61
4.2.3 Ballistic testing	62
4.2.4 Bending stiffness tests	63
4.2.5 3D CT scan analysis	65
4.3. Results and Discussion	66
4.4. Conclusions	76
4.5 Acknowledgement	78
4.6 References	79
Chapter 5: Development of high-performance hypodermic needle penetration resistance flexible cotton fabric using patterned thermoplastic EVA hot film	83
Abstract.....	84
5.1. Introduction	85
5.2. Materials and methods	88
5.2.1 Materials	88
5.2.2 Sample fabrication	88
5.2.3 Needle-stick penetration test	90
5.2.4 Flexibility and stiffness test.....	91
5.2.5 SEM analysis.....	93
5.3. Results and discussion	93
5.3.3 Effect of patterned size of EVA on penetration and flexibility performance	101
5.3.4 Effect of multiple layers of stacked fabrics on penetration and flexibility performance	103
5.4. Conclusions	106
5.5 References	108
Chapter 6: Conclusions	111
6.1 Recommendations for future work	113

List of figures

Fig.2.1. Projectile impact into body armor[8].....	9
Fig.2.2. Projectile impacting single ply of fabric (a) side view, (b) top view and (c) bottom view displaying principal yarns under high stress[8].....	9
Fig. 3.1. Schematic diagram of fabrication method of (a) laminated UHMWPE fabric using pressure-sensitive adhesive (PSA) and cold-pressed at 0.1, 4, or 8 MPa and (b) unlaminated UHMWPE fabric and bonded only at the sides and cold-pressed at 0.1 MPa.....	24
Fig. 3.2. Schematic of ballistic test setup.....	26
Fig. 3.3. Effect of applied pressure on inter-ply adhesion strength of UHMWPE laminate bonded with pressure sensitive adhesive (PSA).....	29
Fig. 3.4. Thickness, areal density, and stiffness of the different UHMWPE laminated and unlaminated test samples.....	30
Fig. 3.5. Cross-section CT-scan images of the impact area of target samples for the 22-layer laminated pressed at (a) 0.1 MPa (b) 4 MPa (c) 8 MPa; 25-layer laminated pressed at (d) 0.1 MPa (e) 4 MPa (f) 8 MPa; unlaminated with (g) 40-layers (h) 45-layers. Impact direction is from top to bottom; The arrows indicate the delamination of fabric layers; The dash-lines show the edge of plug formation at the crater region formed on the strikeface.....	33
Fig. 3.6. Effect of applied pressure on BFS and BFV for (circle) 22-layer and (Square) 25-layer laminates.....	35
Fig. 3.7. Strikeface of target samples after impact for the 22-layer laminated pressed at (a) 0.1 MPa (b) 4 MPa (c) 8 MPa; 25-layer laminated pressed at (d) 0.1 MPa (e) 4 MPa (f) 8 MPa; unlaminated with (g) 40-layers (h) 45-layers. The arrows show the delamination of fabric layers. The dash-lines show the edge of plug formation at the crater region formed on the strikeface.....	38
Fig. 3.8. 3D-view of the backface of target samples after impact for the 22-layer laminated pressed at (a) 0.1 MPa, (b) 4 MPa, (c) 8 MPa; 25-layer laminated pressed at (d) 0.1 MPa, (e) 4 MPa, (f) 8 MPa; unlaminated with (g) 40-layers and (h) 45-layers.....	41
Fig. 3.9. Effect of applied pressure on normalized backface signature (BFSn) and percentage of the unperforated depth to the total thickness.....	42
Fig. A1. Measurement schematic of the BFS of a partially-perforated panel.....	46
Fig. A2. Circular bending stiffness testing according to PED-IOP-008 (5-Mar-2014) standard.....	47
Fig. A3. Adhesive bond strength test according to ASTM D903 standard.....	48
Fig 4.1. Preparation of patterned hot film.....	62

Fig 4.2. Schematic of fabrication method of ballistic panels of (a) 25 layer panel of patterned hot film and (b) 25 layer hybrid panel consisting of 13 layers of patterned hot film and 12 layers of fabric bonded with PSA.....	63
Fig 4.3. Ballistic test set up.....	64
Fig 4.4. Schematic of bending stiffness test (a) 2-dimensional drop test and (b) cantilever test[39].....	65
Fig 4.5. Thickness, areal density, and stiffness of the different UHMWPE laminated and unlaminated test samples.....	70
Fig 4.6. Effect of patterning hot film on BFS and BFV.....	71
Fig 4.7. Effect of patterning hot film on stiffness of ballistic panels.....	72
Fig 4.8. Effect of composite configuration on BFS, BFV and stiffness.....	73
Fig 4.9. 3D images of the backface of target samples after impact (a) HF25 (b) H/P25 (c) Plain25 (d) PSA25 (e) N45.....	74
Fig 4.10. 2D cross sectional view of the partially perforated target samples (a) HF25 (b) H/P25 (c) Plain25 (d) PSA25 (e) N45.....	76
Fig 4.11. Relationship between normalized BFS, BFV, SAR with energy absorbed.....	77
Figure 5.1: Schematic of sample fabrication process.....	90
Figure 5.2: Needle-stick penetration test apparatus.....	92
Figure 5.3: Schematic of test set up using (a) overhang method and (b) tensile tester.....	94
Figure 5.4: SEM images of EVA hot film under different conditions. (a) cotton fabric (b) untreated EVA film (c) treated EVA film (d) treated EVA film on cotton fabric (e) treated EVA film with small size of pattern (f) treated EVA film with XS size of pattern.....	97
Figure 5.5: SEM images of samples under 5N needle stick penetration force. (a) cotton fabric, (b) untreated EVA film, (c) treated EVA film, (d)) treated EVA film on cotton fabric (e) treated EVA film with small size of pattern, (f) treated EVA film with xs size of pattern.....	97
Figure 5.6: Needle resistance, bending angle and bending force for the different fabric samples.....	99
Figure 5.7: Normalized needle resistance and flexibility parameters (bending angle and bending force) by areal density for samples with different coverage area on cotton fabric.....	101
Figure 5.8: Normalized flexibility parameters (bending angle and bending force) by needle penetration force for samples with different coverage area on cotton fabric.....	102

Figure 5.9: Needle penetration force and flexibility parameters of different size of hexagon pattern.....103

Figure 5.10: Normalized flexibility parameters (bending angle and bending force) by needle penetration force for samples with different size of hexagon pattern on cotton fabric.....104

Figure 5.11: Needle penetration force and flexibility parameters of different size of hexagon pattern with different layer of stack.....105

Figure 5.12: Normalized flexibility parameters (bending angle and bending force) by needle penetration force for samples with different size of hexagon pattern with different layer of stack.....106

List of Tables

Table 3.1 Ballistic test results; backface signature (BFS), backface volume (BFV), thickness, areal density, and stiffness of various multi-layered laminated and unlaminated target samples.....	31
Table 4.1. Summary of the tested configurations and ballistic results.....	74
Table 5.1: Illustration of sizes and patterns.....	91
Table 5.2: Layout of stack combinations.....	95

Chapter 1: Introduction

Flexible ballistic and/or puncture resistant materials have become more popular in a range of applications such as ballistic body armor, industrial safety wear and needle resistant gloves. In recent years, novel manufacturing technologies and materials have enabled the development of such materials for Personal Protective Equipment (PPE). Since the development of high-strength fibers (HSFs) in the 1960s, a new era of flexible and soft body armor has been developed that offer protection against small ammunitions and stab attacks. The main parameters that affect the penetration resistance of textiles are mechanical properties of fibers, fabric weave architecture, yarn linear density, fabric areal density, number of filaments per yarn and number of fabric plies. Other parameters which could affect the performance of a multilayer textile structure are type of geometry, velocity and mass of penetrators, boundary condition of the fabric, fabric-projectile and yarn-yarn frictional forces. High strength fibers used for PPE are characterized by high strength, low density, and high energy absorption capability. Currently, common HSFs in the form of woven fabrics or unidirectional sheets which are used for PPE applications are ultra-high molecular weight polyethylene (UHMWPE) such as Dyneema® and Spectra® (these two are the main commercially available UHMWPE fibers with the lowest density of currently used HSFs for body armor), aramids (Technora®, Twaron®, Kevlar®). Fibres and fabrics of UHMWPE are widely used in manufacturing of military helmets, body armors and PPE such as cut-resistant gloves. UHMWPE makes a potential substitute for Kevlar® (DuPont) for body protection due to its high resistance against physical degradation and good chemical resistance although there are considerably less research studies carried out for UHMWPE polymers as compared to Kevlar in the context of PPE. Ballistic performance of a material is based on its ability to locally absorb energy and its capability to spread out energy

efficiently. To meet typical ballistic body protection levels, 20-50 stacked layers of HSFs are generally required. However, textile only body armors tend to be stiff and bulky and provide low energy dissipation which could result in severe injury to the wearer.

Fabric coating can alter energy absorption characteristics of textiles and change the frictional forces (mainly yarn-yarn and projectile-yarn friction). This approach is utilized by several commercial stab resistant fabrics such as Kevlar MTP™ (Dupont), Twaron® SRM™ (Teijin-Twaron) and Argus™ (Barrday Inc.). The coatings increase the toughness of the woven fabrics so that more energy will be needed to separate the yarns and fibers. Another benefit of coated HSFs is that they can be used to construct body armors that offer both ballistic and stab protection. One technique used to improve the mechanical properties of fibers is the nylon coating of UHMWPE which increases the fiber to fiber frictional force resulting in penetration resistance of fabrics [1]. A relatively new approach of improving the penetration resistance of HSFs is the impregnation of non-Newtonian Shear Thickening Fluids (STFs). It has been shown that fabric structure is what determines the effectiveness of STF-impregnation in improving penetration resistance of UHMWPE fabric. For instance, STF-impregnation of 1350-denier UHMWPE provides a higher penetration resistance force than a 400-denier UHMWPE fabric against a spherical head impactor at 4.5 m/s [2]. However, one major limitation of STF-treatment is the high likelihood of fluid-like STF materials to leak because exposure to water and moisture can result in them being washed away easily.

The objective of this thesis focuses on developing novel cold (using pressure sensitive adhesive) and hot (using thermoplastic patterned hot melt film) lamination techniques of fabrics for wearable protective equipment. An investigation on the effect of processing pressure on the ballistic performance of UHMWPE laminated with PSA is carried out and compared to that of

neat as-received fabric layers. Patterning of hot film is also introduced and its use in the lamination of ballistic panels as well as effect on the stiffness of the tested panels is investigated. This technique is also adopted for the lamination of cotton fabric in order to enhance its needle penetration resistance abilities without losing much flexibility. Ballistic composite panels are the main focus of this study followed by needle resistant textiles.

1.1 Scope and organization of this thesis

This study is presented as a sandwich thesis consisting of three publications which are preceded by an overview of literature concerning this study. The general overview presented in this study as well as a brief review of literature to this study are contained in each publication. Henceforth, there are some repetitions although they have been minimized. In this study, the study of the use of PSA to create flexible ballistic composite laminates is presented in Chapter 3 and has been submitted to the journal of Composite Structures . The study of the use of patterned hot film to create flexible ballistic composite laminates is presented in Chapter 4 and will be submitted to the journal of Composites part A. In Chapter 5, an investigation of the use of patterned hot film to create needle resistant textiles is carried out and will be submitted to the journal of Fibres. Lastly, the conclusions from this thesis are presented in Chapter 6 with the recommendations for future work.

In Chapter 3, the paper titled ‘Use of pressure sensitive adhesives to create flexible ballistic composite laminates from UHMWPE fabric’ introduces a novel technique to develop ballistic composite panels using UHMWPE plain weave fabric with pressure sensitive adhesive (PSA). An investigation on the effect of bonding individual fabric layers using PSA was carried out to explore a new cold lamination technique in contrast to common compression processes which require high temperatures and long curing times. Composite laminates were fabricated by

cold pressing the panels at 0.1, 4 and 8 MPa and the effect of the applied pressure levels and the adhesive bond strength on ballistic performance was investigated. The failure mechanism of the composite panels was investigated using a comprehensive analysis of X-Ray Computed Tomography (CT). Increase in processing pressure resulted in a significant improvement in the ballistic performance of the composite laminates with a slight increase in stiffness due to the fibers being more interconnected and hence better at transferring impact energy to nearby regions. No previous research work has ever considered the use of PSA for cold lamination to bond fabric layers for ballistic applications.

Chapter 4 presents a manuscript that will be submitted to Composites part A on developing a novel ballistic composite panel using UHMWPE plain-weave fabric laminated with patterned thermoplastic hot film aiming to provide high ballistic performance without significant loss of flexibility. Unlike the existing ballistic thermoplastic FRCs, this new technique utilizes the hardness of the thermoplastic matrix and the flexibility of the fabric. This was made possible by bonding each individual fabric layer with hot film using a heat press at 100 °C and a patterned heat resistant film was used as a mask to allow only specific regions of the fabric to be laminated. Various configurations are prepared and tested against NIJ standard level II 0.357 mag ammunition. The failure mechanism of the composite panels was investigated using a comprehensive analysis of X-Ray Computed Tomography (CT). The findings show that using patterned thermoplastic hot film lamination significantly improves the ballistic performance of UHMWPE fabric without compromising much of its flexibility.

In Chapter 5, the technique of patterning hot film is adopted to fabricate needle resistant textiles which can be used for applications such as needle resistant gloves. In order to investigate the parameters that affect stiffness and needle resistance using this technique, various samples

with different patterning geometries were made and tested. Patterning of the hot film allows the coated fabric to remain flexible whilst inhibiting high needle resistance capabilities.

The conclusions from this study are presented in Chapter 6 with a summary of the main findings. The advantages of the introduced lamination techniques are highlighted together with their possible applications. Recommendations for future work are also addressed in this section

1.2 Contribution

The existing fabrication methods of ballistic FRCs either require extensive processing time and/or high temperatures such as vacuum assisted compression molding. The resulting panels become very stiff, and this is not desirable in the context of wearable body armor as it restricts mobility due to lack of flexibility. The main contribution of this thesis is to develop novel fabrication methods of flexible ballistic composite laminates from UHMWPE fabric such as the use of PSA to improve its ballistic performance without compromising much flexibility. Application pressure is also used to influence the ballistic performance. Another method which is introduced is the patterning of thermoplastic hot film to produce ballistic composite laminates with the hardness of the treated hot film whilst retaining most of the flexibility from the UHMWPE fabric. The thesis also develops the protocols for the patterning of the hot film. The results show that the techniques introduced significantly improve the ballistic performance of the fabric. Lastly, the technique of patterning of hot film is adopted to produce needle resistant textiles which are flexible and can be of use in several applications such as development of needle resistant glove for security and waste handling personnel. The fabrication methods introduced in this thesis are robust and easy to implement for industrial applications.

Chapter 2: Literature Review

The previous literature on the performance and mechanisms of ballistic composite laminates is reviewed in this chapter. A broad overview is provided in this review while each of the manuscripts presented provide more focused reviews related to this study. A background into ballistic and puncture resistant textiles is presented first, followed by mechanisms influencing ballistic and puncture resistant performance and lastly, fabric coating techniques used to enhance penetration resistant performance of textiles.

2.1 Background

Textiles and compliant laminates have been used for bodily protection since ancient times. Personnel protection aimed to provide protection from the corresponding advances in armaments from the use of leather in Grecian times to chain mail in the Middle Ages. However, these forms of protection were deemed obsolete due to the advancement of firearms until the development of high strength fibers in the 1960s. A new era of body armor was ushered by these materials and offered protection against small ammunitions. The interceptor, containing an outer tactical vest able to stop high-powered handguns is the presently fielded state of the art body armor by the US army [3]. Hard ceramic plates can also be inserted in it to stop rifle projectiles. However, these plates increase the weight and stiffness of the armor which negatively affect the mobility of the wearer.

Puncture and stab resistance have become important features in PPE due to the increase in non-firearm related assaults in countries where firearms are prohibited such as Canada. There is a present threat in incidences of accidental injuries due to broken glass, sharp debris, or razor

wire in certain professionals such as waste management workers [4]. Areal density of fabrics, number of filaments per yarn, number of fabric plies, weave architecture, yarn linear density and mechanical properties of fibers are the main parameters that affect the penetration resistance of textiles [2]. Aramid, UHMWPE, S-glass, polypyridobisimidazole (PIPD), and polyphenylene benzobisoxazole (PBO) are typical textile-based resistant materials comprising of HSFs. They generally possess low density, high tensile and compressive strength, and high energy absorption [5]. Fibres and fabrics of UHMWPE are widely used for military body armors and personal protective equipment (PPE) such as cut-resistant gloves [6]. Two main commercially produced UHMWPE fibers with the lowest densities among HSFs used for armor applications are Dyneema® (Royal DSM) and Spectra® (Honeywell International Inc.,Morristown, NJ,USA). Due to its excellent chemical resistance and high resistance against physical degradation, UHMWPE is a promising alternative of Kevlar® (DuPont) for body protection[7]. However, there are fewer research works of UHMPWE as compared to Kevlar®(DuPont) for body armor application despite its many advantages.

2.2 Ballistic and Puncture penetration mechanisms

2.2.1 Ballistic impact mechanisms

High strength fibers allowed the development of current bullet resistant fabrics and compliant laminates. The yarns experience a sharp increase in stress (magnitude related to impact velocity) upon impact. Longitudinal and transverse waves propagate from the point of impact when a projectile strikes the fiber as shown in Figure.1. Hence the longitudinal tensile wave propagates along the fiber axis at the material sound speed.

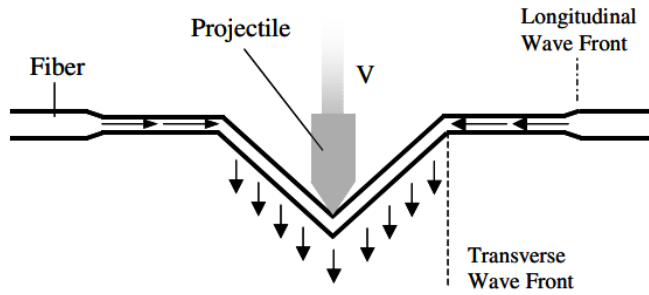


Fig.2.1. Projectile impact into body armor[8]

The material behind the wave front moves towards the impact point along the direction of motion of the projectile as the tensile wave propagates away from the impact point. The transverse wave is the transverse movement of the fiber and is propagated at a velocity lower than that of the material [8].

It has been observed that a transverse deflection in the principal yarns (yarns in direct contact with the projectile) is produced when a projectile impacts the fabric. Longitudinal strain waves are then generated down the axis of the yarns and propagate at the sound speed of the material [9]. Principal yarns pull the orthogonal yarns, which are yarns that intersect the principal yarns, out of the original fabric plane[9]. Just like principal yarns, orthogonal yarns experience a deformation and develop a strain wave.

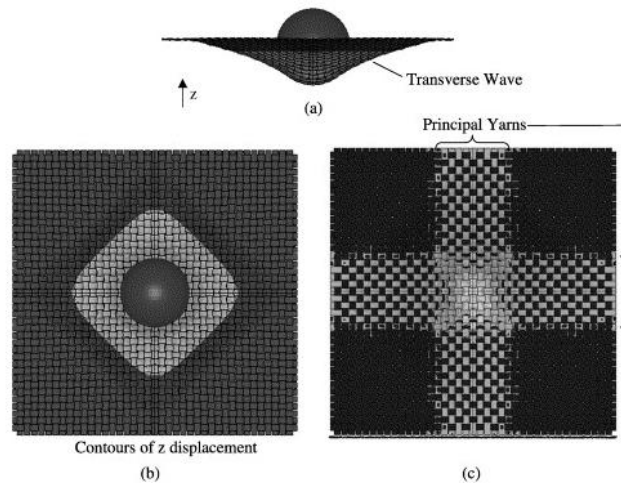


Fig.2.2. Projectile impacting single ply of fabric (a) side view, (b) top view and (c) bottom view displaying principal yarns under high stress[8]

Until a breaking strain is reached by the strain at the impact point, the transverse deflection will proceed. Numerical studies revealed that the contribution of the orthogonal yarns to energy absorption is small whilst most of the kinetic energy of the projectile is transmitted as strain and kinetic energy to the principal yarns. This behaviour can be observed in Fig.2.2c displaying highly stressed principal yarns while the orthogonal yarns are not [8].

Friction, multi ply interactions, fabric structure, impact velocity, far field boundary condition and material properties influence the ballistic performance of fabrics. Fibres possessing high-tensile strengths and large failure strains can absorb considerable amounts of energy. Additionally, a correlation between the levels of impact energy absorbed to the number of broken yarns was observed of which researchers state is a clear sign that the primary mechanism of energy absorption of the ballistic textiles is fiber straining [10]. It has been shown that the strain wave is rapidly dispersed away from the impact point, distributing the energy over a wider area for materials with a high modulus and low density (high wave velocity). This restricts large strains from being formed at the impact point [11].

It has been shown that poor ballistic performance was observed from fabrics with unbalanced weaves as well as loosely woven fabrics [9]. Loosely woven fabrics have higher chances of having a projectile wedge through the yarn mesh by pushing yarns aside instead of breaking them. Basket and plain weaves are the weaves typically used for ballistic applications. Another parameter that influences ballistic performance of fabrics is projectile geometry. Blunt bullets were decelerated quicker than pointed bullets due to their ability to wedge through the fabric [12]. A study was carried out to investigate the effect of projectile geometry on ballistic performance of a single ply of Twaron CT 716 plain weave fabric using projectiles with ogival, flat, conical, and hemispherical head. The fabric was perforated with the least amount of yarn

pull-out by the conical and ogival projectiles. This indicated that the projectiles were able to slip through the weave due to their geometry [13].

Impact velocities affect the ballistic performance of fabrics and compliant laminates. However, sharper projectiles and higher velocities penetrate fabrics through shear failure across the yarns rather than straining them to failure. A study was carried out on a single yarn of Kevlar® and UHMWPE under high velocity impact to study the failure mechanisms. It was found that the yarns fail through shear failure and together with small amounts of fiber melt damage on UHMWPE [14]. In general, shearing failure of the filaments at the strikeface, delamination, and fiber stretching at the backface are the three main stages of perforation of FRCs. Another important parameter that significantly influences the ballistic performance of fabrics is friction. During an impact event, yarn-to-yarn friction and projectile-to-yarn friction are also responsible for amount of energy absorbed. It has been found out that by restricting the movement of yarns out of the path of the projectile using resin increases the amount of impact energy absorbed by the fabric[10]. Coating of fabrics is a common way of increasing these frictional forces in order to enhance the ballistic performance of fabrics and will be discussed in more detail in Section 2.3.

2.2.2 Puncture, stab, and needle resistance mechanisms

Law enforcement and military personnel have an increased threat of knife and stab attacks including accidental injuries due to sharp objects which are a threat to health care workers. The penetration mechanism of sharp objects such as hypodermic needles is dependant on the fabric weave architecture, yarn linear density, areal density of fabrics and number of

filaments per yarn. For fabrics with loosely held yarns, the dominant penetration mechanism by hypodermic needles is the “windowing effect” which is when the penetrator pushes the yarns to the sides as it penetrates through the fabric. However, for tightly woven fabrics, the dominant failure mechanism is fiber breakage and one way of enhancing penetration resistance of textiles is through fabric coating by restricting the yarns from being moved to the sides of the penetrator [2].

2.3 Fabric coating

Frictional forces and energy absorption characteristics of textiles can be altered through fabric coating. Mechanical properties of fibers can be improved through an increase in fiber-to-fiber frictional forces by Nylon coating of UHMWPE and results in higher energy absorption and penetration resistance[1]. UHMWPE fabrics coated with Nylon 6,6 and Nylon 6,12 showed 62% increase in spike puncture resistance due to the mechanical interlocking mechanism of the nylon[2]. In another study, high density polyethylene (HDPE) fabric provided up to 90% increase in normalized penetration resistance to 21G hypodermic needles when impregnated with a mixture of heavily loaded silica and SiC nanoparticles.

Several research works have investigated the use of non-Newtonian (viscosity increases sharply at a critical shear strain) shear thickening fluids (STFs) with HSFs for ballistic protection. Impregnation of HSFs with STF results in a significant improvement in penetration resistance due to reduced yarn mobility, reduction of yarn-pull-out, increase in yarn-to-yarn friction and higher energy absorption[15]. This is because of the shear thickening phenomenon[16]. Under impact with the critical shear rate, STF is able to change from initial liquid state to a near solid state promoting energy distribution and dissipation [17]. When the load disappears, the transformation is reversible. Many researchers have investigated the ballistic

resistance of STF impregnated fabrics. STF impregnated fabrics have been proven to have improved ballistic resistance properties for impact velocities below 300m/s. Ballistic tests were carried out at an impact velocity of 224m/s on ballistic fabrics impregnated with STF and it was observed that the 4-ply STF impregnated fabric absorbed the same amount of energy with that of the 14-ply neat panel whilst being thinner and less stiff[18]. Similar results were also obtained by Majumdar *et al.*[19], Kang *et al.*[20] and Lee *et al.*[21].

However, the effect of STF impregnation with fabric panels regarding energy absorption becomes inconsistent when the impact velocity is set to be higher than 300 m/s. There are certain studies that demonstrated improvement in ballistic performance as a result of STF impregnation such as the one by Wang *et al.*[22] who saw an improvement in ballistic performance of multi-ply fabric panels at impact velocities of 445m/s. In another study, involving the 2 plies of Twaron® fabrics impregnated with STF and tested for ballistic performance showed that energy absorbed was 20% higher than that of the neat fabrics at the impact velocity of 360m/s. In contrast to the mentioned studies, certain studies reported negative effects of STF impregnation for ballistic performance. Kevlar impregnated with STF at impact velocities near 300m/s showed that its ballistic protection was equivalent to that of the neat samples at the same areal density [23]. Similarly, another study showed that neat Kevlar panels had a penetration limit velocity of 340m/s which was higher than that of STF impregnated Kevlar with the same areal density. Another disadvantage of STF-treatment is the likelihood of leakage of fluid-like STF materials because they could be easily washed away when exposed to water[2].

The most common high strength unidirectional (UD) laminated composites are thermoplastic/thermoset impregnated fiber reinforced composites (FRCs). FRCs are manufactured by various methods including vacuum bagging and oven processing, compression

molding, autoclave processing and hand layup technique. Long curing processes and the need for a low temperature storage are some disadvantages that limit the use of thermoset as matrix materials. A better choice is the use of thermoplastic based composites due to their significantly shorter processing times, recyclability, chemical resistant melt processability and long shelf life. Another factor that make thermoplastics a more attractive matrix is the relatively low brittleness transition temperatures which allow improvements in ballistic resistance, higher mechanical toughness and faster fabrication cycles. Major energy absorbing mechanisms of thermoplastic based FRCs are delamination, fiber breakage, fiber straining and matrix cracking. Polypropylene (PP) matrix reinforced with Kevlar® fabrics was used to make ballistic armor panels using the compression molding technique and resulted in a 16-29% reduction in density relative to the use of comparable thermoset matrix. Recent studies show that thermoplastic laminated fabrics significantly improve the stab and puncture resistance of fabrics when dynamic and quasi static stab testing of thermoplastic impregnated woven aramid woven fabrics were carried out[24]. The improvement was due to the increased yarn-spike frictional forces resulting in an increase in cut resistance and reduced windowing effect due to the restricted movement of the yarns. The dominant failure mechanism in thermoplastic FRCs is shear plugging near the impact zone and hole friction. For armor grade composites, low resin content is more desirable due to weak fiber-matrix adhesion allowing additional mechanisms of energy dissipation associated with delamination and debonding to take place. However, common thermoplastic FRCs used for ballistic application are very stiff and that provides discomfort and limits mobility of the wearer.

A number of studies have investigated the ballistic performance of thermoplastic matrix FRCs and their failure mechanisms depend on type of resin, fiber and fiber-resin interface[8]. The processing conditions (e.g., temperature, cooling rate) of thermoplastic-matrix FCR could

affect ballistic performance of composite panels [25]. Processing conditions of thermoplastic-matrix FRC could result in improved wetting characteristics of resin and fiber and increase adhesion strength between fabric layers. As a result, stiffness (flexural strength) of composite panels increases which results in restricted fiber straining (deformation) and mobility. The ballistic impact resistance of composite laminates is consequently reduced when fiber straining is restricted which makes the impact failure more localized accompanied by shear cutting of fibers at the impact area [26]. For example, a UHMWPE composite plate (DSM Dyneema® HB50) with lower matrix shear strength (as a measure of inter-laminar shear strength) shows the highest ballistic limit compared to UHMWPE composite plate (DSM Dyneema® HB26) with a harder matrix [25]. In general, a weaker fiber/matrix interface of FCRs results in lower stiffness and strength which consequently results in greater debonding and fiber-pull-out mechanisms and higher fracture toughness of composite laminate [27].

2.4 References

- [1] D. Firouzi, D.A. Foucher, H. Bougherara, Nylon-coated ultra high molecular weight polyethylene fabric for enhanced penetration resistance, *J. Appl. Polym. Sci.* 131 (2014) 40350. <https://doi.org/10.1002/APP.40350>.
- [2] D. Firouzi, C.Y. Ching, S.N. Rizvi, P.R. Selvaganapathy, Development of oxygen-plasma-surface-treated UHMWPE fabric coated with a mixture of SiC/polyurethane for protection against puncture and needle threats, *Fibers.* (2019). <https://doi.org/10.3390/FIB7050046>.
- [3] S.B. Sapozhnikov, O.A. Kudryavtsev, M. V. Zhikharev, Fragment ballistic performance of homogenous and hybrid thermoplastic composites, *Int. J. Impact Eng.* 81 (2015) 8–16. <https://doi.org/10.1016/j.ijimpeng.2015.03.004>.
- [4] B.A. Cheeseman, T.A. Bogetti, Ballistic impact into fabric and compliant composite laminates, (n.d.). [https://doi.org/10.1016/S0263-8223\(03\)00029-1](https://doi.org/10.1016/S0263-8223(03)00029-1).
- [5] M.J. Decker, C.J. Halbach, C.H. Nam, N.J. Wagner, E.D. Wetzel, Stab resistance of shear thickening fluid (STF)-treated fabrics, (2006). <https://doi.org/10.1016/j.compscitech.2006.08.007>.
- [6] B. Zhang, X. Nian, F. Jin, Z. Xia, H. Fan, Failure analyses of flexible Ultra-High Molecular Weight Polyethylene (UHMWPE) fiber reinforced anti-blast wall under explosion, (2017). <https://doi.org/10.1016/j.compstruct.2017.10.037>.
- [7] S.M. Kurtz, Composite UHMWPE Biomaterials and Fibers, *UHMWPE Biomater. Handb.* (2009) 249–258. <https://doi.org/10.1016/B978-0-12-374721-1.00017-1>.
- [8] S.P. Lin, J.L. Han, J.T. Yeh, F.C. Chang, K.H. Hsieh, Surface Modification and Physical Properties of Various UHMWPE-Fiber-Reinforced Modified Epoxy Composites, *J Appl Polym Sci.* 104 (2007) 655–665. <https://doi.org/10.1002/app.25735>.
- [9] B.A. Cheeseman, T.A. Bogetti, Ballistic impact into fabric and compliant composite laminates, (n.d.). [https://doi.org/10.1016/S0263-8223\(03\)00029-1](https://doi.org/10.1016/S0263-8223(03)00029-1).
- [10] P.M. Cunniff, An Analysis of the System Effects in Woven Fabrics Under Ballistic Impact, *Text. Res. J.* 62 (1992) 495–509.
- [11] B.L. Lee, T.F. Walsh, S.T. Won, H.M. Patts, J.W. Song, A.H. Mayer, Penetration Failure Mechanisms of Armor-Grade Fiber Composites under Impact, *J. Compos. Mater.* 35 (2001). <https://doi.org/10.1106/YRBH-JGT9-U6PT-L555>.
- [12] D. Roylance, S.-S. Wang, PENETRATION MECHANICS OF TEXTILE STRUCTURES o .y, 1980.
- [13] T.G. Montgomery, P.L. Grady, C. Tomasino, The Effects of Projectile Geometry on the Performance of Ballistic Fabrics, *Billica, Soils, Text. Res. J.* 48 (1978) 133–144.
- [14] V.B.C. Tan, C.T. Lim, C.H. Cheong, Perforation of high-strength fabric by projectiles of

different geometry, *Int. J. Impact Eng.* 28 (2003) 207–222. [https://doi.org/10.1016/S0734-743X\(02\)00055-6](https://doi.org/10.1016/S0734-743X(02)00055-6).

[15] D.J. Carr, Failure mechanisms of yarns subjected to ballistic impact, (n.d.).

[16] S. Gürgen, M.C. Kuşhan, The ballistic performance of aramid based fabrics impregnated with multi-phase shear thickening fluids, *Polym. Test.* 64 (2017) 296–306. <https://doi.org/10.1016/J.POLYMERTESTING.2017.11.003>.

[17] S. Arora, A. Majumdar, B.S. Butola, Structure induced effectiveness of shear thickening fluid for modulating impact resistance of UHMWPE fabrics, *Compos. Struct.* 210 (2019) 41–48. <https://doi.org/10.1016/J.COMPSTRUCT.2018.11.028>.

[18] Z. Lu, Z. Yuan, X. Chen, J. Qiu, Evaluation of ballistic performance of STF impregnated fabrics under high velocity impact, (2019). <https://doi.org/10.1016/j.compstruct.2019.111208>.

[19] Y.S. Lee, E.D. Wetzel, N.J. Wagner, The ballistic impact characteristics of Kevlar R woven fabrics impregnated with a colloidal shear thickening fluid, n.d.

[20] A. Majumdar, B.S. Butola, A. Srivastava, Development of soft composite materials with improved impact resistance using Kevlar fabric and nano-silica based shear thickening fluid, *Mater. Des.* 54 (2014) 295–300. <https://doi.org/10.1016/J.MATDES.2013.07.086>.

[21] T.J. Kang, C.Y. Kim, K.H. Hong, Rheological behavior of concentrated silica suspension and its application to soft armor, *J. Appl. Polym. Sci.* 124 (2012) 1534–1541. <https://doi.org/10.1002/APP.34843>.

[22] B.-W. Lee, C.-G. Kim, Computational analysis of shear thickening fluid impregnated fabrics subjected to ballistic impacts, (2012). <https://doi.org/10.1080/09243046.2012.690298>.

[23] Y. Wang, S.K. Li, X.Y. Feng, The Ballistic Performance of Multi-Layer Kevlar Fabrics Impregnated with Shear Thickening Fluids, *Appl. Mech. Mater.* 782 (2015) 153–157. <https://doi.org/10.4028/WWW.SCIENTIFIC.NET/AMM.782.153>.

[24] R.J. Rabb, E.P. Fahrenthold, Evaluation of Shear-Thickening-Fluid Kevlar for Large-Fragment-Containment Applications, <https://doi.org/10.2514/1.C031081>. 48 (2012) 230–234. <https://doi.org/10.2514/1.C031081>.

[25] A. Bhatnagar, *Lightweight Ballistic Composites: Military and Law-Enforcement Applications: Second Edition*, 2016. <https://doi.org/10.1016/C2014-0-03657-X>.

[26] A.K. Bandaru, V. V. Chavan, S. Ahmad, R. Alagirusamy, N. Bhatnagar, Ballistic impact response of Kevlar® reinforced thermoplastic composite armors, *Int. J. Impact Eng.* 89 (2016) 1–13. <https://doi.org/10.1016/j.ijimpeng.2015.10.014>.

[27] J.W. Song, A. Nainesh, P. Stephen, Ballistic Impact Resistance of Thermoplastic Composites, *ANTEC.* (2000) 2391–2395

Chapter 3: Use of pressure sensitive adhesives to create flexible ballistic composite laminates from UHMWPE fabric

Dariush Firouzi^{1,2#}, **Panashe Mudzi**^{1#}, **Chan Y. Ching**¹, **Troy H. Farncombe**², and **P. Ravi Selvaganapathy**^{1,*}

¹ Department of Mechanical Engineering, McMaster University, Hamilton, ON L8S 4L7, Canada

² RONCO PPE, Concord, ON, Canada

³ Department of Radiology, McMaster University, Hamilton, ON L8S 4L7, Canada

dariush.firouzi@gmail.com (D.F.); mudzip@mcmaster.ca (P.M.); chingcy@mcmaster.ca (C.Y.C.); farncom@mcmaster.ca (T.H.F.)

* Corresponding author: selvaga@mcmaster.ca; Tel.: +1 905-525-9140 (ext. 27435)

Equal contributions as first authors

Relative Contributions:

Dariush Firouzi: Carried out interpretation and analysis of the data and 2/3 of the first draft of the manuscript.

Panashe Mudzi: Carried out all experiments, assisted in the interpretation and discussion of results, including figures. Carried out the CT-scan analysis.

Chan Y.Ching: Co-supervisor of Panashe, responsible for the final editing of the paper.

Troy H.Farncombe : Carried out the CT-scans of the ballistic samples and assisted with the Matlab code to interpret the data

P.Ravi Selvaganapathy: Supervisor of Panashe and was responsible for the final editing and submission to the journal.

ABSTRACT

Fiber reinforced composites (FRC) have been widely used for ballistic resistance where hot resin melt is infused into the fabric layers and cured to form the composite. Here, we explore the use of pressure-sensitive adhesive (PSA) and its cold lamination as a simple, rapid and inexpensive method to integrate plain-weave UHMWPE and demonstrate that these composites have attractive ballistic performance. Simple compression lamination of 22 layers of fabric with interlay of PSA, for 1 min at 4 or 8 MPa, was able to confer the ability to stop 9 mm bullets shot at ~357 m/s. Increasing the processing pressure results in an increase of inter-ply bonding strength significantly while only affecting the bending stiffness slightly. It also results in increase in energy absorption of laminate which leads to smaller backface signature and volume and better ballistic performance. They are also more flexible, thinner and lightweight compared with hot melt FRC.

Keywords: Ultra-high molecular weight polyethylene (UHMWPE); Ballistic impact; Body armor; Pressure-sensitive adhesive;

3.1. Introduction

Since the development of synthetic high-strength fibers (HSFs) in the mid-20th century, fiber-reinforced composites have become an integral element of personal protective equipment (PPE) and spawned a new category of flexible and lightweight "soft body armor" protection [1-4]. HSFs have been significantly improved over the past few decades. Currently, aramids (such as Kevlar[®], Twaron[®], and Technora[®]) and ultra-high molecular weight polyethylene (UHMWPE such as Dyneema[®] and Spectra[®]) are the most popular HSFs in the form of unidirectional (UD) sheets or woven fabrics used for PPE and military applications [3-6]. HSFs are generally lightweight and possess higher tenacity, elastic modulus, and energy absorption compared with normal fibers [7,8]. The amount of impact energy absorption of HSFs is mainly related to their high tensile strength, elastic modulus, and elongation to failure [3]. In general, the protection resistance of multi-layer high-strength fabrics is lower when compared to "hard body armors" which are capable of providing high resistance against multi-threats [1]. Generally, 30-50 stacked layers of high-strength fabric are required to meet typical ballistic body protection levels. Hence, textile-only body armors tend to be bulky and stiff [8-10]. Additionally, textile-only soft body armors provide low energy dissipation which could cause a blunt trauma injury from ballistic impact [11].

Fabric coatings can alter frictional force between fibers and change the energy absorption characteristics of textiles [12]. Frictional dissipation of energy is due to a combination of yarn-to-yarn and projectile-yarn interactions [13]. Nylon coating of UHMWPE has been used to improve mechanical properties of fibers and increase fiber-to-fiber frictional force which results in higher energy absorption and penetration resistance of fabrics [14,15]. More commonly, laminated composites of high-strength UD or woven fabrics impregnated with either

thermoplastic or thermoset resin have been developed. The processing methods of manufacturing fiber-reinforced composites (FRC) include compression molding, autoclave processing, vacuum bagging and oven processing, and hand layup technique [16] all of which have some limitations. For instance, the thermoset-matrix FRCs require a long curing process [17]. The curing process of thermoset resins normally takes 75-90 min under 4-8 MPa at 140-160 °C [16]. Alternatively, thermoplastic-matrix FRCs offer shorter processing time and higher ballistic impact resistance at a lighter weight compared to thermoset-matrix composites as thermoplastics have lower stiffness and higher toughness and deformation [17-19]. There are a number of studies of the ballistic performance of thermoplastic-matrix FRC [17-22]. Both of these approaches significantly increase the stiffness as compared with the neat fabrics themselves.

The ballistic failure mechanism of FRC is dependent on different factors such as fiber, resin, fiber-resin interface and the construction of the textile reinforcements [23]. Three main stages of perforation of FRCs are shearing failure of the filaments at the strikeface, delamination, and fiber straining on the backface of the composite panel [17]. For instance, the failure mechanism of thin UD UHMWPE composite laminates are shear plugging and hole friction (between the projectile and test specimen). In the case of thick UD UHMWPE laminates, the dominant failure mechanism are composite delamination, fiber tension and bulge [21].

The use of non-Newtonian shear thickening fluids (STFs) with HSFs for ballistic protection have been studied to improve ballistic performance while maintaining flexibility [24-30]. The improved penetration resistance of STF-impregnated HSFs is mainly due to the increased yarn-to-yarn and yarn-to-impactor frictional force and reduced yarn mobility [6,24], reduction of yarn pull-out and also higher energy absorption due to the shear thickening phenomenon [10,24,30]. The improvement in penetration resistance of STF-treated textiles is

dependent on the impregnation of STF material (i.e., efficient STF intercalation) with textiles rather than a sandwich construction with the STF stacked between fabric layers [28]. STF-treatment is more effective on a loosely woven fabric (infirm structure) compared to a tightly woven fabric (firm structure). Interestingly, the increased yarn friction of firm-structure textiles after STF-impregnation become detrimental with respect to impact energy absorption due to increased stress concentration [30]. Additionally, at high impact velocity of 450-510 m/s, STF impregnation does not have a positive impact to increase energy absorption of Twaron® aramid woven fabric. Interestingly, the ballistic performance of one-layer and multiple-layer STF-impregnated ballistic panel is worse than neat samples with respect to their specific energy absorption [27]. Coating HSFs with added nano- or micron-sized particles in elastomeric mixtures has recently been shown to enhance penetration resistance against various projectiles [31-36]. Higher ballistic resistance of particle-added elastomers is attributed to the changing of crack-propagation path which delays penetration of a projectile into the material [33]. Increasing concentration of hard particles in elastomeric mixtures increases stiffness of the material and restrict its lateral motion under ballistic impact. Additionally, particle density is an important parameter to ballistic performance of particle-laden elastomers [34].

In this work, the use of pressure-sensitive adhesive (PSA) in cold lamination as a flexible binding material for composites prepared from UHMWPE plain-weave fabric is investigated and their ballistic performance, evaluated. Unlike thermoset or thermoplastic resins that require high processing temperatures, the PSA is applied at room temperature and remain flexible even after impregnation into and between the fibers of the fabric. It also inhabits non-Newtonian properties. The degree of inter-ply adhesion can be controlled by the magnitude of the pressing pressure used during cold lamination. The process for fabrication of these composite panels is rapid and

low cost. The panels thus produced demonstrate significant ballistic protection at much lower areal densities and thicknesses compared with that of unlaminated stack of as-received UHMWPE fabric layers. A 22-layer UHMWPE-PSA panel was able to stop 9 mm bullets at 357 m/s with very small back face signature. Analysis using CT-scan of the penetrated panels show that PSA provide strong binding that spread impact forces over larger area and dissipate the energy more efficiently. The energy dissipation was also related to the processing pressure applied during the fabrication of the panels. The material and technology investigated here is very attractive for high performance ballistic protection for body armor and other PPE applications.

3.2. Materials and Methods

3.2.1 Preparation of ballistic target samples

The UHMWPE plain-weave fabric (Spectra[®] 900) with an areal density of 0.233 kg/m², 1200 denier, 1333 dtex, and thread-count of 21 × 21 yarns per inch was supplied by Barrday Inc., Charlotte, NC, USA. Pressure sensitive adhesive (PSA - 9472LE with adhesive thickness of 0.132 mm) was purchased from 3M Canada, Milton, ON, Canada. UHMWPE fabric was cut to 130 mm × 130 mm pieces for the manufacturing of ballistic panels. PSAs form a bond with the adherend when pressure is applied and are widely used in many industries [37]. PSA was cut to the same dimension and laid between the fabric layers (Fig. 3.1(a)) and hand-stacked together. The fabric plies were stacked with the warp and weft directions of fibers aligned in the same directions for all layers to ensure that the effects of processing pressure on ballistic performance can be investigated without any influences from changes in yarn directions . The UHMWPE laminates were formed by cold pressing using a Carver[™] model #4938 hydraulic bench top press (Carver, Inc., Wabash, IN, USA) at 0.1, 4, and 8 MPa to produce panels with 22 and 25

layers. Additionally, samples of 40 and 45-layer neat fabric panels were hand-stacked together but bonded only along the sides and pressed at 0.1 MPa to study the effect of the adhesive bond between layers on the performance of the ballistic panels (Fig. 3.1(b)). The unlaminated impact zone of the neat fabric panels had a diameter of 100 mm to eliminate the influence of PSA on their ballistic performance and thus used as comparison to those that were fully laminated.

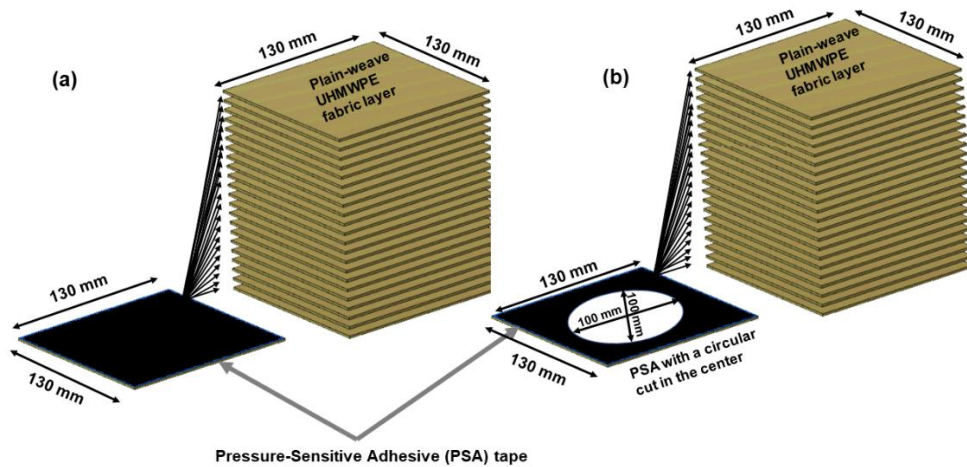


Fig. 3.1. Schematic diagram of fabrication method of (a) laminated UHMWPE fabric using pressure-sensitive adhesive (PSA) and cold-pressed at 0.1, 4, or 8 MPa and (b) unlaminated UHMWPE fabric and bonded only at the sides and cold-pressed at 0.1 MPa.

3.2.2 Ballistic testing

Ballistic tests were performed at NINE35 testing facility in Caledonia, ON, Canada. A schematic of the ballistic test setup is shown in Fig. 3.2. Tests were performed by shooting 9 mm caliber 124-grain Round Nose (RN) Full Metal Jacketed (FMJ) bullets at $90 \pm 5^\circ$ angle to the strikeface of the test frame. The test frame was placed 5 m from the gun muzzle. The ammunition used in our test conforms to NIJ standard- 0101.06 (Ballistic resistance of body armor, U.S. Department of Justice, 2008) for Type IIA protection level. Additionally, NIJ standard- 0101.06 suggests a distance of 5.0 ± 1.0 m from gun muzzle of the test barrel to the target panel when testing for handgun ammunition. The velocity of the bullet was recorded using a chronograph (Beta Master Shooting Chrony[®], Shooting Chrony Inc., Mississauga, ON,

Canada) at approximately half distance between the end of gun muzzle and target sample. The velocity of bullets recorded through the entire set of experiments was 357 ± 8 m/s, close to the suggested velocity in NIJ standard- 0101.06 for similar 9 mm ammunition for Level IIA protection (373 ± 9 m/s). The NIJ standard- 0101.06 classifies partial-perforation of a body armor when the entire portion of projectile is stopped (captured) by the armor. On the contrary, full (or complete) perforation is when any portion passes the armor by creating a hole through it or any projectile fragment is detected in the backing material. The backing material behind test panels was a standard clay (Roma Plastilina #1[®] modeling clay, Sculpture House Inc., Fort Pierce, FL, U.S.) suggested by ASTM E3004 – 15e1 standard (Standard specification for preparation and verification of clay blocks used in ballistic-resistance testing of torso body armor) and NIJ Standard- 0101.06. The clay was housed in a metal frame with a plywood bottom according to ASTM E3004 – 15e1 standard. The panel was held in-place using two elastic straps similar to the suggested procedure in the NIJ standard- 0101.06.

Two samples were made for each multi-layer panel and tested. NIJ standard- 0101.06 defines backface signature (BFS) as the maximum extent of indentation that remains in the backing material (clay) when the bullet is stopped by the armor plate and not perforated on its rear face (i.e., partial perforation). BFS is an important characteristic of ballistic performance and is widely used to compare performance of ballistic panels and trauma resistance as it is related to the amount of impact energy transferred to the body from non-perforated projectiles [38,39]. The injury caused by BFS after ballistic impact is called behind-armor blunt trauma (BABT) and could result in injury or death [11,40]. The maximum allowable BFS (depth of indentation or bulge height) is 44 mm according to the NIJ standard- 0101.06 for acceptable protection against BABT to prevent injuries of internal organs [39]. Here, the BFS of a partially-deformed panel

(Fig. A1 in Appendix) was determined from computed tomography (CT)-scan images which are described in Section 2.4.

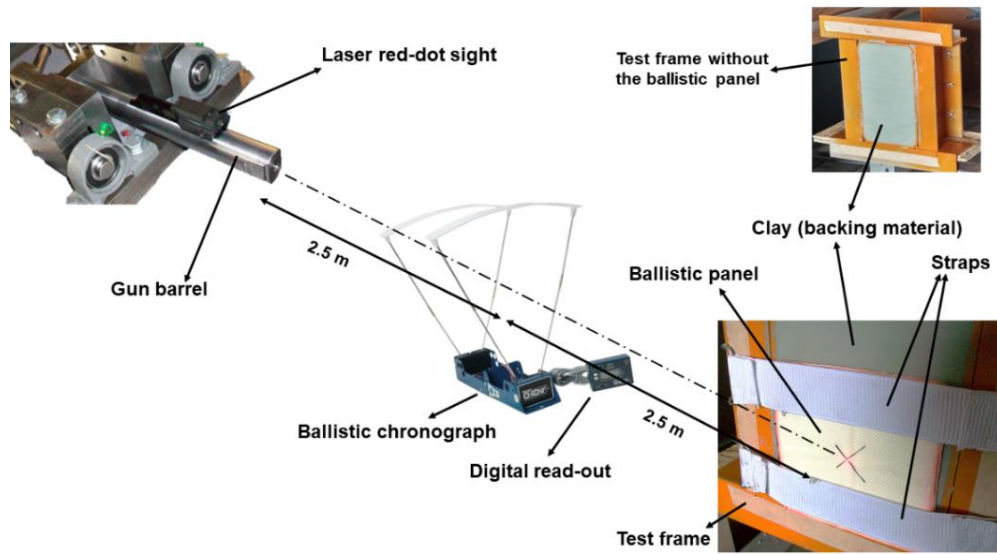


Fig. 3.2. Schematic of ballistic test setup.

3.2.3 Bending stiffness and adhesive bond strength testing

The stiffness of the multi-layer composite panels was determined similar to PED-IOP-008 (5-Mar-2014) which is an approved flexibility test for soft body armor panels in U.S. Army Aberdeen Test Center [16,41]. Identical test samples to those used in the ballistic tests, but of size 160 mm × 160 mm, were prepared for these tests. The samples were centered and allowed to rest freely on a rigid platform (170 mm × 170 mm) that had a 127 mm diameter orifice (with a 12.7 mm edge radius [41]). The platform is fixed onto the bottom frame of a Shimadzu AG-X series tensile tester with a 5 kN load cell (Fig. A2 in Appendix). A 25.4 mm diameter spherical plunger is fixed to the upper grip of the tensile tester that is aligned concentrically with respect to the 127 mm diameter orifice plate [41]. The plunger pushes the samples downward at the rate of 1 m/min for a total stroke length of 57 mm into the orifice plate [42], similar to the testing

procedure of ASTM D4032 – 08 (Standard test method for stiffness of fabric by the circular bend procedure) to address complex multiaxial bending motion of protective garments. The maximum force is recorded from three samples for each sample configuration. This force is an indication of the stiffness of the ballistic panels and their resistance to bending. A lower force means higher flexibility (lower stiffness) of the ballistic panel.

The bonding strength (peel or stripping strength) of PSA with UHMWPE fabric under different pressure levels (0.1, 1, 4, 8, and 12 MPa) was evaluated according to ASTM D903 – 98 (Standard test method for peel or stripping strength of adhesive bonds, 2017). UHMWPE fabric is cut into two strips (width of 25.4 mm). The strips were laminated using PSA over a length of 152.4 mm and firmly held at the grips of a Shimadzu AG-X series tensile tester with a 500 N load cell (Fig. A3 in Appendix). The strips were then peeled away from each other (at a separation angle of 180°) at a rate of 152.4 mm/min. The average adhesion strength is calculated from the force-displacement graph for 127 mm of separation. The adhesive bond strength (N/mm) was then calculated by dividing the average force over the width of strips (i.e., 25.4 mm). The average adhesion strength was then calculated from five samples for each PSA pressure level.

3.2.4 CT-scan analysis

The tested panels were analyzed using a non-destructive testing (NDT) technique of X-Ray Computed Tomography (CT) scans to characterize delamination failure and study the failure mechanisms under ballistic impact. The CT-scans were conducted on a Gamma Medica X-SPECT™ Small Animal Scanner operating at 75 kVp and 310 μ A X-ray. The FLEX X-O CT System software was used to acquire 2184 \times 2240 pixel-projections (0.05 mm \times 0.05 mm pixels)

over 512 projection angles. The projection images are reconstructed using a Feldkamp cone-beam reconstruction algorithm (COBRA, Exxim Computing Corporation) into $512 \times 512 \times 512$ arrays (0.115 mm voxels). The visualization and measurement processing were done using Amira software and MATLAB[®] (MathWorks, Natick, MA, USA). The BFS of partially-perforated panels after impact was determined from the CT-scan images by measuring the maximum bulging height on the backface relative to the average baseline obtained from the four corners. The remaining depth of unperforated panels was also determined by measuring the thickness of remaining material from the X-Z view of the images and was used to calculate the percentage of the unperforated (i.e., intact) depth of composite laminates through the direction of impact (transverse direction). Additionally, a 3D-view of the backface after impact was also rendered from the 2D image slices for all the panels in order to calculate backface volume (BFV) in MATLAB[®]. The BFV was determined over a $45 \text{ mm} \times 45 \text{ mm}$ region for all the samples as all of them were able to fit within this region while accounting for off-center hits on the target.

3.3. Results and Discussion

3.3.1 Effects of processing pressure on properties of composite laminates

Tests were performed to determine the effect of the applied pressure on the inter-ply bond strength and stiffness of the composite laminates. Various pressures between 1-12 MPa were applied during processing and the adhesive strength measured. A condition of 0.1 MPa pressure was used as a control to simulate the no/gentle applied pressure condition. The results as shown in Fig. 3.3 indicate that the inter-ply bond strength increased from $0.281 \pm 0.048 \text{ N/mm}$ at the lowest applied pressure of 0.1 MPa (control) to 0.546 ± 0.026 , 0.668 ± 0.051 , 0.755 ± 0.055 , and $0.908 \pm 0.032 \text{ N/mm}$ as the processing pressure was increased to 1, 4, 8 and 12 MPa, respectively.

This behaviour is inherent to the PSA where application of the pressure initiates the adhesion process.

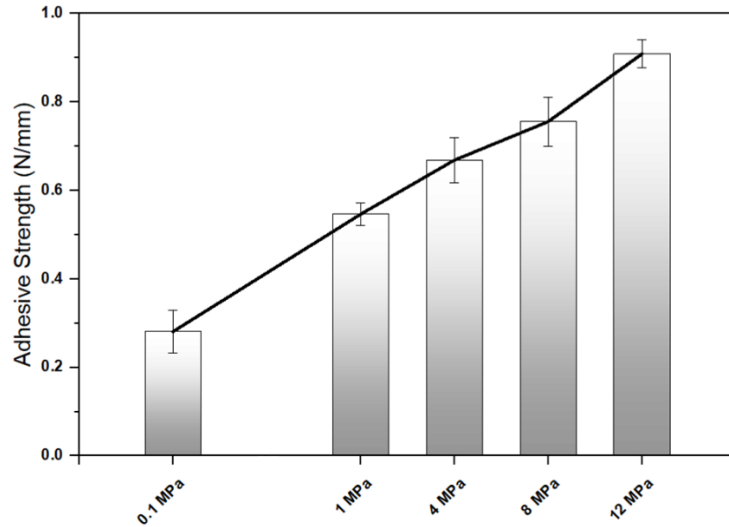


Fig. 3.3. Effect of applied pressure on inter-ply adhesion strength of UHMWPE laminate bonded with pressure sensitive adhesive (PSA).

The thickness, areal density and stiffness of the fabricated panels are presented in Fig. 3.4. Each individual layer of neat UHMWPE fabric has a thickness of 0.45 mm, which would yield a thickness of approximately 9.9 mm and 11.2 mm for a stack of 22 and 25-layer unlaminate panels, respectively. The measured thickness of a 22-layer laminate is 11.1 ± 0.4 mm when pressed at 0.1 MPa, and this decreased to 9.3 ± 0.2 and 8.8 ± 0.2 mm when pressed at 4 and 8 MPa, respectively. Similarly, the thickness of a 25-layer laminate is measured at 12.4 ± 0.1 mm when pressed at 0.1 MPa and decreased to 10.8 ± 0.2 and 10.3 ± 0.3 mm when pressed at 4 and 8 MPa, respectively. This indicates the PSA infuses more effectively into the depth of the fabric layers between fibers at higher applied pressures, resulting in higher bond strength. In comparison, a 45-layer unlaminate target sample is about 82 to 130% and about 63 to 96% thicker than 22 and 25-layer laminated panels, respectively. Similarly, the areal density of 45-layer unlaminate

target sample is approximately 30 and 12% higher than 22 and 25-layer laminated panels, respectively.

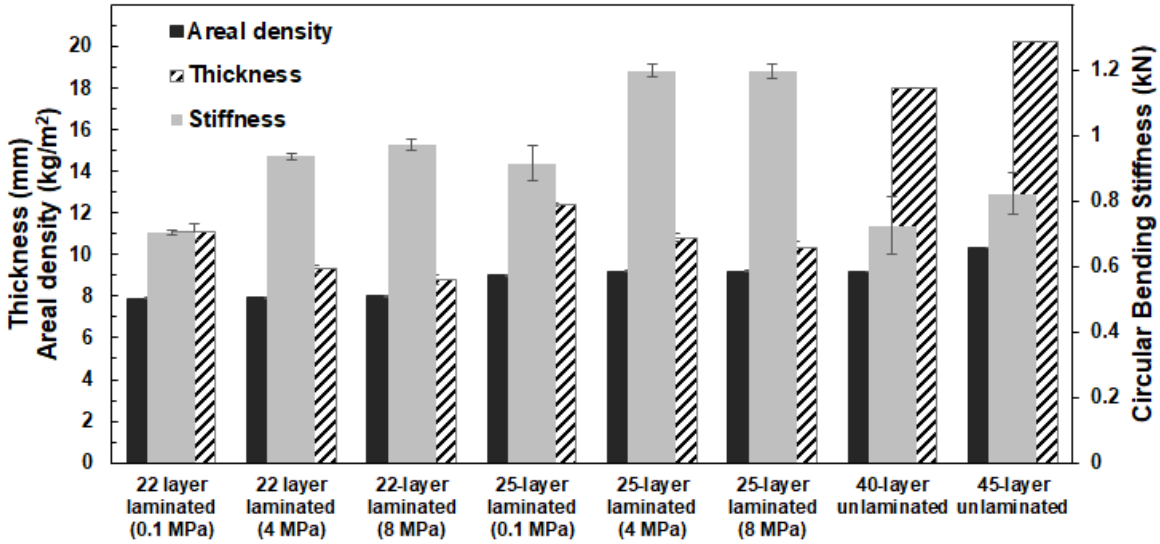


Fig. 3.4. Thickness, areal density, and stiffness of the different UHMWPE laminated and unlaminated test samples.

In general, peel (adhesion) strength, cohesive resistance, and tack of different PSAs depend on the rheological properties (i.e., viscoelastic response) of the bulk adhesives [37,43] as well as the surface energies of the adhesives and adherend [43] and other process conditions including substrate surface roughness, contact time, applied pressure and temperature on tack (instantaneous) adhesion properties of PSA [44,45]. At low pressure and/or short contact times, PSA tack force (or energy) is dependent on bonding conditions (i.e., pressure and time of contact) and was found to increase with applied pressure similar to the results observed here.

Table 3.1 Ballistic test results; backface signature (BFS), backface volume (BFV), thickness, areal density, and stiffness of various multi-layered laminated and unlaminated target samples.

No. of stacked fabric layers	Processing pressure (MPa)	Partial perforation (PP) vs. Full perforation (FP)	Average BFS (mm)	Average BFV (mm ³)	Normalized BFS (mm)	Average areal density (kg/m ²)	Circular bending stiffness (kN)	Average thickness (mm)
22	0.1	FP	-	-	-	7.90±0.04	0.702 ±0.008	11.1±0.4
	4	PP	15.2±1.6	11,338 ±1492	17.3	7.95±0.02	0.936 ±0.009	9.3±0.2
	8	PP	12.6±0.2	9,640 ± 753	14.9	8.00±0.02	0.973 ±0.018	8.8±0.2
25	0.1	PP	18.9±0.1	~14,983	21.0	9.00±0.04	0.915 ±0.052	12.4±0.1
	4	PP	13.8±0.1	11,170 ± 1485	20.1	9.20±0.02	1.197 ±0.020	10.8±0.2
	8	PP	11.7±0.5	8,272 ± 208	17.0	9.21±0.03	1.196 ±0.020	10.3±0.3
40	Unlaminated	FP	-	-	-	9.20*	0.724 ±0.087	~18.0**
45	Unlaminated	PP	19.2±0.2	19,835 ± 399	19.2	10.35*	0.822 ±0.062	~20.2**

The circular bending stiffness of the various laminated panels with PSA under different processing pressures are compared based on the amount of force needed to push the panels through an orifice (Section 2.3). The maximum recorded force for the 22-layer composite laminates is 702±8 N at the lowest applied pressure of 0.1 MPa and this increased to 936±9 and 973±18 N as the pressure was increased to 4 and 8 MPa. Similarly, the maximum recorded force for the 25-layer composite laminates is 915±52, 1197±20 and 1196±20 N at applied pressures of 0.1, 4 and 8 MPa. The 22- and 25-layer composite laminates become stiffer (less flexible) by about 31-33% while the inter-ply bonding strength (between adjacent fabric layers) increases (by about 138%) as the applied processing pressure increased from 0.1 to 4 MPa. This observation is analogous to the changes in the processing conditions of thermoplastic-matrix fiber-reinforced composites (FRCs) as an increase in inter-ply adhesion strength results in higher stiffness

(flexural modulus) [46,47]. Moreover, the stiffness of the composite laminates did not change significantly, but inter-ply bonding strength increased by about 13% when the applied pressure was further increased from 4 to 8 MPa. Therefore, the lamination of PSA with fabric layers is preferable at 8 MPa as it results in higher interplay bond strength, reduced thickness, and without additional increase in stiffness (compared to the processing pressure at 4 MPa). For comparison, the maximum recorded bending force for 40 and 45-layer unlaminated panels is 724 ± 87 and 866 ± 62 N, respectively. Interestingly, the bending stiffness of the 22-layer laminate pressed at 0.1 MPa was found to be lower than 40 and 45-layer unlaminated panels. However, the bending stiffness of 22-layer laminated pressed at 4 and 8 MPa was only ~ 14-18% higher than the 45-layer unlaminated panel.

3.3.2 Failure and deformation analysis of target samples

The ballistic performance of the 22 and 25 layer laminated PSA-UHMWPE composite panels were measured (Table 1) and compared with 40 and 45 layers of unlaminated neat UHMWPE panels to determine the improvement conferred due to the use of PSA and lamination. Since the 22 layer samples pressed at 0.1 MPa failed to stop the projectile, panels with fewer number of layers were not considered in this study. It can be seen that 40 layers of neat, unlaminated UHMWPE was completely perforated by the bullet while 45 layers was able to stop it. In comparison, 22 layer PSA laminates pressed at higher pressures and all of the 25 layer PSA laminates were able to stop the bullet. It is notable that the areal densities of the 22 layer laminates (8 MPa applied pressure) were considerably lower (~30%) and were also thinner (more than 50%) than the 45 layer neat UHMWPE while the flexibility was comparable, which

makes the 22 layer PSA laminate pressed at higher pressures that most ideal among the ballistic panels tested.

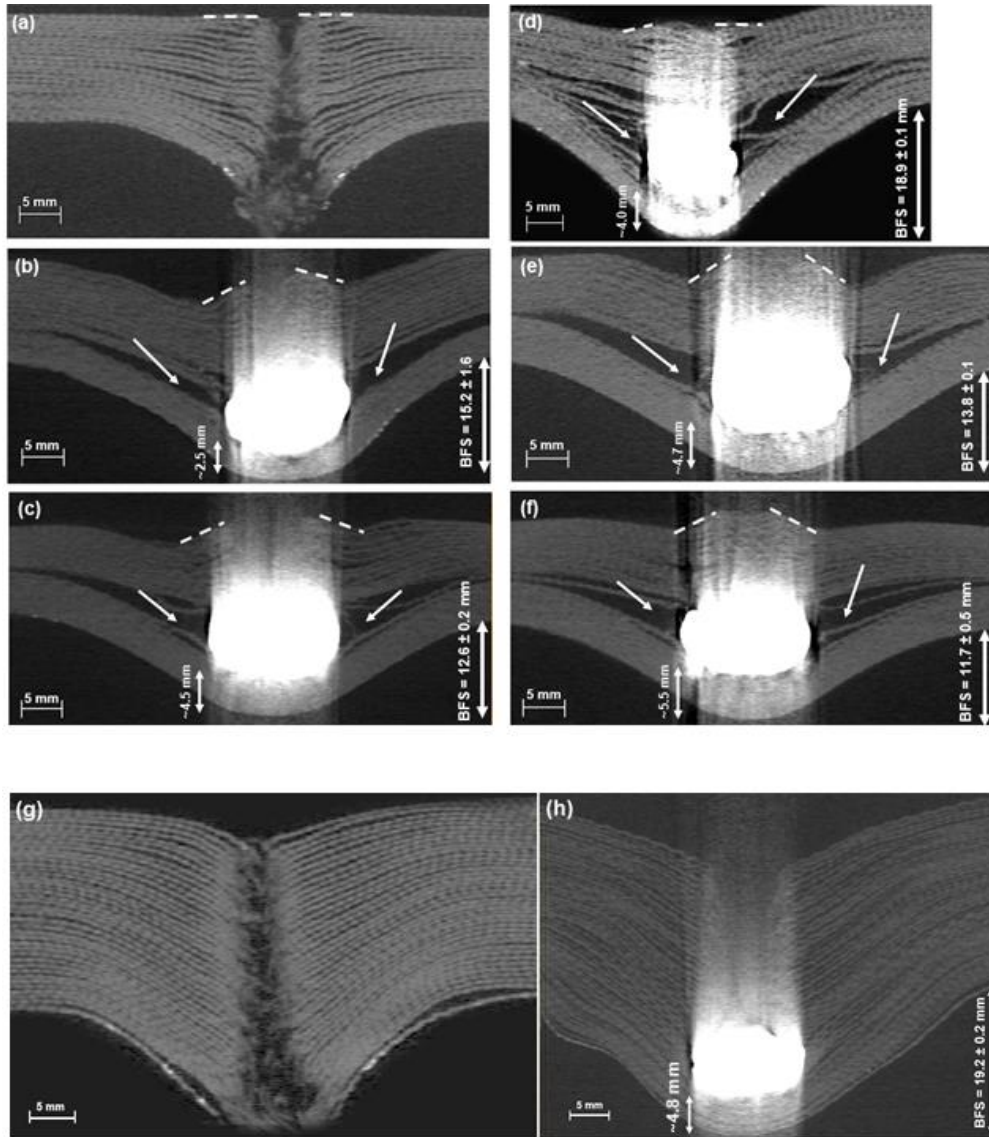


Fig. 3.5. Cross-section CT-scan images of the impact area of target samples for the 22-layer laminated pressed at (a) 0.1 MPa (b) 4 MPa (c) 8 MPa; 25-layer laminated pressed at (d) 0.1 MPa (e) 4 MPa (f) 8 MPa; un laminated with (g) 40-layers (h) 45-layers. Impact direction is from top to bottom; The arrows indicate the delamination of fabric layers; The dash-lines show the edge of plug formation at the crater region formed on the strikeface.

Cross-sectional images of the bullet perforation from the ballistic tests were also obtained from the CT-scans. The reconstructed images for the 22 and 25-layer laminates for different applied pressures are shown in Fig. 3.5. The corresponding images for a 40- and 45-layer un laminated panel are also shown in this figure. The average BFS of the partially-perforated panels measured from the CT-scan images are presented in Fig. 3.6 and listed in Table 1. The 22-layer laminate pressed at 0.1 MPa (Fig. 3.5(a)) were completely perforated and allowed the bullet to pass through. Fiber fracture (initial shear cut-out followed by fiber failure under tensile forces [48]) and delamination of the individual layers can be observed indicating that the adhesive was not able to hold the layers together at impact. The samples that were laminated at higher processing pressure (Fig. 3.5(b-c)) and all the 25-layer laminates (Fig. 3.5(d-f)) were not completely perforated and was able to stop the bullet. It can be seen that the fibers were fractured at the front of the panels while the fibers at the back were stretched and deformed creating a permanent BFS. The BFS of target samples was detected from cone-shape bulges that was formed at the backface of the laminates (Fig. 3.5(b-f)). The bullet was flattened (mushroomed) as it was stopped (grabbed) by the panel. It is estimated that about 25% of the impact energy dissipation is through the deformation of the bullet into a “mushroom” form through a UD-based armor panel [49]. Once deformed, the bullet tends to stretch the fibers (rather than fiber fracture) at the rear of the panel and compress the target toward the backing material. The deformation and fiber cutting and stretching decelerates the bullet through the panel layers. As the flattened bullet shear-cuts through the layers, the panel starts to bend which results in greater tensile fiber breakage, which absorbs more energy of impact before the bullet is stopped. Extensive delamination of partially-perforated target samples was observed mainly occurs near the backface where the bullet is stopped (similar to [22,50]). Therefore, the energy dissipation in the

in-plane direction is spread over a larger surface area. In other words, the delamination failure occurred close to the penetration and propagated to the sides of the composite laminates [22]. The place where the bullet starts to deform is also where the panel is deformed to its maximum extent [49].

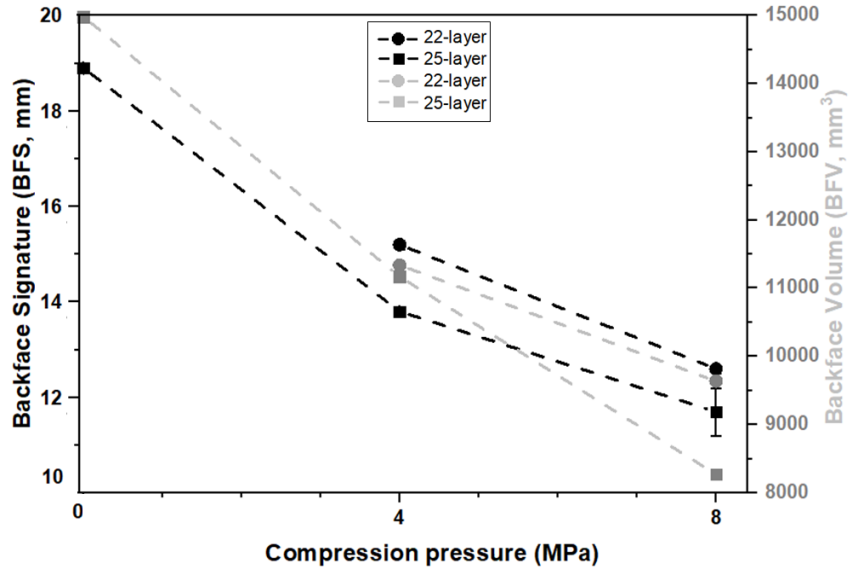


Fig. 3.6. Effect of applied pressure on BFS and BFV for (circle) 22-layer and (Square) 25-layer laminates.

The extensive propagation of delamination was more noticeable for the partially-perforated 22 and 25-layer panels (Fig. 3.5(b,c,e, and f)) which were compressed at 4 and 8 MPa. The delamination creates an interface between the perforated layers and the remaining plies at the backface which were strained without breakage. The delamination failure was less observed for panels pressed at the 0.1 MPa pressure (Fig 3.5(d)) when compared to panels pressed at higher pressured (Fig. 3.5(b, c, e, and f)). The panels pressed at 0.1 MPa pressure had low inter-ply bond strength which significantly reduced mechanical coupling of the layers. Therefore, most of the energy of the impact is dispersed through fiber straining at the backface (i.e., bulging)

rather than extensive delamination. This likely explains the higher BFS for the 25-layer laminate pressed at 0.1 MPa (i.e., 18.9 ± 0.1 mm) compared to 25-layer laminates pressed at 4 and 8 MPa (i.e., 13.8 ± 0.1 and 11.7 ± 0.5 mm, respectively). The extent of delamination to the sides of the panel was more noticeable in the laminate pressed at 8 MPa (Fig. 3.5(f)) when compared to the laminate pressed at 4 MPa (Fig. 3.5(e)). This is also evident in the 22-layer laminate when comparing Fig. 3.5(b) and Fig. 3.5(c), which explains its higher energy dissipation and smaller BFS. The increase in lamination pressure results in a change in energy dissipation mode from primarily “fiber fracture” to one where a significant amount of fiber straining is involved that can result in a higher energy dissipation per unit volume. Similar results were observed when the processing pressure of cross-ply laminates of DSM Dyneema® HB26 (UD UHMWPE prepreg plies) was increased. It resulted in reducing the thickness of the interply resin layer which leads to increased interlaminar delamination (fiber/matrix debonding) and thus more ply splitting near the backface. A higher degree of fiber damage and ply splitting is evidence of the panel being exposed to a greater compressive stress under ballistic impact [51].

An inverse co-relation between the applied processing pressure and BFS was also observed which was unique to PSA laminates. While the 22-layer composite laminate pressed at 0.1 MPa was fully perforated (minimal energy dissipation due to mainly fiber fracture rather than fiber straining), the 22-layer laminate compressed at 4 MPa was only partially perforated with a BFS of only 15.2 ± 1.6 mm. The BFS of the 22-layer laminate reduces further to 12.6 ± 0.2 mm when compressed at 8 MPa (Fig. 3.5(c)). The increase in applied pressure results in higher interply bond strength of the PSA which provides higher dissipation of impact energy as the layers are delaminated resulting in smaller BFS. The total thickness of unperforated layers in the partially-perforated samples was estimated from Fig. 3.5 (b-f and h). For the 22-layer laminated

panels at 4 and 8 MPa, the thickness of unperforated layers was about 2.5 and 4.5 mm, respectively. For the 25-layer laminated panels pressed at 0.1, 4, and 8 MPa, the thickness of unperforated layers was about 4, 4.7, and 5.5 mm, respectively, while it was about 4.8 mm for the 45-layer unlaminated panel. The percentage of the unperforated depth of 25-layer composite laminates increased from about 32 to 43 and 53%, when processing pressure increase from 0.1 to 4 and 8 MPa, respectively, which demonstrates a higher energy absorption of the laminates manufactured at higher pressure. Similarly, the percentage of the unperforated depth of 22-layer composite laminates increases from 0 to about 27 and 51% when processing pressure increase from 0.1 to 4 and 8 MPa, respectively (Table 1). This indicates that the composite is potentially capable of withstanding bullets even at higher velocities. From the ballistic test results, the unlaminated samples with 40 layers of fabric were fully perforated and failed (Fig. 3.5(g)). However, the unlaminated samples with 45 layers of fabric were only partially perforated (Fig. 3.5(h)) with BFS of 19.2 ± 0.2 mm, which is about 26 and 52% higher than 22-layer laminates compressed at 4 and 8 MPa, and about 1.6, 39, and 64% higher than 25-layer laminates compressed at 0.1, 4, and 8 MPa. Additionally, the percentage of the unperforated depth of 45-layer unlaminated panel is about 24% which is smaller than that of 22- and 25-layer partially-perforated laminates.

The strikeface of target samples from the CT-scans are shown in Fig. 3.7. The compression of target sample forms an upward flow (compressive pulse [48]) of the material which creates a plug formation at the crater (formed on strikeface due to shear plugging and fracture of fibers [29]). Plug formation at the crater region of target samples is also noticeable from cross-section CT-scan images in Fig. 3.5. For the 22-layer composite laminate compressed at 0.1 MPa (Fig. 3.7(a)), there was complete bullet perforation through all the layers with

minimal straining at the backface and no visible plug formation on the strikeface because of minimal upward flow of the materials due to low inter-ply bond strength. Similarly, no plug formation was detected in the 25-layer composite laminate compressed at 0.1 MPa (Fig. 3.7(d)), and in the 40- and 45-layer un laminated target samples (Fig. 3.7(g and h)), where the dominant failure mechanism is the shear failure of the fibers at the strikeface.

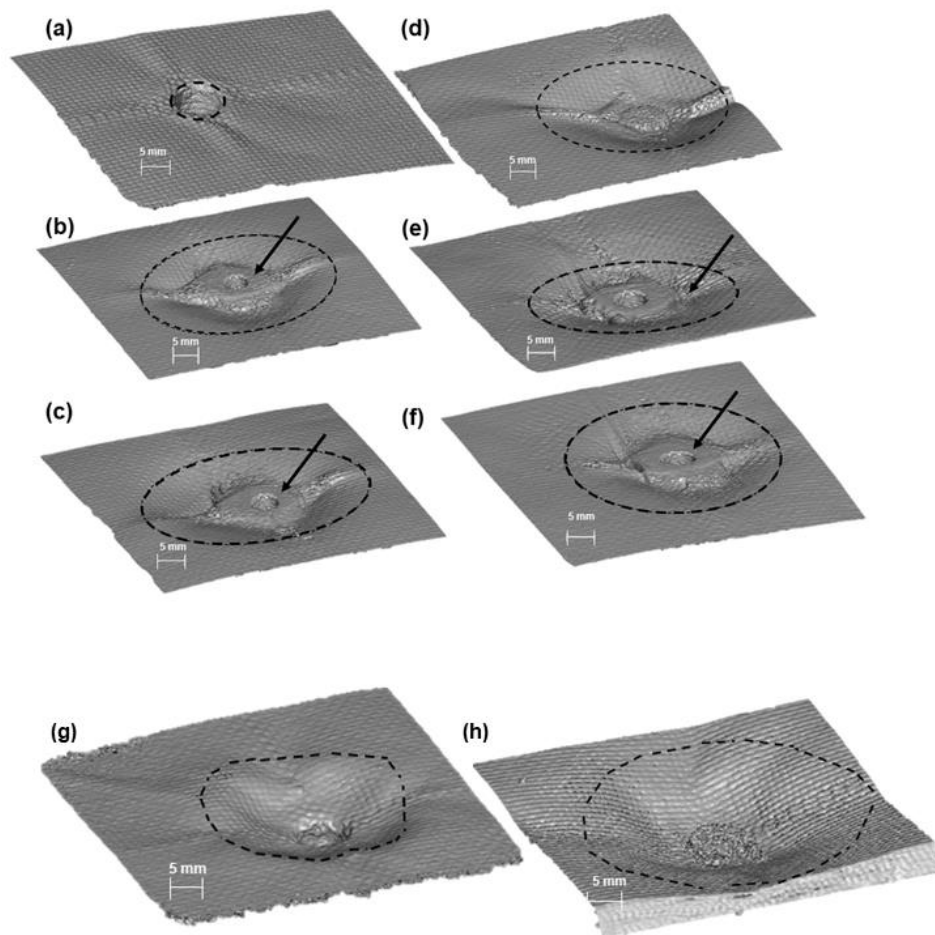


Fig. 3.7. Strikeface of target samples after impact for the 22-layer laminated pressed at (a) 0.1 MPa (b) 4 MPa (c) 8 MPa; 25-layer laminated pressed at (d) 0.1 MPa (e) 4 MPa (f) 8 MPa; un laminated with (g) 40-layers (h) 45-layers. The arrows show the delamination of fabric layers. The dash-lines show the edge of plug formation at the crater region formed on the strikeface.

On the other hand, a noticeable strikeface plug formation was observed in all the 22- and 25-layer composite laminates compressed at 4 and 8 MPa (Fig. 3.7(b,c,e, and f)). In general, the dominant failure mechanisms of woven fabric composites under ballistic impact is elastic deformation of secondary yarns, cone formation on the rear face of target samples, tensile failure of primary yarns/fibers, delamination, shear plugging, matrix cracking, and friction between projectile and target sample during penetration [52] rather than yarn pull-out and "windowing" effect [53]. Here, the strikeface plug formation in composite laminate pressed at 4 and 8 MPa indicates higher energy dissipation throughout the panel which results in lower BFS (compared to laminated panels at 0.1 MPa).

NIJ standard- 0101.06 only suggests the measurement of BFS (i.e. the extent of indentation depth in the backing material). However, it was noted that the volume of backface deformation should also be considered in damage analysis to determine energy absorption capacity and energy transmitted to the back side of ballistic panels [40]. In [40], the depth and diameter of trauma formed in the backing material were determined by measuring the dimension of a mold created inside the indentation cavity of the backing material (i.e. clay) after impact. The volume of trauma geometry was determined from these dimensions to calculate the impact energy transmitted to the back of the fabric layers.

The CT-scans obtained here provide a convenient means to calculate the Backface volume (BFV) using in-house image processing software. Here, the BFV of partially-perforated target samples were calculated from the 3D images (Fig. 3.8) of the backface target samples after impact and presented in Fig. 3.6 and listed in Table 1. The BFV in partially-perforated target samples is related to the amount of impact energy transmitted to the back of the target sample. A higher BFV means more energy of impact is transmitted to the back of the panel which results in

more trauma. In other words, if the impact energy is propagated to a larger area of the panel and absorbed more by the fabric layers, the trauma volume will be lower (i.e. smaller diameter of trauma) [40]. From the results, the BFV of 22-layer laminated panels decreases about 15% when the processing pressure is increased from 4 to 8 MPa. Similarly, the BFV of 25-layer laminated panels decreases about 25 and 45% when the processing pressure is increased from 0.1 to 4 and 8 MPa. Moreover, the 45-layer unlaminated fabric panel has about 32 to 140% higher BFV compared to all 22- and 25-layer partially-perforated laminated panels. As the processing pressure is increased from 0.1 to 4 and 8 MPa, the fibers within the laminated layers are more interconnected and held together more strongly (i.e. higher inter-ply adhesion) with better strain resistance and therefore impact energy is transferred to a larger area of the panel. Hence, the bulge formed on the backface has smaller depth and diameter which results in lower BFS and BFV, respectively. Similarly, the 45-layer unlaminated panel has significantly higher BFS and BFV (and lower trauma resistance) compared to all 22- and 25-layer partially-perforated laminated panels.

The BFS extent of partially-perforated samples were normalized (BFS_n) with respect to the flexibility of 45-layer neat fabric (which is the thickest analyzed panel among all the tested samples) similar to [38,39] as

$$BFS_n = \frac{BFS \times (f)}{(f_{45\text{-layer as-received UHMWPE})}} \quad (1)$$

where f is the flexural stiffness (N) of the panel, BFS (mm) is the extent of deformation on the backface, BFS_n (mm) is the normalized BFS, and $f_{45\text{-layer as-received}}$ is the bending stiffness of 45-layer stack unlaminated panel as the reference. The BFS_n of partially-perforated panels along with the percentage of the unperforated depth for the 22- and 25- layer panels with the

processing pressure are presented in Fig. 3.9. The BFS_n of the 22-layer partially-perforated laminates reduced from 17.3 to 14.9 mm when the applied pressure was increased from 4 to 8 MPa, confirming that the panels pressed at higher pressure have better ballistic performance with respect to BFS although they become slightly stiffer in an absolute sense.

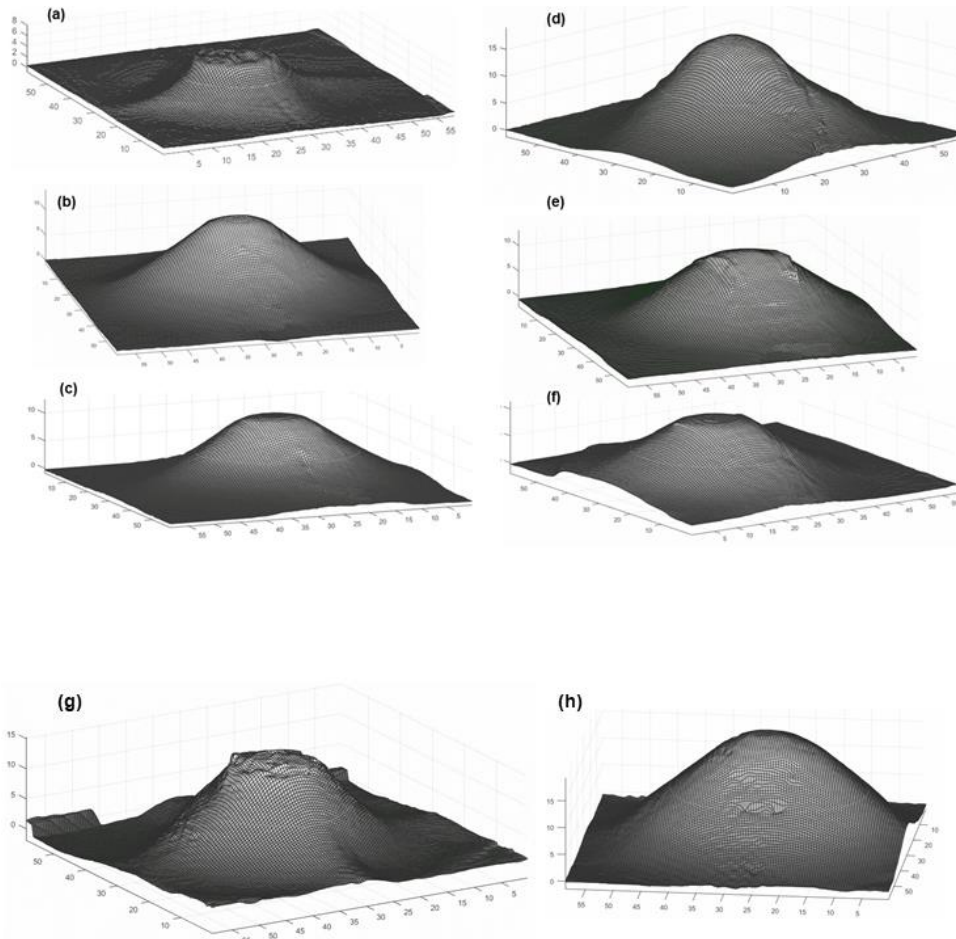


Fig. 3.8. 3D-view of the backface of target samples after impact for the 22-layer laminated pressed at (a) 0.1 MPa, (b) 4 MPa, (c) 8 MPa; 25-layer laminated pressed at (d) 0.1 MPa, (e) 4 MPa, (f) 8 MPa; un laminated with (g) 40-layers and (h) 45-layers.

Similarly, BFS_n of 25-layer partially-perforated laminates reduced from 21 to 20.1 and 17 mm when the applied processing pressure was increased from 0.1 to 4 and 8 MPa, respectively. On the other hand, the BFS_n of 45-layer partially-perforated un laminated target sample is the highest

(except for 25-layer laminated at 0.1 and 4 MPa) which is up to about 29 % higher than that of laminated samples, confirming the superior performance of laminated target samples with respect to their thickness and BFS.

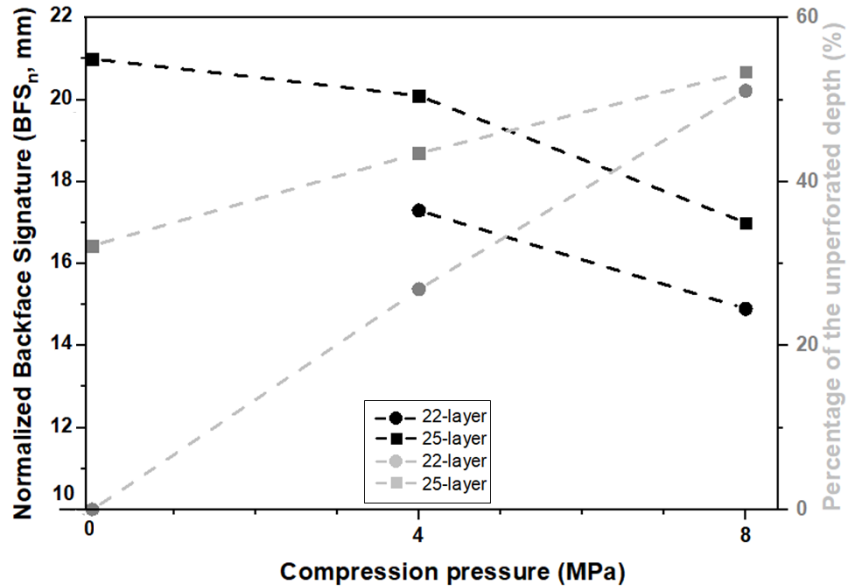


Fig. 3.9. Effect of applied pressure on normalized backface signature (BFS_n) and percentage of the unperforated depth to the total thickness.

The improvement in ballistic performance of multi-layer fabric by laminating individual layers using PSA in this work is analogous to the influence of STF to increase ballistic impact energy absorption of multi-layer fabric. A multi-layer Kevlar[®] impregnated with shear thickening fluids (STFs) absorbs more impact energy as STF act as a “bridging matrix” which transforms the stack of fabric layers into a coherent structure. Therefore, a larger portion of fabric is involved in load-bearing and energy-absorption mechanisms in addition to primary yarns [10]. Primary (principal) yarns are those in direct contact with the projectile and intersect with orthogonal yarns. Generally, primary (principal) yarns deform more (highly stressed) and

contribute more to disperse kinetic energy of projectile [23]. Unlike the STF the PSA is a solid state material and therefore more amenable to manufacturing and integration within a body armor. Furthermore, issues such as leakage of fluids are not of concern in PSA. Finally, due to its nature, further cold processing by application of pressure can restore the inter-ply adhesion and enhanced performance of these composites.

The laminated panels pressed at higher pressure (and resulting slightly higher bending stiffness) provides better ballistic performance with respect to BFS and BFV. This property is unique to PSA based laminate material and has not been reported before. This observation is unlike that of thermoplastic-matrix FRC where flexural stiffness of composite laminates is inversely related to ballistic resistance. For instance, processing conditions of thermoplastic-matrix FRC could result in improved wetting characteristics of resin and fiber and increase adhesion strength between fabric layers. As a result, stiffness (flexural strength) of composite panels increases which results in restricted fiber straining (deformation) and mobility. The ballistic impact resistance of composite laminates is consequently reduced when fiber straining is restricted which makes the impact failure more localized accompanied by shear cutting of fibers at the impact area [46,47]. For another example, a UHMWPE composite plate (DSM Dyneema[®] HB50) with lower matrix shear strength (as a measure of inter-laminar shear strength) shows the highest ballistic limit compared to UHMWPE composite plate (DSM Dyneema[®] HB26) with a harder matrix [54]. Overall, it is concluded that all the laminated composite panels at processing pressure of 4 and 8 MPa performed better from ballistic testing compared to 40- and 45-layer of unlaminated target samples. Cold lamination is a simple, rapid, low-cost and effective processing technique that in combination with the PSA can be used to create composite panels that provide

superior ballistic performance at lower areal density and still maintain the flexibility of neat stitched ballistic fabrics such as UHMWPE.

3.4. Conclusions

The ballistic performance of composite laminates prepared by cold-press compression of plain-weave UHMWPE fabrics using pressure-sensitive adhesive (PSA) was studied. Laminated composite panels consisting of 22 and 25 layers of UHMWPE were cold pressed at 0.1, 4 and 8 MPa. In addition, 40 and 45 layers of UHMWPE neat fabric were stacked together in order to compare their ballistic performance with the laminated panels. Ballistic tests using 9 mm ammunition at ~357 m/s were performed in order to determine the bullet penetration resistance and impact energy absorption capability of the panels. The tested laminate samples were analyzed using X-Ray Computed Tomography (CT) scans to study failure mechanism under impact and calculate backface signature (BFS), backface volume (BFV), and percentage of unperforated layers.

There was a significant improvement in bullet penetration resistance and energy absorption of laminated panels when the compression pressure was increased as shown by the decrease in BFS, BFV, and increase in percentage of the unperforated layers. All the 22- and 25-layer laminated target samples stopped the bullet and were only partially perforated (except 22-layer laminate pressed at 0.1 MPa). The energy of impact was found to be dispersed through fiber straining and delamination at the backface and compression of the panel forming a permanent deformation on the backface (BFS), in addition to an upward flow of the material forming a plug at the strikeface. Increasing the processing pressure to 4 and 8 MPa resulted in a decrease in BFS and BFV due to an increased energy dissipation upon impact through an extensive delamination mechanism which propagated to the sides of the panel. A 45-layer stack

of unlaminated layers was able to stop the bullet (while the 40-layer unlaminated failed the test) and was partially-perforated but showed lower ballistic performance (higher thickness, areal density, normalized BFS (BFS_n) with flexibility, BFV and also lower percentage of unperforated layers) compared to the partially-perforated 22- and 25-layer laminated samples at 8 MPa.

Inter-ply bond strength and stiffness tests were performed to determine the effect of the processing pressure on these parameters. An increase in applied pressure was found to increase the inter-ply bond strength. The composite laminate becomes stiffer (specifically when processing pressure increased from 0.1 to 4 MPa) with an increase in inter-ply bonding strength due to the PSA spreading more effectively into the depth of fabric layers when processing pressure is increased. However, increasing the processing pressure from 4 to 8 MPa resulted in only a small increase in bending stiffness while the inter-ply bond strength was increased. The BFS_n decreased in both 22 and 25-layer laminates when processing pressure increased from 0.1 to 8 MPa.

3.5 Acknowledgements

The authors would like to thank Mr. Rod Rhem for performing the CT-scans. The authors would also like to thank Mr. Ron Lodewyck from NINE35, Caledonia, ON, Canada, for helping with the ballistic testing and providing valuable insight into ballistic materials and testing. DF would like to thank Ron Pecheolli for supporting his continued participation in this research.

3.6 Funding sources

This work was supported by the Natural Science and Engineering Research Council (NSERC) of Canada; the Ontario Centers of Excellence (OCE); and the Canada Research Chairs Program.

3.7 Compliance with ethical standards

The authors declare that they have no known competing financial interests or personal relationships that could have appeared to influence the work reported in this paper.

3.8 Appendix

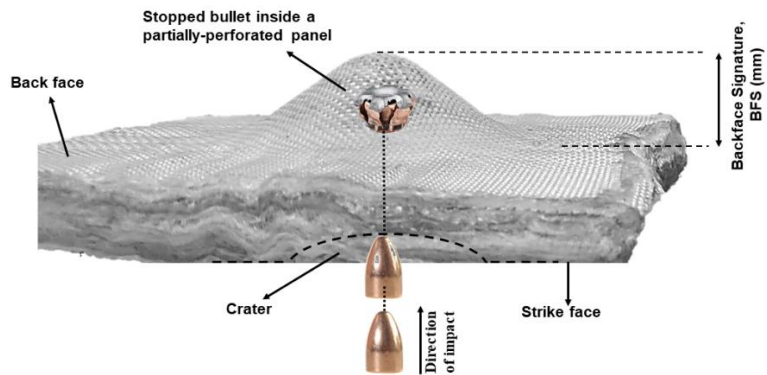


Fig. A1. Measurement schematic of the BFS of a partially-perforated panel.

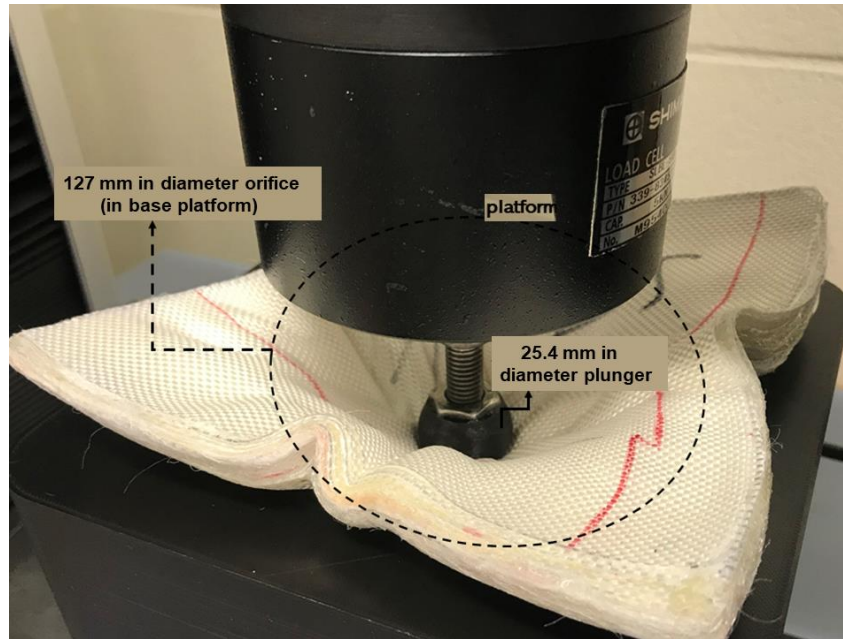


Fig. A2. Circular bending stiffness testing according to PED-IOP-008 (5-Mar-2014) standard.

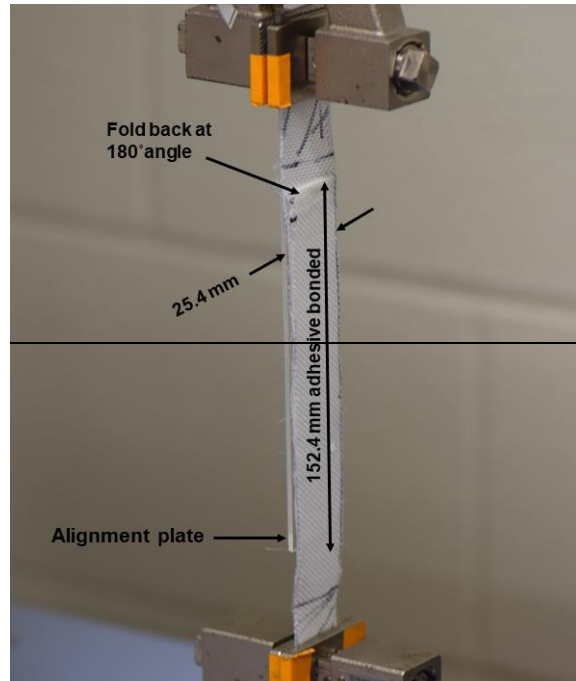


Fig. A3. Adhesive bond strength test according to ASTM D903 standard.

3.9 References

- [1] Majumdar A, Butola BS, Srivastava A. Development of soft composite materials with improved impact resistance using Kevlar fabric and nano-silica based shear thickening fluid. *Mater Des* 2014. <https://doi.org/10.1016/j.matdes.2013.07.086>.
- [2] Hosur M V., Mayo JB, Wetzel E, Jeelani S. Studies on the fabrication and stab resistance characterization of novel thermoplastic-kevlar composites. *Solid State Phenom.*, 2008. <https://doi.org/10.4028/www.scientific.net/SSP.136.83>.
- [3] Lane RA. High Performance Fibers for Personnel and Vehicle Armor Systems. *AMPTIAC Q* 2005;9:10.
- [4] Chen X. Advanced Fibrous Composite Materials for Ballistic Protection. 2016. <https://doi.org/10.1016/C2014-0-01733-9>.
- [5] Wang H, Hazell PJ, Shankar K, Morozov E V., Escobedo JP, Wang C. Effects of fabric folding and thickness on the impact behaviour of multi-ply UHMWPE woven fabrics. *J Mater Sci* 2017. <https://doi.org/10.1007/s10853-017-1482-y>.
- [6] Gürgen S, Kuşhan MC. The ballistic performance of aramid based fabrics impregnated with multi-phase shear thickening fluids. *Polym Test* 2017. <https://doi.org/10.1016/j.polymertesting.2017.11.003>.
- [7] Tan VBC, Tay TE, Teo WK. Strengthening fabric armour with silica colloidal suspensions. *Int J Solids Struct* 2005. <https://doi.org/10.1016/j.ijsolstr.2004.08.013>.
- [8] Lee YS, Wetzel ED, Wagner NJ. The ballistic impact characteristics of Kevlar® woven fabrics impregnated with a colloidal shear thickening fluid. *J Mater Sci* 2003. <https://doi.org/10.1023/A:1024424200221>.
- [9] Srivastava A, Majumdar A, Butola BS. Improving the impact resistance performance of Kevlar fabrics using silica based shear thickening fluid. *Mater Sci Eng A* 2011. <https://doi.org/10.1016/j.msea.2011.09.021>.
- [10] Majumdar A, Butola BS, Srivastava A. An analysis of deformation and energy absorption modes of shear thickening fluid treated Kevlar fabrics as soft body armour materials. *Mater Des* 2013. <https://doi.org/10.1016/j.matdes.2013.04.016>.
- [11] Haro Albuja E, Szpunar JA, Odeshi AG. Ballistic impact response of laminated hybrid materials made of 5086-H32 aluminum alloy, epoxy and Kevlar® fabrics impregnated with shear thickening fluid. *Compos Part A Appl Sci Manuf* 2016. <https://doi.org/10.1016/j.compositesa.2016.04.007>.
- [12] Ahmad MR, Ahmad WYW, Salleh J, Samsuri A. Effect of fabric stitching on ballistic impact resistance of natural rubber coated fabric systems. *Mater Des* 2008. <https://doi.org/10.1016/j.matdes.2007.06.007>.

- [13] Yang CC, Ngo T, Tran P. Influences of weaving architectures on the impact resistance of multi-layer fabrics. *Mater Des* 2015. <https://doi.org/10.1016/j.matdes.2015.07.014>.
- [14] Firouzi D, Foucher DA, Bougherara H. Nylon-coated ultra high molecular weight polyethylene fabric for enhanced penetration resistance. *J Appl Polym Sci* 2014. <https://doi.org/10.1002/app.40350>.
- [15] Firouzi D, Youssef A, Amer M, Srouji R, Amleh A, Foucher DA, et al. A new technique to improve the mechanical and biological performance of ultra high molecular weight polyethylene using a nylon coating. *J Mech Behav Biomed Mater* 2014. <https://doi.org/10.1016/j.jmbbm.2014.01.001>.
- [16] Bhatnagar A. *Lightweight Ballistic Composites: Military and Law-Enforcement Applications: Second Edition*. 2016. <https://doi.org/10.1016/C2014-0-03657-X>.
- [17] Bandaru AK, Chavan V V., Ahmad S, Alagirusamy R, Bhatnagar N. Ballistic impact response of Kevlar® reinforced thermoplastic composite armors. *Int J Impact Eng* 2016. <https://doi.org/10.1016/j.ijimpeng.2015.10.014>.
- [18] Sapozhnikov SB, Kudryavtsev OA, Zhikharev M V. Fragment ballistic performance of homogenous and hybrid thermoplastic composites. *Int J Impact Eng* 2015. <https://doi.org/10.1016/j.ijimpeng.2015.03.004>.
- [19] Carrillo JG, Gamboa RA, Flores-Johnson EA, Gonzalez-Chi PI. Ballistic performance of thermoplastic composite laminates made from aramid woven fabric and polypropylene matrix. *Polym Test* 2012. <https://doi.org/10.1016/j.polymertesting.2012.02.010>.
- [20] Dos Santos Alves AL, Nascimento LFC, Suarez JCM. Influence of weathering and gamma irradiation on the mechanical and ballistic behavior of UHMWPE composite armor. *Polym Test* 2005. <https://doi.org/10.1016/j.polymertesting.2004.06.003>.
- [21] Zhang D, Sun Y, Chen L, Zhang S, Pan N. Influence of fabric structure and thickness on the ballistic impact behavior of Ultrahigh molecular weight polyethylene composite laminate. *Mater Des* 2014. <https://doi.org/10.1016/j.matdes.2013.08.074>.
- [22] Zhang TG, Satapathy SS, Vargas-Gonzalez LR, Walsh SM. Ballistic impact response of Ultra-High-Molecular-Weight Polyethylene (UHMWPE). *Compos Struct* 2015. <https://doi.org/10.1016/j.compstruct.2015.06.081>.
- [23] Cheeseman BA, Bogetti TA. Ballistic impact into fabric and compliant composite laminates. *Compos Struct* 2003. [https://doi.org/10.1016/S0263-8223\(03\)00029-1](https://doi.org/10.1016/S0263-8223(03)00029-1).
- [24] Kalman DP, Merrill RL, Wagner NJ, Wetzel ED. Effect of particle hardness on the penetration behavior of fabrics intercalated with dry particles and concentrated particle-fluid suspensions. *ACS Appl Mater Interfaces* 2009. <https://doi.org/10.1021/am900516w>.
- [25] Majumdar A, Butola BS, Srivastava A. Optimal designing of soft body armour materials using shear thickening fluid. *Mater Des* 2013. <https://doi.org/10.1016/j.matdes.2012.10.018>.

- [26] Petel OE, Ouellet S, Loiseau J, Frost DL, Higgins AJ. A comparison of the ballistic performance of shear thickening fluids based on particle strength and volume fraction. *Int J Impact Eng* 2015. <https://doi.org/10.1016/j.ijimpeng.2015.06.004>.
- [27] Lu Z, Yuan Z, Chen X, Qiu J. Evaluation of ballistic performance of STF impregnated fabrics under high velocity impact. *Compos Struct* 2019. <https://doi.org/10.1016/j.compstruct.2019.111208>.
- [28] Asija N, Chouhan H, Gebremeskel SA, Bhatnagar N. Impact Response of Shear Thickening Fluid (STF) Treated High Strength Polymer Composites - Effect of STF Intercalation Method. *Procedia Eng.*, 2017. <https://doi.org/10.1016/j.proeng.2016.12.133>.
- [29] Haro EE, Odeshi AG, Szpunar JA. The energy absorption behavior of hybrid composite laminates containing nano-fillers under ballistic impact. *Int J Impact Eng* 2016. <https://doi.org/10.1016/j.ijimpeng.2016.05.012>.
- [30] Arora S, Majumdar A, Butola BS. Structure induced effectiveness of shear thickening fluid for modulating impact resistance of UHMWPE fabrics. *Compos Struct* 2019. <https://doi.org/10.1016/j.compstruct.2018.11.028>.
- [31] Petel OE, Higgins AJ. Shock wave propagation in dense particle suspensions. *J Appl Phys* 2010. <https://doi.org/10.1063/1.3504858>.
- [32] Petel OE, Frost DL, Higgins AJ, Ouellet S. Formation of a disordered solid via a shock-induced transition in a dense particle suspension. *Phys Rev E - Stat Nonlinear, Soft Matter Phys* 2012. <https://doi.org/10.1103/PhysRevE.85.021401>.
- [33] Petel OE, Ouellet S, Marr BJ, Higgins AJ, Frost DL. Ballistic penetration of particle-laden elastomers. *Proc. - 27th Int. Symp. Ballist. Ballist.* 2013, 2013.
- [34] Comtois-Arnaldo C, Ouellet S, Petel OE. A ballistic performance study on particle-infused elastomeric systems. *AIP Conf. Proc.*, 2018. <https://doi.org/10.1063/1.5044940>.
- [35] Firouzi D, Russel MK, Rizvi SN, Ching CY, Selvaganapathy PR. Development of flexible particle-laden elastomeric textiles with improved penetration resistance to hypodermic needles. *Mater Des* 2018. <https://doi.org/10.1016/j.matdes.2018.07.011>.
- [36] Firouzi D, Ching CY, Rizvi SN, Selvaganapathy PR. Development of oxygen-plasma-surface-treated UHMWPE fabric coated with a mixture of SiC/polyurethane for protection against puncture and needle threats. *Fibers* 2019. <https://doi.org/10.3390/FIB7050046>.
- [37] Sun S, Li M, Liu A. A review on mechanical properties of pressure sensitive adhesives. *Int J Adhes Adhes* 2013. <https://doi.org/10.1016/j.ijadhadh.2012.10.011>.
- [38] Liu X, Li M, Li X, Deng X, Zhang X, Yan Y, et al. Ballistic performance of UHMWPE fabrics/EAMS hybrid panel. *J Mater Sci* 2018;53:7357–71. <https://doi.org/10.1007/s10853-018-2055-4>.

- [39] Kędzierski P, Popławski A, Gieleta R, Morka A, Sławiński G. Experimental and numerical investigation of fabric impact behavior. *Compos Part B Eng* 2015. <https://doi.org/10.1016/j.compositesb.2014.10.028>.
- [40] Karahan M, Kuş A, Eren R. An investigation into ballistic performance and energy absorption capabilities of woven aramid fabrics. *Int J Impact Eng* 2008. <https://doi.org/10.1016/j.ijimpeng.2007.04.003>.
- [41] George TC, Benjamin KJ. Soft Ballistic Resistant Armor. US20170314894A1, 2017.
- [42] Chin W, Gasset S, Slusarski K, Hibbert N, Long L, Dalzell M, et al. Comfort Characterization of Various Fabrics for Extremity Protection. Army Res Lab 2013;ARL-TR-661.
- [43] Chu SG. Dynamic Mechanical Properties of Pressure-Sensitive Adhesives. *Adhes. Bond.*, 1991. https://doi.org/10.1007/978-1-4757-9006-1_5.
- [44] Tordjeman P, Papon E, Villenave JJ. Tack properties of pressure-sensitive adhesives. *J Polym Sci Part B Polym Phys* 2000. [https://doi.org/10.1002/\(SICI\)1099-0488\(20000501\)38:9<1201::AID-POLB12>3.0.CO;2-#](https://doi.org/10.1002/(SICI)1099-0488(20000501)38:9<1201::AID-POLB12>3.0.CO;2-#).
- [45] Creton C, Leibler L. How does tack depend on time of contact and contact pressure? *J Polym Sci Part B Polym Phys* 1996. [https://doi.org/10.1002/\(SICI\)1099-0488\(199602\)34:3<545::AID-POLB13>3.0.CO;2-I](https://doi.org/10.1002/(SICI)1099-0488(199602)34:3<545::AID-POLB13>3.0.CO;2-I).
- [46] Choi J, McCarthy SP, Song JW. Effect of processing conditions on ballistic impact resistance of thermoplastic composites. *Annu. Tech. Conf. - ANTEC, Conf. Proc.*, 1997.
- [47] Song JW, N A, S P. Ballistic impact resistance of thermoplastic composites. *Plast. Magic. Solut. Conf. proceedings, ANTEC 2000, Orlando: 2000*.
- [48] Liu S, Wang J, Wang Y, Wang Y. Improving the ballistic performance of ultra high molecular weight polyethylene fiber reinforced composites using conch particles. *Mater Des* 2010. <https://doi.org/10.1016/j.matdes.2009.01.044>.
- [49] Jacobs MJN, Van Dingenen JLJ. Ballistic protection mechanisms in personal armour. *J Mater Sci* 2001. <https://doi.org/10.1023/A:1017922000090>.
- [50] Min S, Chen X, Chai Y, Lowe T. Effect of reinforcement continuity on the ballistic performance of composites reinforced with multiply plain weave fabric. *Compos Part B Eng* 2016. <https://doi.org/10.1016/j.compositesb.2015.12.001>.
- [51] Greenhalgh ES, Bloodworth VM, Iannucci L, Pope D. Fractographic observations on Dyneema® composites under ballistic impact. *Compos Part A Appl Sci Manuf* 2013. <https://doi.org/10.1016/j.compositesa.2012.08.012>.
- [52] Naik NK, Shrirao P. Composite structures under ballistic impact. *Compos Struct* 2004. <https://doi.org/10.1016/j.compstruct.2004.05.006>.

[53] Nilakantan G, Merrill RL, Keefe M, Gillespie JW, Wetzel ED. Experimental investigation of the role of frictional yarn pull-out and windowing on the probabilistic impact response of kevlar fabrics. *Compos Part B Eng* 2015. <https://doi.org/10.1016/j.compositesb.2014.08.033>.

[54] Karthikeyan K, Russell BP, Fleck NA, Wadley HNG, Deshpande VS. The effect of shear strength on the ballistic response of laminated composite plates. *Eur J Mech A/Solids* 2013. <https://doi.org/10.1016/j.euromechsol.2013.04.002>.

Chapter 4: Use of patterned thermoplastic hot film to create flexible ballistic composite laminates from UHMWPE fabric

Panashe Mudzi^{1#}, **Rong Wu**^{1#}, **Dariush Firouzi**^{1,2}, **Chan Y. Ching**¹, **Troy H. Farncombe**², and **P. Ravi Selvaganapathy**^{1,*}

¹ Department of Mechanical Engineering, McMaster University, Hamilton, ON L8S 4L7, Canada

² RONCO PPE, Concord, ON, Canada

³ Department of Radiology, McMaster University, Hamilton, ON L8S 4L7, Canada
mudzip@mcmaster.ca (P.M.); wur31@mcmaster.ca (R.W.); dariush.firouzi@gmail.com (D.F.);
chingcy@mcmaster.ca (C.Y.C.); farncom@mcmaster.ca (T.H.F.)

* Corresponding author: selvaga@mcmaster.ca; Tel.: +1 905-525-9140 (ext. 27435)

Equal contributions as first authors

Relative Contributions:

Panashe Mudzi: Carried out all experiments, interpretation, and analysis of the data and the first draft of the manuscript including all figures.

Rong Wu: Carried out all experiments, assisted in the interpretation and discussion of results.

Dariush Firouzi : Assisted with fabric materials needed for the experiments and helped with final editing of paper.

Chan Y. Ching: Co-supervisor of Panashe, responsible for the final editing of the paper.

Troy H.Farncombe: Carried out the CT-scans and assisted with constructing MATLAB code to interpret results

P.Ravi Selvaganapathy: Supervisor of Panashe and was responsible for the final editing and submission to the journal.

Abstract

Thermoplastic resin is infused into fabric layers to form fiber reinforced composites (FRCs) which are commonly used for ballistic resistance purposes. Here, we explore the use of patterned thermoplastic hot film as a simple and rapid method to laminate plain-weave UHMWPE and demonstrate that these composites have attractive ballistic and stiffness properties. Lamination of 25 layers of fabric using hot press compression lamination of each individual layer with hot film was able to confer the ability to stop .357 magnum ammunition shot at 435.9 ± 9 m/s. Patterning the hot film resulted in the composite panels to retain most of their flexibility without losing their ballistic performance as compared to when they are laminated with plain (not patterned) hot film. Using the hot film for lamination results in an increase in energy absorption of the laminates with a smaller backface signature and backface volume. These laminates are lighter and more flexible than the commonly used hot resin infused FRC.

Keywords: Ultra-high molecular weight polyethylene (UHMWPE); Ballistic impact; Body armor; Hot film;

4.1 Introduction

With the rapid technological advancement in firearms over the last few decades, there is an increased demand for personal protective equipment (PPE) with greater firearm protection without compromising weight and flexibility. Since the development of high strength fibers (HSFs), fiber reinforced composites have been widely adopted for ballistic protection for personal and military applications [1,2]. HSFs are characterised by high energy absorption capability, low density, and high strength [3]. The most common HSFs used for ballistic protection purposes include aramid fibers (Kevlar[®], Nomex[®], Technora[®], Twaron[®]) and Ultra High Molecular Weight Polyethylene (UHMWPE) fibers (such as Dyneema[®] and Spectra[®]) [4,5]. However, without any further treatment, they remain heavy, bulky, and stiff because stacks of multiple layers (generally 30-50) are needed to obtain the required ballistic and/or stab protection. This greatly affects the mobility and comfort of the wearer [6].

The ballistic performance of a material mainly depends on its ability to locally absorb energy of the projectile and its capability to spread it out quick and efficiently [3]. Studies review that most of the kinetic energy of the projectile is transferred to the principal yarns (yarns in direct contact with the projectile) as strain and kinetic energy [7]. Orthogonal yarns (yarns that intersect primary yarns) have a smaller influence on energy absorption as they are not highly stressed as much as the primary yarns at the time of impact. Other material properties that influence the ballistic performance are friction, far-field boundary conditions, fabric structure, impact velocity, projectile geometry and multiple ply interactions [8]. Ballistic damage mechanisms differ and depend on whether the projectile strikes at high or low velocities. At high velocities (350-500m/s), the damage occurs through localized loading of the fabric and yarn

uncrimping, leading to plastic deformation of the fiber and fracture [8–10]. However, yarn uncrimping and translation which are normally referred to as yarn pull-out are dominant at relatively lower velocities (i.e. about 244 m/s) [11]. Another major factor affecting the energy absorption of fabrics is weaving architecture. It has been observed that plain weave fabrics perform better than other weaving structures (i.e. twill, satin and basket architectures) [12].

The backface signature (BFS) or trauma depth in the backing material plays an important role to ensure the wearer is protected from injury by minimizing the projectile's probability of severely damaging internal organs through the torso. According to NIJ standard-0101.04, the BFS in the backing material should not exceed 44mm [13]. A combination of yarn-to-yarn and projectile-to-yarn friction form the frictional energy absorption from the interaction of fabric layers during impact [8]. One popular way of reducing the BFS which is widely used is coating of fabrics because it can alter frictional forces and energy absorption characteristics of textiles [14,15]. High strength woven fabrics coated with natural rubber latex (NRL) showed significant improvements in ballistic impact performance of the fabric systems involving neat and coated fabric layers due to the decreased mobility of the yarns upon impact thus altering frictional interactions [15]. The ballistic performance of unidirectional UHMWPE 12-ply fabric systems coated with NRL was compared to all-neat fabric systems and results showed that NRL coated panels possessed superior energy absorption characteristics [16]. Nylon coating is another technique that has shown to improve mechanical properties of fibers and increase fiber-to-fiber frictional force which results in higher penetration resistance of fabrics [17].

There are many studies of enhancing the ballistic/stab performance of materials by increasing friction between the yarns using shear thickening fluids (STF) and silica-water suspension (SWS). High strain rate properties of STF-treated UHMWPE ballistic composites

were investigated by subjecting both STF-treated and neat compression moulded UHMWPE variant (Gold Shield[®]) to high strain rate loading. It was revealed that STF treatment enhanced the ballistic resistance of Gold Shield[®] [18]. In another study, UHMWPE woven fabrics of varying thread densities were treated with 65% w/w STF and investigated for energy impact absorption. All tested levels of yarn linear densities resulted in an increase in yarn pull-out force which was correlated to an increase in inter-yarn friction [19]. Kevlar fabrics were impregnated with STF consisting of sphere silica and fumed silica as silica particles with ethylene glycol and polyethylene glycol (PEG 200) as the fluid medium and it was observed that the STF improved the stab and ballistic resistance of Kevlar[®] fabric [6]. In another study, the ballistic performance of woven Kevlar[®] impregnated with colloidal STF (containing 450 nm silica particles) was investigated and the results showed a significant improvement in ballistic penetration resistance without any loss in material flexibility as compared to the neat fabrics with comparable areal density [20]. This suggested that the STF restricts the yarns as they are pulled through the fabric increasing the force needed to pullout each yarn from the fabric resulting in increase in energy dissipation [20]. STF impregnated aramid fabrics under high velocity impact were investigated at high impact velocities of around 500 m/s and the findings indicated that the specific energy absorption of the single ply and 10-ply STF impregnated fabric panels was 44.8% and 64.1% lower than the corresponding neat fabric panels respectively. This was found to be due to the change in failure mode from being tensile dominant to shear dominant which resulted in decrease in energy absorption due to increased possibility of earlier damage [21]. Therefore, the effect of STF becomes less predictable at high impact velocities which can be a drawback. Another research work manufactured sandwich composite panels using 3D-mats containing interconnected channels sandwiched between Kevlar[®] layers and filled the core with 600 nm

silica based STF's dispersed in PEG-200 to investigate its effect in energy dissipation of the material. It was found that the sandwich panels were able to absorb 96.3% of the incident energy accounting to 67.4% increase in energy absorbed as compared to hollow sandwich composite panels [22]. However, despite the improvement in ballistic performance and mechanical properties of STF, they remain inconveniently cumbersome to incorporate and have leakage issues [23].

Thermoplastic (TP)/thermoset impregnated fiber reinforced composites (FRCs) are the most common high strength unidirectional (UD) laminated composites. Compression molding, vacuum bagging and oven processing, autoclave processing, and hand layup technique are some of the processing methods of manufacturing fiber reinforced composites [24]. The use of thermosets as matrix materials is limited due to some disadvantages such as long curing processing and the requirement for low temperature storage [25]. However, thermoplastic based composites are a better choice because of their short processing times, long shelf life, recyclability, and chemical resistant melt processability [26,27]. Having relatively low brittleness transition temperatures allowing improvements in ballistic resistance, fast fabrication cycles and higher mechanical toughness also makes thermoplastics a more attractive matrix [28,29]. Fiber breakage, matrix cracking, delamination and fiber straining are the major energy absorbing mechanisms of thermoplastic based FRCs [25]. Due to their lower tensile strength as compared to thermosets, thermoplastics are used with fibers of high elastic modulus such as Kevlar[®] to improve the matrix stiffness [26]. Kevlar[®] fabrics of different architectures were used as reinforcements with polypropylene (PP) matrix to make ballistic armor panels using compression molding and 16-29% reduced density was observed in Kevlar[®] thermoplastic based composites relative to that of the thermoset based ones [25]. Dynamic and quasi static stab testing of TP

impregnated woven aramid fabrics were carried out and the results showed that the TP laminated fabrics significantly improve the stab and puncture resistance of fabrics due to a combination of reduced windowing by prohibiting the yarns from being pushed aside and increased cut resistance by increasing the friction between the target and the spike [1]. It was observed that shear plugging near the impact zone is the dominant energy absorption mechanism in thermoplastic composites [30]. Heating process of thermoplastic composites affect the wetting characteristics and the cooling process greatly affects the molecular packing characteristics which influences the stiffness of the composite [31]. Another study compared the ballistic performance of composites processed at different temperatures and the ones processed at 260 °C (tension mode of failure dominant) had significantly higher ballistic impact resistance than composites processed at 350 °C (shear cut dominant) in which fiber straining and delamination are the desired failure mechanisms [32]. Low resin content is more attractive for armor-grade composites due to the weak fiber-matrix adhesion which allows fibers to deform pull-out as well as additional mechanisms of energy dissipation associated with delamination and debonding [33]. However, despite having good ballistic properties, TP impregnated fiber reinforced composites are very stiff and require long processing times and high temperatures[32].

The objective of this work is to develop a novel ballistic composite panel with uniform hardened regions using UHWPE plain-weave fabric and patterned thermoplastic hot film (HF) that will provide high ballistic performance without significantly compromising on flexibility. The panels were developed using multiple layers of fabric bonded with a thermoplastic HF using a heat press at 100°C. A patterned heat resistant film was used so that only the patterned areas of the fabric were laminated, leaving a network of unlaminated channels to allow a greater degree of flexibility. The layers are offset from one another by ensuring interacting plies provide

complete coverage of the HF over the layers. The composite panels were prepared with varying number of layers ranging from 20 to 30 and tested against NIJ standard II 0.357 magnum ammo. The failure mechanism of the composite panels was investigated using a comprehensive analysis of X-Ray Computed Tomography (CT). This fabrication technique provides useful insights in creating a soft ballistic body armor with great flexibility. The materials and methods are presented in the following section, followed by results, discussion, and conclusions.

4.2. Materials and Methods

4.2.1 Preparation of patterned hot film

Thermoplastic hot melt film (with application temperature range of 190-219 °C) was supplied from Adheco Ltd, Scarborough, ON, Canada. Hot melt film (HF) melts when heated to its melting temperature which allows it to form a physical bond with a substrate, then solidifies when cooled and are used for many applications [34]. The UHMWPE plain-weave fabric (Spectra® 900) with thread-count of 21 × 21 yarns per inch, areal density of 0.233 kg/m², 1200 denier and 1333 dtex, was supplied by Barrday Inc., Charlotte, NC, USA. A heat transfer vinyl carrier sheet cut to 130 mm × 130 mm was attached to an adhesive backing and patterned using a Silhouette CAMEO 3 vinyl cutter programmed using Silhouette Studio® software to cut out uniform hexagonal regions from the carrier sheet as shown in Fig.4.1. The patterns had a nominal diameter of 27.9 mm with a 1 mm gap between each region. A hexagon pattern was chosen because it allows the fabric to freely bend in 6 different directions along the gaps and provides degrees of freedom of motion to the wearer of such body armor. The patterned heat transfer carrier sheet was stacked in-between a 130 mm × 130 mm single layer of HF and a single ply of UHMPWE fabric of similar dimensions. Heat was then applied to the stack at 210 °C for 120 s as shown in Fig.4.1(b). After cooling down at room temperature the patterned heat

transfer carrier sheet is peeled off the fabric by hand leaving solid hexagonal patched coated to the UHMPWE fabric as shown in Fig.4.1(c).

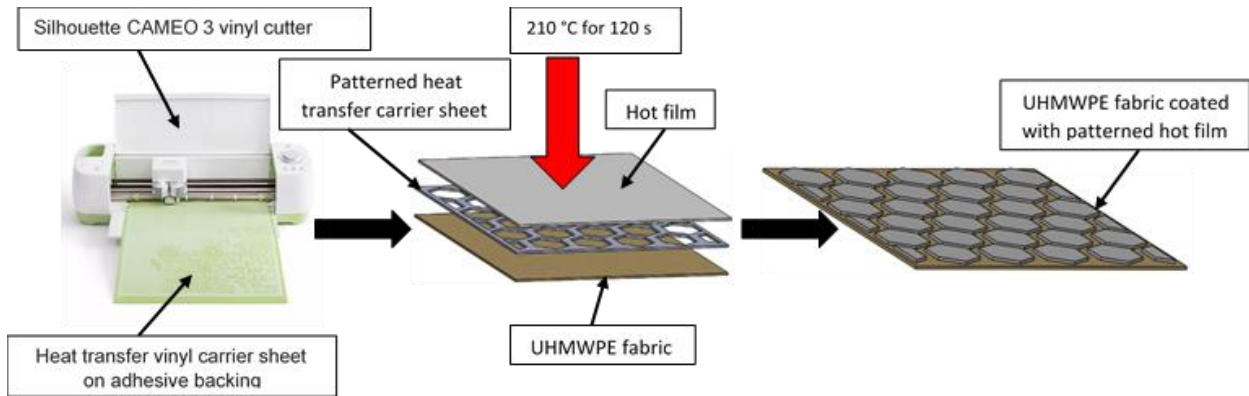


Fig 4.1. Preparation of patterned hot film

4.2.2 Preparation of ballistic target samples

Fabric samples coated with the patterned HF were hand stacked together with the weft and warp directions of fibers aligned in the same direction and pressure sensitive adhesive (PSA) bonded along the sides and pressed at 0.1 MPa as shown in Fig.4.2(a). Samples were also prepared with fabric coated uniformly with HF without using a heat transfer carrier sheet to investigate the effect of patterning the HF on ballistic performance and stiffness. PSA (9472LE) with adhesive thickness of 0.132 mm was purchased from 3M Canada, Milton, ON, Canada. Another set of panels (H/P25) were prepared in which only half of the layers are bonded as in Fig.4.2(a) at the strike face and the other half completely bonded with PSA at the back face throughout the entire surface and pressed at 8 MPa as shown in Fig.4.2(b). HF was used at the strike face because of its hardness properties when treated to the fabric is highly favourable during initial impact with a projectile[35]. These panels were prepared with 25 layers of fabric stacked. Alternatively, a 45-layer sample was prepared using only neat fabric samples with PSA

only bonded at the sides similar to Fig.4.2(a) in order to compare how the fabric lamination affect ballistic mechanism and performance in relation to neat fabric.

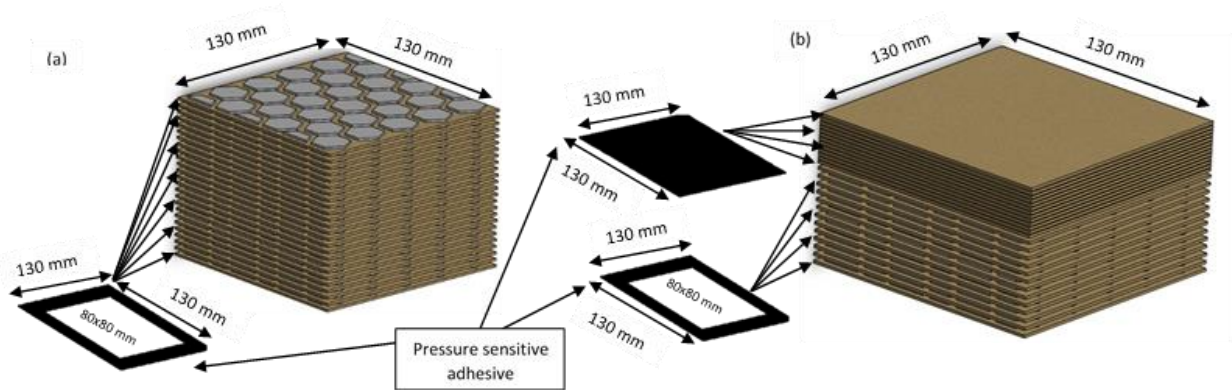


Fig 4.2. Schematic of fabrication method of ballistic panels of (a)25 layer panel of patterned hot film and (b) 25 layer hybrid panel consisting of 13 layers of patterned hot film and 12 layers of fabric bonded with PSA

4.2.3 Ballistic testing

Ballistic tests were carried out by shooting .357 Magnum Jacketed Soft Point (JSP) bullets with a specified mass of 10.2 g (158 gr) at 90° to the strike face of the test frame as shown in Fig.4.3. The tests were performed at NINE35 testing facility in Caledonia, ON, Canada. The ballistic sample was positioned 5 m from the gun muzzle and the ammunition used is in accordance with NIJ standard-0101.06 (Ballistic resistance of body armor, U.S. Department of Justice, 2008) for Type II protection level [36]. For handgun ammunition, the suggested distance between the gun muzzle of the barrel and the test frame is 5.0 ± 1.0 m according to NIJ standard-0101.06. A chronograph (Beta Master Shooting Chrony®, Shooting Chrony Inc., Mississauga, ON, Canada) was used to measure and record the velocities of the bullets at about halfway the distance between the target and the end of the gun muzzle. All recorded velocities of the bullets throughout the entire set of experiments were within the range of 435.9 ± 9 m/s which is the suggested velocity in NIJ standard- 0101.06 for similar .357 magnum ammunition for Level II

protection. Partial perforation is classified when the bullet is completely stopped by the armor and full perforation is when a hole is created through it or if any fragments enter the backing material. Standard clay (from Roma Plastilina #1[®] modeling clay, Sculpture House Inc., Fort Pierce, FL, U.S.) was used as the backing material behind target panels suggested by ASTM E3004 – 15e1 (Standard specification for preparation and verification of clay blocks used in ballistic-resistance testing of torso body armor) and NIJ Standard- 0101.06 [37]. In accordance to ASTM E304 – 15e1 standard, a metal frame with a plywood bottom was used to house the clay. Elastic straps were used to hold the target sample in position according to NIJ standard- 0101.06. Three samples were made for each multi-layer configuration and tested.

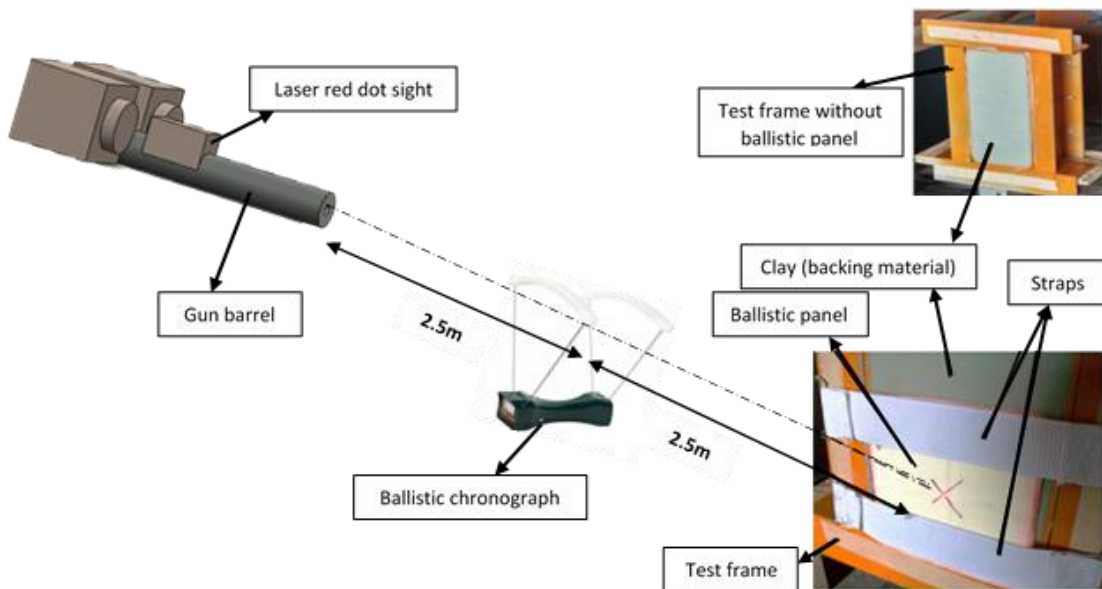


Fig 4.3. Ballistic test set up

4.2.4 Bending stiffness tests

Two separate tests were performed to investigate the effect of the patterned hot film as well as composite configuration (respective lamination arrangements of hot film and/or PSA) on the stiffness of the samples. The first method shown in Fig.4.5(a) is a two-dimensional drop test used to measure flexibility of 25 layer samples of 50 mm x 160 mm of all the four configurations

mentioned earlier in addition to a 45 layer sample of neat UHMPWE fabric that was sealed tightly in a polyethylene bag using a Manual Impulse Bag Sealer. One half of the sample (80 mm) is allowed to hang from a right-angled edge of a table with a 60 g weight hanging at the end. The other half of held firmly in position as shown in Fig.4.4(a) and the bending angle (BA) was measured with a protractor [20,38], which is a measure of the flexibility where a larger angle indicates a higher flexibility.

The second method is the cantilever test shown in Fig.4.4(b) which employs the principle of cantilever bending of fabric under its own mass in accordance to ASTM D1388-18 [39]. Single layered fabric samples of 25mm x 200 mm were clamped and slid at a constant rate of approximately 120 mm/min in a direction parallel to its long dimension until the edge of the specimen touches the knife edge which is at 41.5° to the horizontal. The overhang length (O) from the linear scale is recorded from which the bending length (c) are calculated from Eq.1[39].

$$c = O/2 \tag{1}$$

Smaller bending length corresponds to greater flexibility.

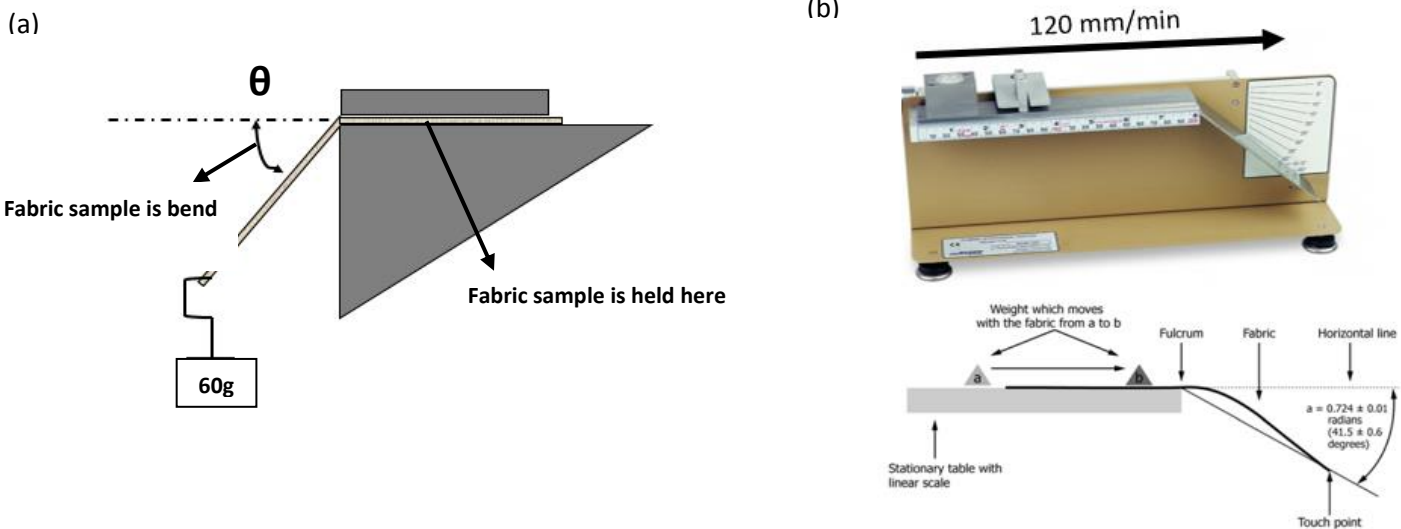


Fig 4.4. Schematic of bending stiffness test (a)2-dimensional drop test and (b) cantilever test[39]

4.2.5 3D CT scan analysis

After the ballistic tests, the panels were analyzed using a non-destructive testing (NDT) technique of X-Ray Computed Topography (CT-scans) to study delamination failure mechanisms in greater depth. A Gamma Medica X-SPECT™ Small Animal Scanner was used to conduct the CT-scans at 75 kVp and 310 μ A X-ray. In order to acquire projections from the scanned samples, FLEX X-O CT System software was capable of producing 512 projection angles of 2184 \times 2240 pixel-projections (0.05 mm \times 0.05 mm pixels). Reconstruction of the projection images into 512 \times 512 \times 512 arrays (0.115 mm voxels) was done using Feldkamp cone-beam reconstruction algorithm (COBRA, Exxim Computing Corporation) and Amira software and MATLAB® (MathWorks, Natick, MA, USA) were used for visualization and quantitative processing.

The maximum bulge height on the backface of the partially-perforated panel produced from the ballistic impact was measured from the CT-scan images in order to acquire the BFS. To determine the amount of unperforated layers of the composite laminates, the thickness of remaining material from the X-Z view of the images was measured as well as manually counting the number of sheared layers. A new metric called Area at Half-Height was calculated by measuring the cross-sectional area at half the height of the bulge. This metric acts to indicate the extent in which the fibers are able to transfer the kinetic energy to nearby regions. Thus, a high Area at Half Height indicates that the energy was transmitted over a wider area. The backface volume (BFV) was measured by calculating the volume of the bulge over a 45 mm \times 45 mm region for all the samples. This was made possible by rendering 3D-views of the backface after impact from the 2D slices in MATLAB®.

4.3. Results and Discussion

Despite having different configurations, the 25 layered samples of the same area have comparable areal densities within the same range of values which shows how the different adhesives have little (2.9 to 13.3% difference) influence on the weight of the panels as shown in Fig.4.5. As expected, the N45 has the highest areal density of 10.57 kg/m^2 since the fabric layers are the main contributors to its weight. Neat samples tested had 45 layers because the minimum number of neat fabric layers required to stop a 9mm ammo at $\sim 350\text{m/s}$ was 45. The N45 is 96% thicker than the thinnest sample (PSA25) and is the thickest among the tested configurations. Patterning of HF does not show to have any effect on the thickness of the panels as shown in Fig.4.5, where HF25 and Plain25 have similar thicknesses of around 14.5 mm which is 41% thicker than PSA25. However, panels that involved cold compression (H/P25 and PSA25) have the smallest thicknesses of 10.7 mm and 10.3 mm respectively. Unlike areal density, thickness shows to be significantly influenced by the type of adhesives used for lamination of the panels.

Patterning of HF results in a 21% increase in bending angle of the 25 layer samples and 9.5% reduction in bending length of the single plies. This is very beneficial for ballistic applications since patterning of the hot film did not have a significant effect on ballistic performance. Processing conditions of common thermoplastic- matrix fiber reinforced composites influence their flexural modulus, and they usually require high processing temperatures resulting in the composites being extremely rigid [40,41]. The unlaminated 45 layer neat sample has about 53% and 26% higher bending angle and 35% and 28% lower bending length than the Plain25 and HF25 respectively. This shows how lamination generally reduces the stiffness of ballistic panels which is why patterning of HF allows for some of the lost flexibility

to be recovered without compromising ballistic performance. A summary of the ballistic and stiffness performance results of the tested configuration is shown in Table.1

Stiffness of the tested samples is shown to be strongly influenced by the type of lamination and configuration used. PSA25 has the lowest bending angle of 5.4° which is 90% lower than that of the 45-layer neat unlaminated sample (N45). Interestingly H/P25 having half of its layers laminated with patterned HF and the other half laminated with PSA has a bending angle of 13.2° indicating that patterned hot film has attractive stiffness characteristics on ballistic panels. This is further supported by HF25 that has a bending angle of approximately 41° which is a steep increase in flexibility from that of HF25 despite having similar AHH. An attractive performance combination will be having a lower BFS and BFV but higher bending angle and AHH meaning that the impact energy is absorbed and distributed within the fibers more effectively resulting in less injury to the wearer. Overall, it is evident that patterning of hot film allows ballistic panels to remain relatively flexible without compromising ballistic performance.

Images of the cross-section of the partially perforated panels were obtained from the CT-scans and reconstructed. The reconstructed 2D images of the 5 different configurations (a-e) tested are shown in Fig.4.10. There is partial penetration by the bullet of all the samples presented and the failure mechanisms involved can be analyzed. It is evident that there is occurrence of fiber fracture followed by fiber failure (under tensile forces) for all the samples [42]. Delamination of individual layers is shown in Fig.4.10(a-d) in which the fibers are stretched absorbing the residual kinetic energy from the bullet until it is stopped near the backface [43,44]. However, the extent of delamination is more noticeable in Fig.4.10(a-c) due to high restriction of the motion of the fibers by the HF. There is no visible delamination in Fig.4.10(e) for the unlaminated panel due to lower bond strength as compared to the laminated

panels. Hence the dominant failure mechanism in which the impact energy is absorbed is through fiber straining rather than delamination which explains the high BFS. Delamination takes place at the penetration point and extends to the sides of the panel and the wider it propagates the more energy dissipated to the in-plane fibers. There is noticeably lower extent of delamination on PSA25 as compared to the rest of the laminated panels which results in a greater BFS due to fiber straining being more dominant than delamination. Additionally, the bullet is seen to flatten into a mushroom-like shape which increases its surface area of contact with the nearby fibers resulting in more energy distribution across the fibers and is more noticeable with HF25 and Plain25. This stretching of the fibers at the back deforms the panel and creates a BFS. Deformation of the bullet into the mushroom-like shape constitutes to approximately 25% of the impact energy dissipation in unidirectional based armor panels [45]. A similar study carried out ballistic tests on composite material composed of aramid fabric and polypropylene films as the matrix and the failure mechanisms were delamination, fabric/matrix debonding and matrix cracking [46]. Interestingly, it is observed that patterning of hot film has no noticeable effect in the ballistic perforation mechanism of the panels by comparing HF25 and Plain25 which appear to have comparable extents of delamination as well as number of sheared layers. This is a significant advantage for body armor applications because it allows the flexibility to improve without limiting the ballistic performance.

Patterning of HF was observed to have insignificant effect on the BFS of the ballistic samples where both HF25 and Plain25 panels have BFS within the range of values of 12.67-14.72 mm as shown in Fig.4.6. BFS is an important parameter of quantitatively analyzing ballistic performance and is used to weigh the trauma resistance since it is directly related to the amount of impact energy transferred to the torso of the wearer [47,48]. According to NIJ

standard- 0101.06, the maximum allowable depth of indentation (BFS) for acceptable protection against behind-armor blunt trauma (BABT) to prevent internal organs from being injured is 44 mm [47]. However, BFS remains an insufficient parameter to fully characterise the protective properties of ballistic panels against blunt trauma. To quantify the amount of energy absorbed by the ballistic panel, BFV provides useful information alongside BFS regarding ballistic performance. When the impact energy absorbed more by the fabric layers and transmitted to a larger area of the ballistic panel, a lower trauma volume is produced [49]. When more energy of impact is transmitted to the back of the panel, a higher BFV is produced resulting in less trauma resistance. This parameter is related to how well the fibers can distribute the energy of the bullet globally within the panel. The BFV can be calculated using in-house image processing software from the CT-scans.

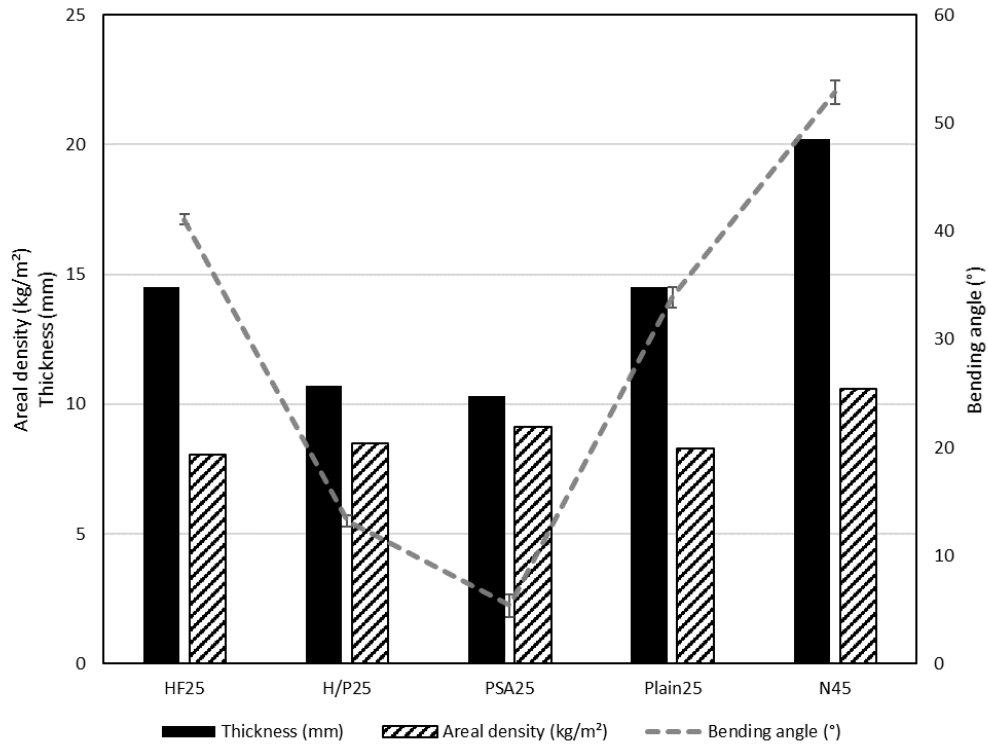


Fig 4.5. Thickness, areal density, and stiffness of the different UHMWPE laminated and unlaminated test samples

Additionally, the 3D images of the backface target samples after impact shown in Fig.4.9 were used to calculate the BFV of partially perforated target samples.

From the results in Fig.4.6, even though patterning on the HF had no significant effect on the BFS of the panels but results in about 20.8% increase in BFV which differentiates how much energy is absorbed between HF25 and Plain25. This shows that in the patterned HF laminated samples, energy is distributed over a larger area by the fibers since the BFS remains similar for both the HF25 and Plain25. The unlaminated regions on the patterned HF allow the fibers to absorb energy through fiber stretching more effectively since they are less restricted resulting in a higher BFV as compared to the Plain25 where all the fibers are relatively more restricted to stretching. Interestingly, the BFV of the patterned HF laminated sample is like the one of the 45-layered unlaminated sample even though the latter has about 5% higher BFS.

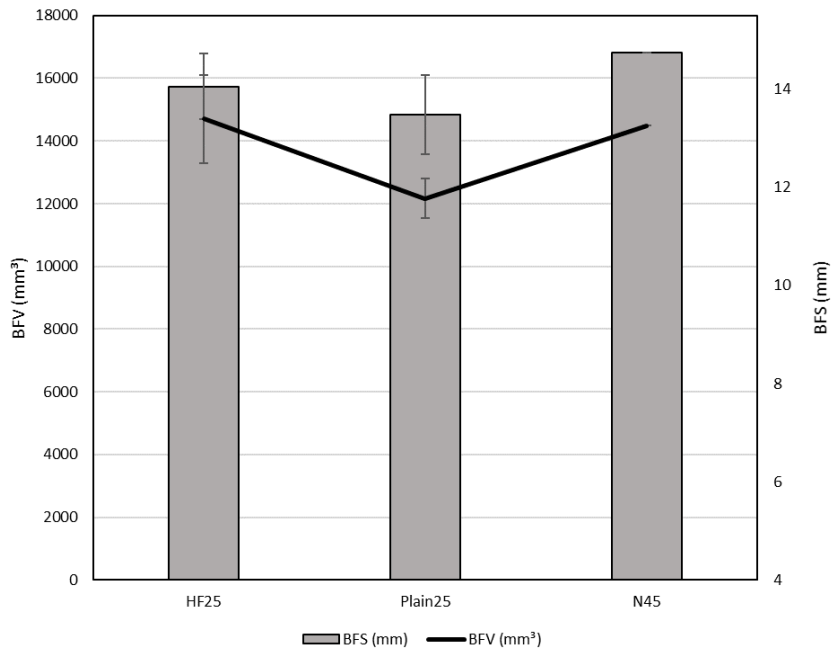


Fig 4.6. Effect of patterning hot film on BFS and BFV

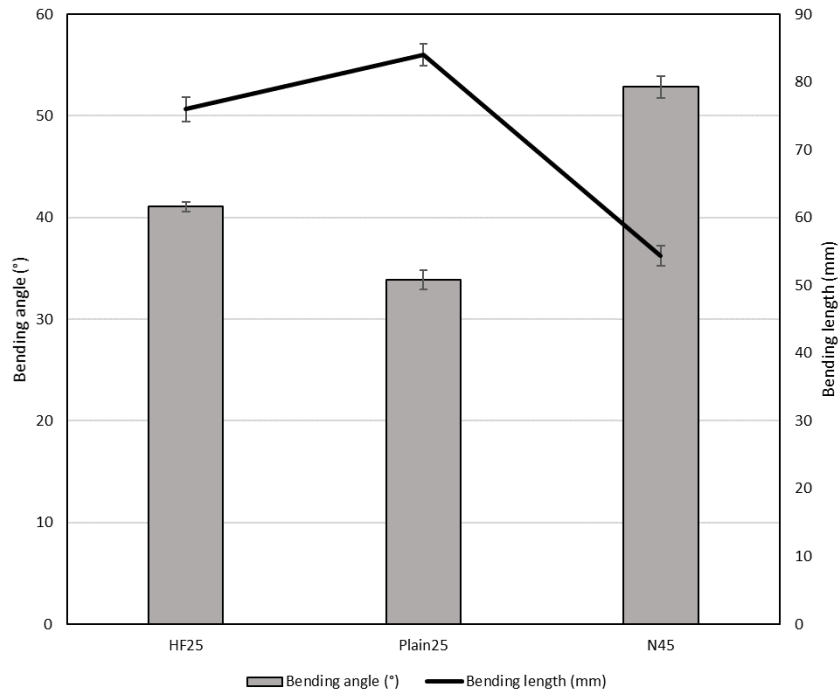


Fig 4.7. Effect of patterning hot film on stiffness of ballistic panels

A similar study calculated the BFV of partially perforated samples by using mold clay to obtain the exact mold of trauma geometry and forming millimetric divisions on the mold to obtain the depth value for each value of the diameter[49].

The effects of composite configuration on BFS, BFV, Stiffness and Area at half Height (AHH) was analyzed and presented in Fig.4.8. Samples which were partially or fully laminated with PSA (H/P25 and PSA25 respectively) has the highest measured BFS ranging from 17.7 mm to 19.8 mm indicating that lamination with PSA resulting with fiber straining being the dominant failure mechanism of the ballistic panels. However, as discussed earlier HF25 and Plain25 have comparable BFS within the same range of values that are approximately 25% less than that of PSA25 and H/P25. Despite having 45 layers, unlaminated samples have a BFS of 14.7 mm which is comparable to that of the HF25 indicating high effectiveness of using HF lamination which only required 25 layers to stop the same bullet. Additionally, H/P25 and PSA25 have the

highest BFV of 19017.29 mm³ and 18870.57 mm³ respectively which indicates that they transferred more energy to the backing material than the rest of the configurations. It is noticeable that PSA has a more significant effect on the amount of impact energy transferred to the backing material since H/P25 has approximately 29% higher BFV than HF25. This can be explained by how less restrictive PSA is to the motion of the fibers is as compared to hot film. A new parameter is introduced in this study called Area at half height (AHH) which is the cross-sectional area at half the height of the backface after impact and can be used to understand energy distribution mechanisms more effectively. A higher AHH indicates that energy has been transferred across a wider area of the panel meaning that the fibers were able to transfer the impact energy to nearby regions more effectively. Interestingly, HF25 and PSA25 have similar AHH despite the later having a 28% higher BFV.

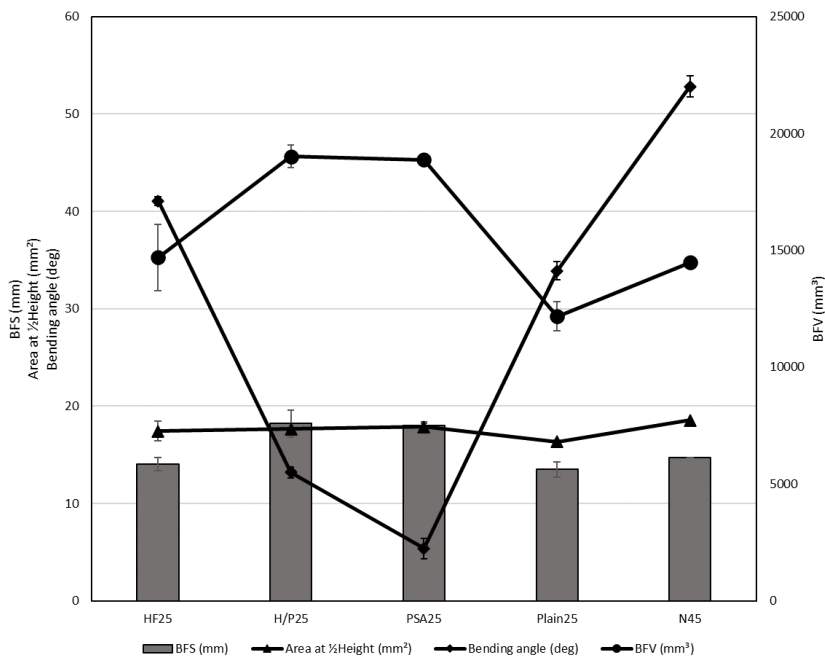


Fig 4.8. Effect of composite configuration on BFS, BFV and stiffness

This shows that for HF25 energy was distributed within the fibers more effectively with less energy being transferred to the backing material as compared to PSA25. As a result, there is less

blunt trauma experience by some wearing a body armor of such configuration. It is observed that patterning of the hot film results in a decrease in AHH by comparing HF25 and Plain 25 indicating how patterning can improve distribution of impact energy across nearby regions of the fibers.

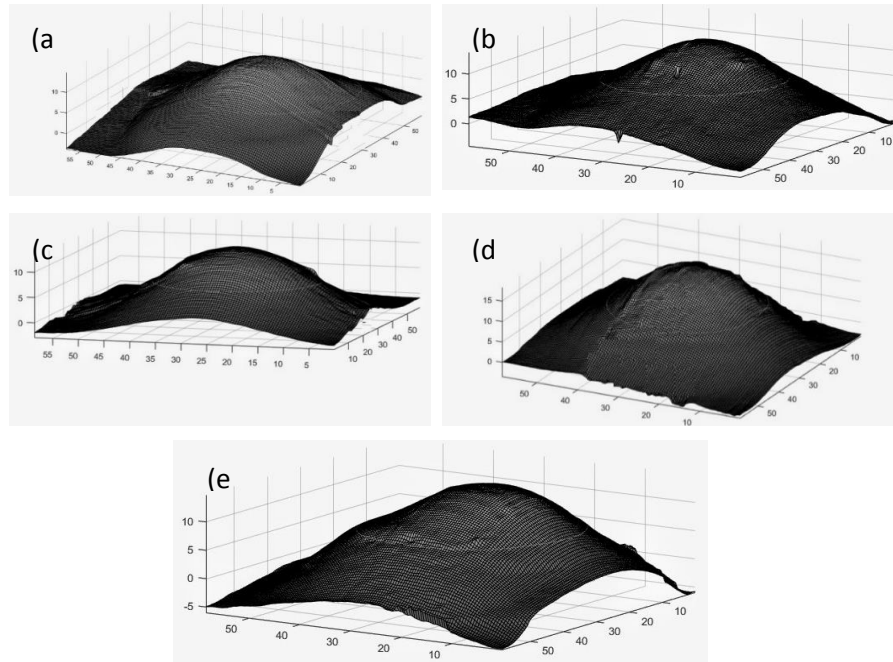


Fig 4.9. 3D images of the backface of target samples after impact(a) HF25 (b) H/P25 (c) Plain25 (d)PSA25 (e)N45

Table 4.1. Summary of the tested configurations and ballistic results

	Sample	Average thickness (mm)	lamination type	BFS (mm)	BFV (mm ³)	Bending angle (°)
(a)	HF25	14.5±?	25 layers laminated with patterned hot film	14±0.668	14696.3±1412.5	41.1±0.47
(b)	H/P25	10.7	13 layers laminated with patterned hot film + 12 layers laminated with PSA	18.2±1.352	19017.3±486.2	13.2±0.56
(c)	Plain25	14.5	25 layers laminated with plain hot film	13.5±0.811	12170.3±621.6	33.9±0.95
(d)	PSA25	10.3	25 layers laminated with PSA	18±0.407	18870.6±162.4	5.4±1.02
(e)	N45	20.2	45 layers of unlaminated fabric	~14.7	~14481.9	52.8±1.11

Upon impact with a projectile, the target sample is compressed forming a compressive pulse of the fibers creating a plug formation at the strikeface due to shear plugging and fracture of fibers [50]. There is no visible plug formation for the composite laminates with HF (Fig.4.10 (a-c) due to low inter-ply bond strength since the plies are stacked on top of each other resulting in minimal up-ward flow of the material. Therefore, their dominant failure mechanism at the strikeface is mainly shearing failure and friction between projectile and target sample due to the increased hardness of the HF lamination which results in restrictions to the motion of the fibers to spread out the upward flow of the material upon impact. Similarly, no plug formation is noticed in the 45-layer un laminated panel where the dominant failure mechanism is shearing failure with a noticeable upward flow of the material spread out more widely due to no fiber motion restrictions. In contrast, PSA25 has a noticeable and significant strikeface plug formation due to its high inter-ply bond strength. In general, delamination, shear plugging, tensile failure and friction are the main dominant failure mechanisms of woven fabric composite materials under ballistic impact[51,52].

Since the main idea of ballistic composite materials is to efficiently absorb the impact energy and transmit less of it to the wearer, BFS and BFV are normalized by dividing them with the bullet energy absorbed per areal density as shown below:

$$\text{Normalized BFS (mm)} = \frac{\text{BFS (mm)} \times \text{Areal density } \left(\frac{\text{kg}}{\text{mm}^2}\right)}{\text{Energy absorbed (J)}} \quad (2)$$

$$\text{Normalized BFV (mm}^3\text{)} = \frac{\text{BFV (mm}^3\text{)} \times \text{Areal density } \left(\frac{\text{kg}}{\text{mm}^2}\right)}{\text{Energy absorbed (J)}} \quad (3)$$

$$\text{Energy absorbed (J)} = 0.5 \times 0.0102 \times (\text{bullet velocity})^2 \quad (4)$$

Kinetic energy of the projectile is mainly dispersed by primary yarns which are the yarns in direct contact with the projectile and intersect with orthogonal yarns[8]. The normalized performance parameters are displayed in Fig.4.11 and a new parameter that can summarize the extent of energy dissipation is the ratio height: Full Width at Half Height (FWHH) which is the ratio between the BFS and the extrapolated diameter of the area at half height.

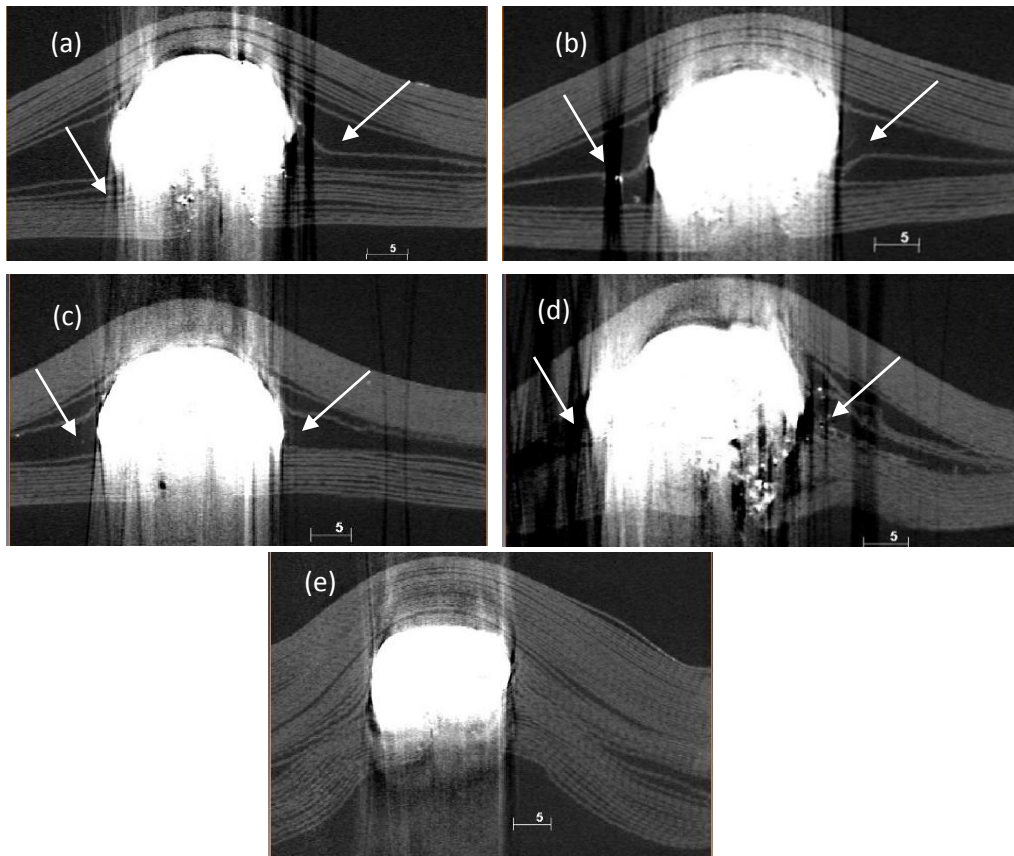


Fig 4.10. 2D cross sectional view of the partially perforated target samples (a) HF25 (b) H/P25 (c) Plain25 (d)PSA25 (e)N45

This means a lower ratio means there is less blunt trauma with the impact energy dissipated over a larger area on the backface which is more favourable. From Fig.4.11 it is noticeable that after normalizing the parameters, HF25 is the most favourable having the lowest

Height : FWHH ratio, low normalized BFS and BFV, and high energy absorbed per areal density.

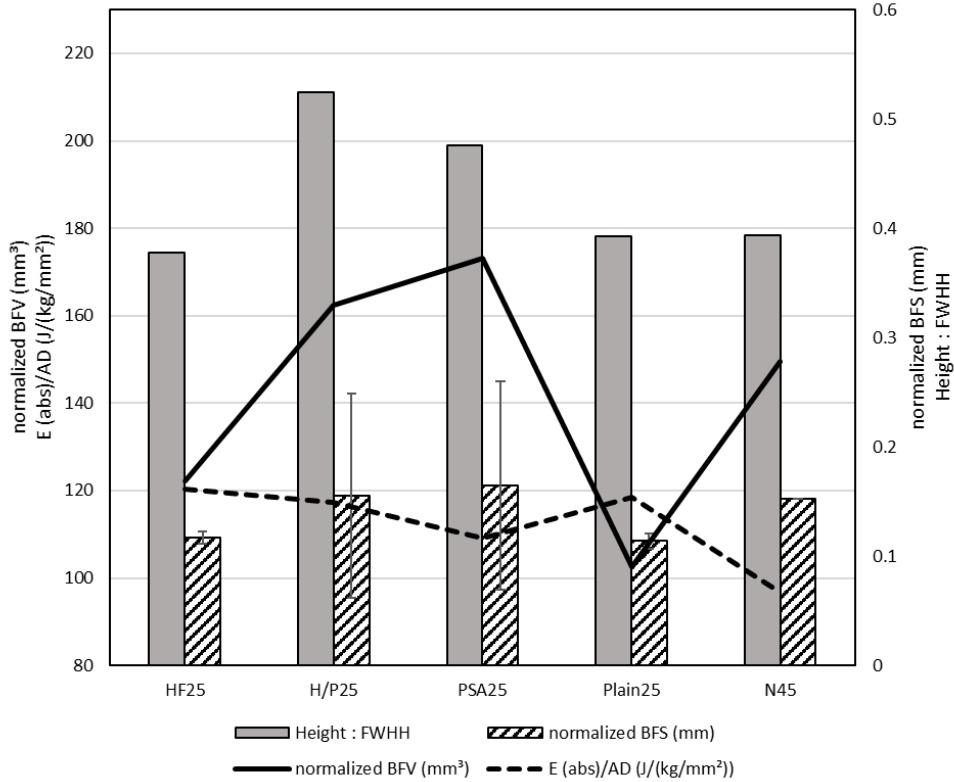


Fig 4.11. Relationship between normalized BFS, BFV,SAR with energy absorbed

However, HF25 and Plain25 seem to have similar ballistic performances, but the former has more superior flexural properties making it the best candidate among the tested samples.

4.4. Conclusions

The ballistic performance of 25 layered composite laminates fabricated from plain weave UHMPWE were characterized. The samples were prepared by either hot-pressing the plain weave UHMPWE with thermoplastic hot film, cold-press compression with pressure sensitive adhesive (PSA) or both. The hot film (HF) used for the laminates was either patterned into

distinct uniform hardened hexagonal regions (nominal diameter of 27.9 mm with a 1 mm gap between each region) or applied without any patterning. Samples consisting of 25 layer panels laminated with PSA and cold-pressed at 8MPa and a 45 layer unlaminated UHMWPE neat fabric stacked together were also tested to contrast their ballistic performance with that of the hot film laminated 25 layered samples. Ballistic tests were performed using 0.357 magnum ammunition at ~435 m/s. The failure mechanisms of the laminate samples under the ballistic impact were analyzed using X-Ray Computed Tomography (CT) scans to calculate metrics such as backface signature (BFS), backface volume (BFV), area at half height (AHH) and ratio of height to full width at half height (Height:FWHH).

A significant increase in bullet penetration resistance and energy absorption was observed on the laminated panels as compared to the neat UHMPWE samples as shown by the decrease in BFS, BFV, Height:FWHH and increase in AHH. Specifically, the 25 layer panel laminated with HF had the least BFS, BFV and Height:FWHH. Use of the patterned hot film did not have any significant effect on the ballistic performance of the panels as compared to using plain HF. However, the panels laminated with 25 layers of HF had the highest energy absorbed per areal density making them the most superior among the tested configurations. This is also shown by having the lowest Height:FWHH ratio meaning that the impact energy was transferred to nearby regions of the fibers more effectively. The main impact energy absorption mechanisms observed were fiber fracture at the strikeface and fiber straining and delamination at the backface of the panels. Panels laminated with PSA had an upward flow of the material forming a plug at the strikeface. Stiffness tests were performed in order to analyse the effect of patterning of HF on the flexibility of a single ply as well as the entire 25 layer panel. Patterning of HF was found to increase the bending angle of the composite panel by 20.9 % and significantly reduced the

bending length of the laminated ply by 8 mm making it more flexible. The flexibility tests were also performed to analyze the effect of the different tested composite configurations on the stiffness of the panels. Among the laminated samples, the 25 layer panel with patterned HF had the highest bending angle with the one laminated with PSA having the lowest bending angle. Patterning of HF has shown to give attractive ballistic and stiffness properties which are favorable in body armor applications.

4.5 Acknowledgement

The authors would like to thank Mr. Ron Lodewyks from NINE35, Caledonia, ON, Canada for carrying out the ballistic tests and Dr. Troy Farncombe for performing the CT-scans.

4.6 References

- [1] Sapozhnikov SB, Kudryavtsev OA, Zhikharev M V. Fragment ballistic performance of homogenous and hybrid thermoplastic composites 2015. <https://doi.org/10.1016/j.ijimpeng.2015.03.004>.
- [2] Bhatnagar A. *Lightweight Ballistic Composites: Military and Law-Enforcement Applications: Second Edition*. 2016. <https://doi.org/10.1016/C2014-0-03657-X>.
- [3] Jacobs MJN, Van Dingenen JLJ. *Ballistic protection mechanisms in personal armour*. n.d.
- [4] David N V., Gao XL, Zheng JQ. Ballistic resistant body armor: Contemporary and prospective materials and related protection mechanisms. *Appl Mech Rev* 2009;62:1–20. <https://doi.org/10.1115/1.3124644>.
- [5] Kulkarni SG, Gao X-L, Horner SE, Zheng JQ, David N V. *Ballistic helmets-Their design, materials, and performance against traumatic brain injury* 2013. <https://doi.org/10.1016/j.compstruct.2013.02.014>.
- [6] Jin Kang T, Youn Kim C, Hwa Hong K. Rheological Behavior of Concentrated Silica Suspension and Its Application to Soft Armor. *J Appl Polym Sci* 2011;124:1534–41. <https://doi.org/10.1002/app.34843>.
- [7] Faur-Csukat G. *A Study on the Ballistic Performance of Composites* n.d. <https://doi.org/10.1002/masy.200650728>.
- [8] Cheeseman BA, Bogetti TA. *Ballistic impact into fabric and compliant composite laminates* n.d. [https://doi.org/10.1016/S0263-8223\(03\)00029-1](https://doi.org/10.1016/S0263-8223(03)00029-1).
- [9] Lim CT, Tan VBC, Cheong CH. Perforation of high-strength double-ply fabric system by varying shaped projectiles. *Int J Impact Eng* 2002;27:577–91. [https://doi.org/10.1016/S0734-743X\(02\)00004-0](https://doi.org/10.1016/S0734-743X(02)00004-0).
- [10] Shim VPW, Tan VBC, Tay TE. Modelling deformation and damage characteristics of woven fabric under small projectile impact. *Int J Impact Eng* 1995;16:585–605. [https://doi.org/10.1016/0734-743X\(94\)00063-3](https://doi.org/10.1016/0734-743X(94)00063-3).
- [11] Kirkwood KM, Kirkwood JE, Lee S, Egres RG, Wagner NJ, Wetzel ED. *Yarn Pull-Out as a Mechanism for Dissipating Ballistic Impact Energy in Kevlar®; KM-2 Fabric Part I: Quasi-Static Characterization of Yarn Pull-Out*. n.d.
- [12] Yang CC, Ngo T, Tran P. Influences of weaving architectures on the impact resistance of multi-layer fabrics. *Mater Des* 2015;85:282–95. <https://doi.org/10.1016/j.matdes.2015.07.014>.
- [13] *Ballistic Resistance of Personal Body Armor*. n.d.
- [14] Hassim N, Ahmad MR, David N V., Ahmad WYW, Yahya MHM. Effect of coating on the ballistic protection of unidirectional fabric systems. *BEIAC 2013 - 2013 IEEE Bus. Eng. Ind. Appl. Colloq.*, 2013, p. 443–7. <https://doi.org/10.1109/BEIAC.2013.6560167>.

- [15] Briscoe BJ, Motamedi F. The ballistic impact characteristics of aramid fabrics: The influence of interface friction. *Wear* 1992;158:229–47. [https://doi.org/10.1016/0043-1648\(92\)90041-6](https://doi.org/10.1016/0043-1648(92)90041-6).
- [16] Ahmad MR, Hassim N, Ahmad WYW, Samsuri A, Yahya MHM. Preliminary Investigation on the ballistic limit of ultra high molecular weight polyethylene unidirectional coated fabric system. *Fibres Text East Eur* 2013;99:89–94.
- [17] Firouzi D, Foucher DA, Bougherara H. Nylon-coated ultra high molecular weight polyethylene fabric for enhanced penetration resistance. *J Appl Polym Sci* 2014;131:40350. <https://doi.org/10.1002/APP.40350>.
- [18] Asijad X, Chouhand X, Xshishay X, Gebremeskeld A, Xrama X, Singhd K, et al. High strain rate behavior of STF-treated UHMWPE composites. *Int J Impact Eng* 2017;110:359–64. <https://doi.org/10.1016/j.ijimpeng.2017.02.019>.
- [19] Arora S, Majumdar A, Singh Butola B. Structure induced effectiveness of shear thickening fluid for modulating impact resistance of UHMWPE fabrics 2018. <https://doi.org/10.1016/j.compstruct.2018.11.028>.
- [20] Lee YS, Wetzel ED, Wagner NJ. The ballistic impact characteristics of Kevlar R woven fabrics impregnated with a colloidal shear thickening fluid. n.d.
- [21] Lu Z, Yuan Z, Chen X, Qiu J. Evaluation of ballistic performance of STF impregnated fabrics under high velocity impact 2019. <https://doi.org/10.1016/j.compstruct.2019.111208>.
- [22] Chatterjee VA, Verma SK, Bhattacharjee D, Biswas I, Neogi S. Enhancement of energy absorption by incorporation of shear thickening fluids in 3D-mat sandwich composite panels upon ballistic impact. *Compos Struct* 2019;225:111148. <https://doi.org/10.1016/j.compstruct.2019.111148>.
- [23] Ding J, Li W, Shen SZ. Research and Applications of Shear Thickening Fluids. *Mater Sci Eng* n.d.
- [24] Bhatnagar A. *Lightweight Ballistic Composites: Military and Law-Enforcement Applications: Second Edition*. 2016. <https://doi.org/10.1016/C2014-0-03657-X>.
- [25] Bandaru AK, Chavan V V., Ahmad S, Alagirusamy R, Bhatnagar N. Ballistic impact response of Kevlar® reinforced thermoplastic composite armors. *Int J Impact Eng* 2016;89:1–13. <https://doi.org/10.1016/j.ijimpeng.2015.10.014>.
- [26] Kulkarni SG, Gao XL, Horner SE, Zheng JQ, David N V. Ballistic helmets - Their design, materials, and performance against traumatic brain injury. *Compos Struct* 2013;101:313–31. <https://doi.org/10.1016/j.compstruct.2013.02.014>.
- [27] Vieille B, Casado VM, Bouvet C. About the impact behavior of woven-ply carbon fiber-reinforced thermoplastic- and thermosetting-composites: A comparative study. *Compos Struct* 2013;101:9–21. <https://doi.org/10.1016/j.compstruct.2013.01.025>.
- [28] Walsh SM, Scott BR, Spagnuolo DM. *The Development of a Hybrid Thermoplastic Ballistic Material With Application to Helmets*. 2005.

- [29] Walsh SM, Scott BR, Spagnuolo DM, Wolbert JP. HYBRIDIZED THERMOPLASTIC ARAMIDS: ENABLING MATERIAL TECHNOLOGY FOR FUTURE FORCE HEADGEAR. n.d.
- [30] Bandaru AK, Ahmad S. Ballistic Impact Behaviour of Thermoplastic Kevlar Composites: Parametric Studies. *Procedia Eng* 2017;173:355–62. <https://doi.org/10.1016/j.proeng.2016.12.029>.
- [31] De Ruijter C, Van Der Zwaag S, Stolze R, Dingemans TJ. Liquid crystalline matrix polymers for aramid ballistic composites. *Polym Compos* 2010;31:612–9. <https://doi.org/10.1002/pc.20835>.
- [32] Song JW, Nainesh A, Stephen P. Ballistic Impact Resistance of Thermoplastic Composites. *ANTEC 2000*:2391–5.
- [33] Sapozhnikov SB, Kudryavtsev OA, Zhikharev M V. Fragment ballistic performance of homogenous and hybrid thermoplastic composites. *Int J Impact Eng* 2015;81:8–16. <https://doi.org/10.1016/j.ijimpeng.2015.03.004>.
- [34] Ageorges C, Ye L, Hou M. Advances in fusion bonding techniques for joining thermoplastic matrix composites: A review. *Compos - Part A Appl Sci Manuf* 2001;32:839–57. [https://doi.org/10.1016/S1359-835X\(00\)00166-4](https://doi.org/10.1016/S1359-835X(00)00166-4).
- [35] Naebe M, Sandlin J, Crouch I, Fox B. Novel polymer-ceramic composites for protection against ballistic fragments. *Polym Compos* 2013;34:180–6. <https://doi.org/10.1002/PC.22397>.
- [36] NIJ Standard-0101.06. Ballistic Resistance of Personal Body Armor. *NIJ Stand* 2008:89.
- [37] ASTM E3004-15e1 - Standard Specification for Preparation and Verification of Clay Blocks Used in Ballistic-Resistance Testing of Torso Body Armor n.d. <https://webstore.ansi.org/standards/astm/astme300415e1> (accessed June 25, 2021).
- [38] Hassan TA, Rangari VK, Jeelani S. Synthesis, processing and characterization of shear thickening fluid (STF) impregnated fabric composites. *Mater Sci Eng A* 2010. <https://doi.org/10.1016/j.msea.2010.01.018>.
- [39] ASTM D1388 - Standard Test Method for Stiffness of Fabrics | *Engineering360*. n.d.
- [40] (PDF) Ballistic Impact of Thermoplastic Composites Reinforced with Carbon Fibers n.d. https://www.researchgate.net/publication/265385274_Ballistic_Impact_of_Thermoplastic_Composites_Reinforced_with_Carbon_Fibers (accessed July 7, 2021).
- [41] Cook FP, Case SW. The effect of processing conditions on the properties of thermoplastic composites. *Conf Proc Soc Exp Mech Ser* 2011;6:591–7. https://doi.org/10.1007/978-1-4419-9792-0_87.
- [42] Liu S, Wang J, Wang Y, Wang Y. Improving the ballistic performance of ultra high molecular weight polyethylene fiber reinforced composites using conch particles. *Mater Des* 2010. <https://doi.org/10.1016/j.matdes.2009.01.044>.
- [43] Zhang TG, Satapathy SS, Vargas-Gonzalez LR, Walsh SM. Ballistic impact response of Ultra-High-Molecular-Weight Polyethylene (UHMWPE) 2015.

<https://doi.org/10.1016/j.compstruct.2015.06.081>.

[44] Min S, Chen X, Chai Y, Lowe T. Effect of reinforcement continuity on the ballistic performance of composites reinforced with multiply plain weave fabric 2015.

<https://doi.org/10.1016/j.compositesb.2015.12.001>.

[45] Jacobs MJN, Van Dingenen JLJ. Ballistic protection mechanisms in personal armour n.d.

[46] Carrillo JG, Gamboa RA, Flores-Johnson EA, Gonzalez-Chi PI. Ballistic performance of thermoplastic composite laminates made from aramid woven fabric and polypropylene matrix. *Polym Test* 2012. <https://doi.org/10.1016/j.polymertesting.2012.02.010>.

[47] Experimental and numerical investigation of fabric impact behavior | Elsevier Enhanced Reader n.d.

<https://reader.elsevier.com/reader/sd/pii/S1359836814004843?token=8B93DF5A3E97B910D490BE361E1AAAE0F9C83E08DC58535D68E6C00479906A2BBE46C41F36F446B7922C6BFD AF99EC08&originRegion=us-east-1&originCreation=20210706021745> (accessed July 5, 2021).

[48] Liu X, Li M, Li X, Deng X, Zhang X, Yan Y, et al. Ballistic performance of UHMWPE fabrics/EAMS hybrid panel 2055. <https://doi.org/10.1007/s10853-018-2055-4>.

[49] Karahan M, Kuş A, Eren R. An investigation into ballistic performance and energy absorption capabilities of woven aramid fabrics. *Int J Impact Eng* 2008;35:499–510.

<https://doi.org/10.1016/J.IJIMPENG.2007.04.003>.

[50] Liu S, Wang J, Wang Y, Wang Y. Improving the ballistic performance of ultra high molecular weight polyethylene fiber reinforced composites using conch particles 2009.

<https://doi.org/10.1016/j.matdes.2009.01.044>.

[51] Nilakantan G, Merrill RL, Keefe M, Gillespie JWD, Wetzel ED. Experimental investigation of the role of frictional yarn pull-out and windowing on the probabilistic impact response of kevlar fabrics 2014. <https://doi.org/10.1016/j.compositesb.2014.08.033>.

[52] Naik NK, Shrirao P. Composite structures under ballistic impact 2004.

<https://doi.org/10.1016/j.compstruct.2004.05.006>.

Chapter 5: Development of high-performance hypodermic needle penetration resistance flexible cotton fabric using patterned thermoplastic EVA hot film

R. Wu¹, P. Mudzi¹, D. Firouzi², C.Y. Ching¹, P.R. Selvaganapathy^{1*}

¹Department of Mechanical Engineering, McMaster University, Hamilton, ON L8S 4L7, Canada

²RONCO, 70 Planchet Road, Concord, ON L4K 2C7, Canada

*Correspondence: selvaga@mcmaster.ca; Tel.: +1 905-525-9140 (ext. 27435)

Relative Contributions:

Rong Wu: Carried out all experiments, interpretation, and analysis of the data and 2/3 of the first draft of the manuscript including all figures.

Panashe Mudzi: Carried out all experiments, assisted in the interpretation and discussion of results.

Dariush Firouzi : Assisted with fabric materials needed for the experiments and helped with final editing of paper.

Chan Y.Ching: Co-supervisor of Panashe, responsible for the final editing of the paper.

P.Ravi Selvaganapathy: Supervisor of Panashe and was responsible for the final editing and submission to the journal.

Abstract

Injuries caused by needle stick puncture are common and a concern in many industries, such as health services and waste collection. Personal protection against needle stick punctures currently use high-cost materials like high-density polyethylene (HDPE) woven fabric and Kevlar which compromises flexibility. In this paper, a low-cost, easy to produce needle puncture resistant material is developed. Here, cotton fabric is overlaid by patterned Ethylene-Vinyl Acetate (EVA) hot film and multiple layers are used that increase the needle penetration resistance by up to 478 percent compared with single layer of laminated fabric, while the flexibility decreased by 12-49%. Patterns of different shapes (hexagons and hexagons with triangles) and sizes with nominal diameters ranging from 2.6 to 13.5 mm were used and tested. The results showed that reducing the pattern size improves flexibility by up to 30%. Patterning the hot film did not significantly reduce the needle penetration resistant as compared to using plain hot film whilst the flexibility was not severely affected. Increasing the number of laminated fabric layers from 1 to 3 resulted in an increase in needle penetration resistance force from 2N up to 8N. Since the fabrication method is simple and rapid, it may be attractive for the manufacturing of personal protective equipment such as needle resistant gloves for healthcare workers, waste management workers and other relevant occupations

5.1. Introduction

In many professions, such as law enforcement, sanitation and medical, the personnel handle a variety of sharp objects such as hypodermic needles and face a significant risk of workplace injuries. The most common injuries are wounds due to penetration of sharp objects into the skin. In addition to puncture wounds, these sharp objects could be severely contaminated by harmful substances that may transmit serious diseases. Due to these reasons, there is increased demand of protective clothing for protection against punctures from hypodermic needles and other sharp objects. For these protective materials to be incorporated into clothing such as gloves, they need to be lightweight and flexible [1].

Two classes are used to categorize stab weapons which are edged or pointed [2]. Edged weapons such as knives consist of a continuous cutting edge and pointed weapons such as spikes have a sharp tip on a slender rod. Penetration from stab attacks is more difficult to prevent than slash attacks [3]. Hypodermic needles with a pointed tip and sloped edge belong to both edged and pointed categories. The main mechanism in which hypodermic needles puncture through untreated woven fabrics is the "windowing" effect in which the yarns spread apart to allow the foreign object to penetrate with low fiber fracture [4]. This mechanism is more repressed in tightly woven fabrics with a high yarn count. Penetration resistance of textiles is affected by several parameters including fabric weave architecture, number of filaments per yarn, number of plies, yarn linear density, areal density of fabric and mechanical properties of fibers [5].

One commonly accepted approach to avoid puncture resistance is to stack layers of fabric together but this results in increased areal density and stiffness [1]. Therefore, there is a need to improve performance of protective clothing whilst keeping them light and flexible. Commonly

used materials for protective clothing are High Strength Fibres (HSF) such as Kevlar[®] and ultra high molecular weight polyethylene (UHMWPE). There are several commercially available products with a high yarn count to resist hypodermic needles such as TurtleSkin[™] fabric from Warwick Mills Inc. with a black polymer coating[6].

Coating of fabrics is one technique that has proven to significantly improve the penetration resistance of textiles. There are different types of fabric coating techniques such as nylon coating [7], natural rubber latex coating, and Shear Thickening Fluid (STF) impregnation [8] to name a few. Several commercially stab resistant fabrics use the approach of incorporating polymer coating into woven fabrics such as Argus[™] (Barrday Inc.) and Kevlar MTP[™] (DuPont) [9]. The polymer matrix restricts “windowing” by prohibiting the fibers and yarns from being pushed aside by the spike resulting in more energy being required to separate the fibers and yarns. Coating Nylon 6,6 and 6,12 of UHMWPE improved the spike resistance by 77% and 86% respectively over a neat fabric target of equivalent areal densities [10]. A higher creep resistance of 14-37% and breaking force of 17-36% was observed from Nylon coated UHMPWE as compared with the neat fibers at various temperatures[7]. However, the coating process is time consuming as it requires several hours to cure. In another study, rubber latex (NRL)-coated unidirectional (UD) UHMWPE fabrics were produced which gave a higher puncture resistance of up to 62% as compared to uncoated fabric [11]. Non-Newtonian STFs have been used to make flexible high stab resistance ‘fluid armor’[12] and was shown to provide about 40-100% higher puncture and stab resistant performance in terms of energy absorption in comparison to textile only samples of comparable areal densities[13], [14]. However, STF have a number of limitations such as propensity to leak because of their liquid state[15] their hygroscopic properties degradation when exposed to moisture[16]. Nanoparticle-loaded elastomer impregnated into

UHMWPE plain-weave fabric was shown to increase the needle penetration resistance of single layer uncoated fabric by approximately 225% [17]. Coating Twaron© fabric with silicon carbide polymer matrix composite was shown to provide a better stab resistance in comparison to the untreated fabric[18]. A material known as SuperFabric® is made from flexible fabric consisting of printed arrays of hard ceramic-polymer platelets on its surface in order to resist needle stick penetration[19]–[21]. However, the plates have spaces in between which act as weak points resulting in the need for a multi-layer construction.

Ethylene-Vinyl Acetate (EVA) copolymer-based thermoplastics are an attractive matrix for fabric coating due to their flexibility and thermal stability. Due to these properties, they are the most widely used base polymers for HMA in industry [22]. Molecular branching, molecular weight and distribution and wt.% vinyl acetate are three main structural attributes of EVA copolymers that determine the properties of any copolymer grade. EVA copolymers are used in hot melt adhesives (HMA) because of their strength, flexibility, adhesion to substrates and low melting temperatures [23][24].

The objective here is to demonstrate that coating woven cotton fabric with EVA based thermoplastic hot film significantly improves its 25G needle penetration resistance as compared to the uncoated fabric. We also introduce a method of using layers of patterned hot film for increased needle penetration resistance whilst not significantly affecting the stiffness of the material. This is an important consideration for use in needle resistant protective gloves. Various samples were made with different patterning geometries to determine parameters that affect stiffness and needle resistance using this technique. The materials and methods are presented in the next section, followed by a presentation and discussion of the results. Finally, the conclusions from this study are presented.

5.2. Materials and methods

5.2.1 Materials

The needle resistant fabric was fabricated using layers of patterned Ethylene-Vinyl Acetate (EVA) sandwiched between layers of cotton fabric. A Silhouette CAMEO 3 (Silhouette America, Inc, USA) xurography cutter which can operate on substrate materials up to 12 inches wide was used to cut patterns on Heat Transfer Vinyl (HTV) sheets. The HTV sheets were purchased from XPCARE and consisted of polyurethane which is heat resistant up to 150°C as a transfer mold. Ethylene-vinyl acetate (EVA) is a thermoplastic copolymer with ethylene and vinyl acetate (VA) and is widely used as a hot melt adhesive [25]. The EVA sheets in this study were purchased from Adheco Ltd, Scarborough, ON, Canada, with 0.254 mm thickness and softening point at 96.7 to 100°C. Swing Away Clamshell Heat Press Machine was purchased from VIVOHOME, City of industry, CA, USA, which can operate within the temperature range - 17.8 to 215.6°C to create even surfaces under pressure. A high-density twill cotton fabric with an areal density of 386 g/m² and thickness of 0.7 mm was used in this study.

5.2.2 Sample fabrication

An imprint lithography technique was adopted in this study for sample fabrication, and a schematic of the fabrication process is shown in Figure 5.1. Firstly, the patterns corresponding to various coverage areas and sizes were designed using the Silhouette Studio[®] software. To have multiple orientations of the gaps between the patterns to improve the flexibility of the fabric, a triangular and hexagonal pattern and their combinations were tested. Details of the patterns are provided in Table 5.1. Once the patterns were created by xurography on the HTV sheets, the patterns were aligned between cotton fabric and EVA film. Two sets of patterns, offset from

each other by 1 mm in the x-direction (creating an overlap for greater overall coverage), were used to obtain a staggered pattern structure over multiple layers. The samples were heat pressed at a temperature of 98°C for four different time durations of 90, 120, 150 and 180 seconds to deposit the patterned EVA film on the fabric. After the heat treatment, the samples were cooled down under a fume hood at ambient temperature for around 2 minutes under a high air circulation and the HTV patterned sheet was removed from the fabric. Samples where the patterned EVA hot films were used to cover either one side or both sides of the fabric with different design and size were fabricated.

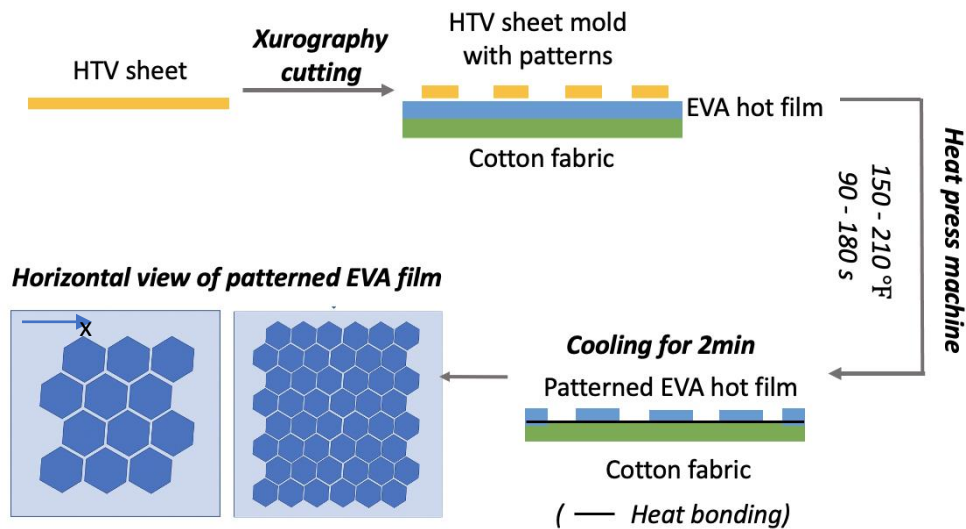
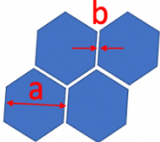
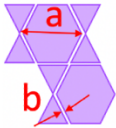


Figure 5.1: Schematic of sample fabrication process

Table 5.1: Illustration of sizes and patterns

Illustration	Pattern	Abbreviation	Dimension of pattern-a (mm)	Dimension of gap-b (mm)	Coverage
	Hexagon	XL	13.5	1.8	73%
		L	9.0	1.2	
		S	4.6	0.6	
		XS	2.6	0.3	
	Hexagon and triangle	Tri/hex	11.1	0.5	63%

5.2.3 Needle-stick penetration test

The prepared fabric samples were tested for needle stick penetration using the test setup shown in Figure 5.2. The test setup was designed and fabricated based on ASTM F2878-10 standard and is similar to the apparatuses used in [5] and patent [26]. The setup consists of four parts: (i) Fabric sample holder, (ii) Needle and stick holder, (iv) Load cell and stepper motor as well as the power supply. The fabric sample holder consists of two holding plates with concentric 20 mm circular openings. The fabric is sandwiched between these two plates with O-rings placed around the circular opening and clamped together using two clamps to hold the fabric sample firmly between the two holding plates with no slippage. The concentric circle opening is aligned to the tip of the needle-stick with the sample holder. The needle stick holder is mounted on a screw-thread which traverses in a direction normal to the fabric sample. The screw-thread is driven by a stepper motor connected to a 30V power supply and controlled and monitored via computer by QuickControl. A 5 kg load cell was mounted at the end of the needle-

stick holder to measure the force applied on the needle tip. The calibration and accuracy of the test setup was performed according to ASTM F2878-10. Additional information about the experimental setup can be found in [5]. A 25G 25.4 mm long hypodermic needle (BD305125) was used for all tests and five independent tests were performed for each fabric sample. The needle was traversed at a speed of 380 mm/min and the distance moved was set to 5 cm for each test. The highest penetration force was recorded and defined as the Penetration Resistance Force (PRF) and used to evaluate the needle resistance provided by the fabric samples.

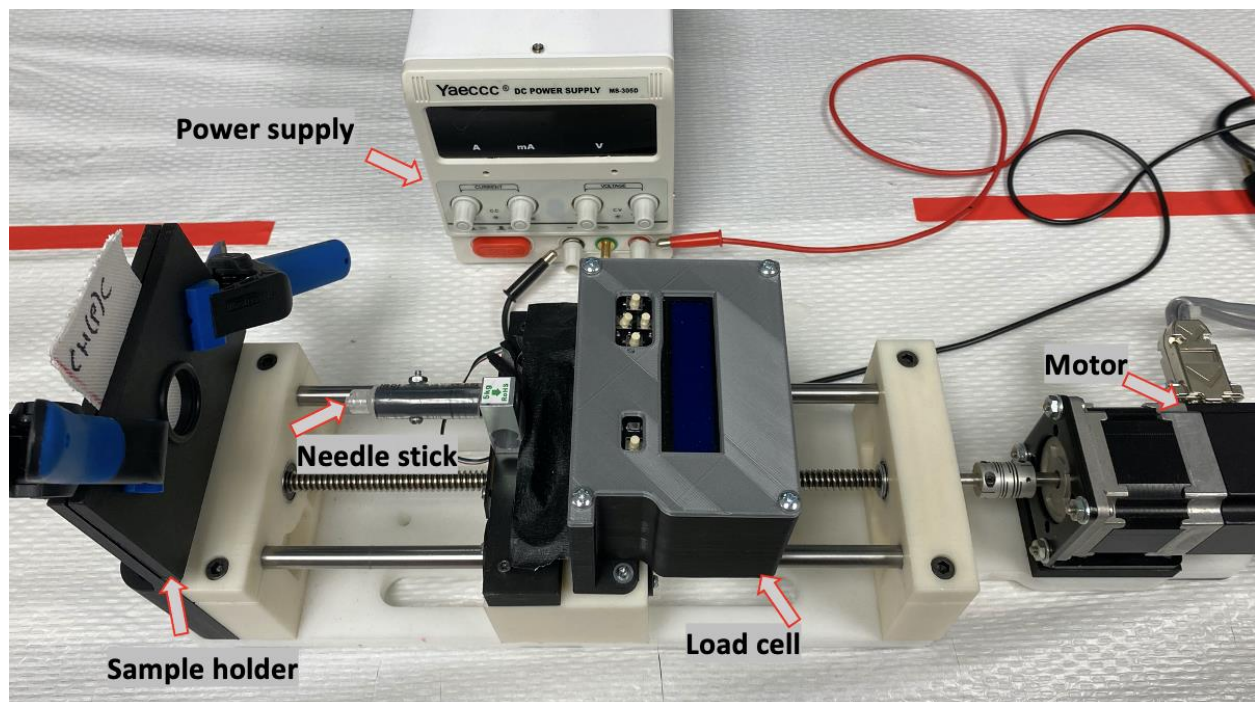


Figure 5.2: Needle-stick penetration test apparatus.

5.2.4 Flexibility and stiffness test

Tests were performed on 5cm × 10cm fabric samples to characterize the flexibility of the fabric. The first tests were done using the setup shown in Figure 5.3a and similar to the principles of ASTM D1388. Here, the sample is sealed completely in a soft polyethylene bag and firmly held at the 90-degree edge of the horizontal workbench. The overhang length of the

fabric was set to 3.8cm and a 20 g weight was attached to the middle end of the sample. The ensuing bending angle (BA) due to the weight was measured by capturing images from one side at a consistent distance and angle. The bending angle is used to characterize the flexibility as in [27][28]. Tests were repeated at least five times on three samples for each combination of fabric. Stiffness tests were also carried out on 127mm × 127mm fabric samples using a SHIMADZU tensile tester according to ASTM D4032-08 shown schematically in Figure 5.3b. This follows the multiaxial bending motion of protective garments evaluation following the modification by an approved flexibility test PED-IOP-008 for soft fabrics [29][30]. The fabric samples were aligned and placed freely on top of a 3D printed platform which was a 127 mm × 127 mm block with a hollow circular opening of 44 mm diameter with a 45-degree clearance angle and 4.8 mm width edge facing up in the center. A 25.4 mm diameter spherical head plunger was fixed to the upper grip of the tester and aligned concentrically to the platform fixed on the bottom of the tester with a 500 N load cell. The plunger was traversed downward at 1 m/min with a total stroke length of 27 mm into the orifice plate. The Stiffness Force (SF) was measured and recorded directly by the SHIMADZU tensile tester. The maximum value is used to characterize the fabric stiffness in this study and indicates the stiffness of the fabric samples and the resistance to bending in all directions.

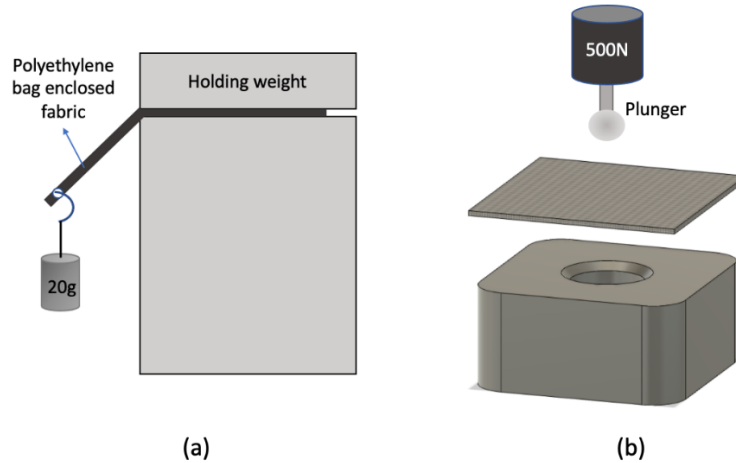


Figure 5.3: Schematic of test set up using (a) overhang method and (b) tensile tester

5.2.5 SEM analysis

Scanning electron microscope (SEM) analysis was performed by TESCAN VEGA SEM to observe and study the morphology of the EVA hot film before and after thermal treatment as well as analysis of the puncture mechanism of the fabric. The samples were coated with a thin layer of gold before loading into the SEM to make the surface conductive and prevent charging due to the material property.

5.3. Results and discussion

A total of 30 different combinations of fabric laminate samples were tested for needle penetration force and flexibility to determine the effectiveness of EVA hot film and the patterned design. The different combinations of stacked fabrics are summarized in Table 5.2 in which the pattern sizes are provided in Table 5.1.

Table 5.2: Layout of stack combinations

Layer of stack	EVA hot film coating on fabric	pattern
1	One side	Hexagon XL/L/S/XS
2		Hexagon/ triangle
3		
1	Double side	Hexagon XL/L/S/XS
2		Hexagon/ triangle
3		

The prepared samples, including untreated and heat-treated EVA hot film and the EVA hot film on cotton fabric without a pattern and with two sizes of hexagon pattern (S and XS) were observed under a SEM with two magnifications to investigate the morphology of the EVA hot film and failure mechanism after needle penetration. The images are presented in Figure 5.4. The surface of the cotton fabric (Figure 5.4a) and as-received EVA hot film sheet (Figure 5.4b) shows a rough finish with uneven structures. After heat treatment under pressure, the surface of the EVA hot film sheet (Figure 5.4c) is relatively smooth compared to the untreated surface; however, small holes are visible on the surface that are likely caused by the trapped air within the untreated film. The nonuniformity is significantly improved when the EVA is heat pressed on the cotton fabric and the holes observed in the heat-treated EVA are visibly reduced (Figure 5.4d); nevertheless, some uneven breaks are still present on the surface. Due to the adhesive property of the EVA hot film, it melts once it is heated and likely allows some of the trapped air to pass through the pores of the fabric resulting in the smoother surface. Once cooled, the fabric layer can be considered as a support for the hot film layer. The SEM images from the two different hexagon pattern sizes (Small and XSmall) are shown in Figure 5.4 e, f. There is greater

nonuniformity in the sample with the smaller hexagon patterns and is likely because the narrower gaps trap some air under pressure.

Corresponding SEM images after subjecting the samples to a 5N penetration force by the needle stick are shown in Figure 5.5. For the neat cotton fabric, the fibers are split apart rather than broken as seen in Figure 5.5a. There is a break or puncture due to the needle stick penetrating through the untreated EVA film as seen in Figure 5.5b. The puncture hole on the hot film treated cotton fabric and needle stick diameter are comparable due to the localized penetration as a result of the treated hot film holding the nearby fibers intact (Figures 5.5 d-f). This is in contrast to the untreated EVA film in Figure 5.5b showing the film breaking away from the penetration point. The narrow holes, having a diameter which is comparable to that of the needle, provides additional resistance to the movement of the needle through needle to fabric frictional forces [9]. The heat treatment performed on the EVA hot film sheet is a physical process and its copolymers, due to their properties, contributed to the strength and toughness of the coated fibers during the adhesive bonding [31]. Thus, the morphology of the surface plays an important role in determining the properties of the material.

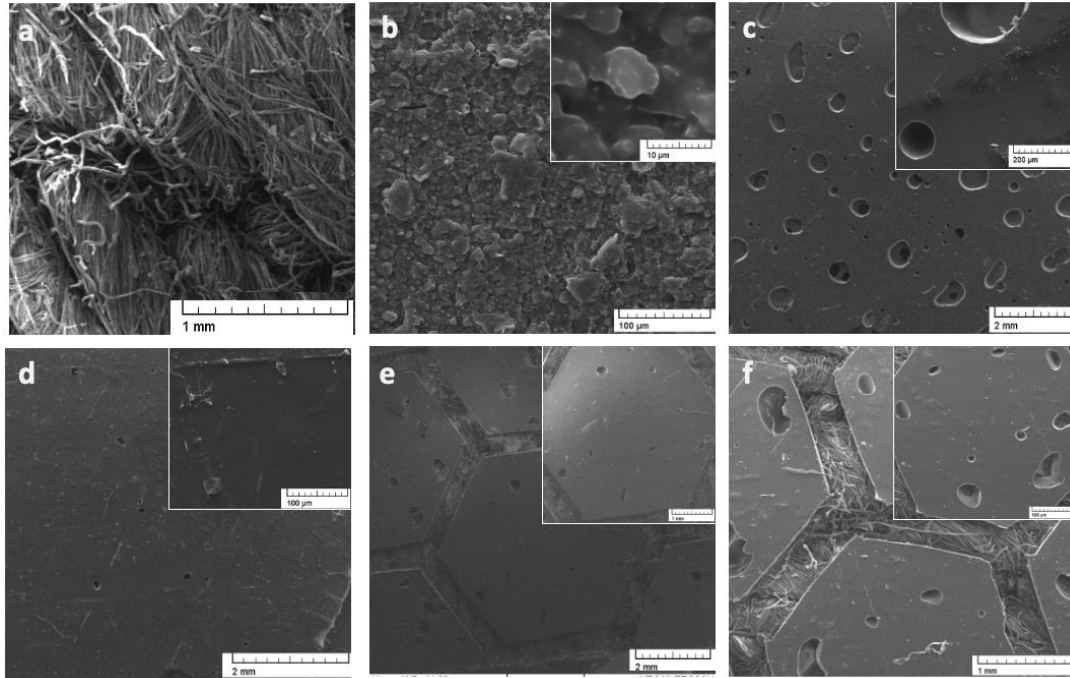


Figure 5.4: SEM images of EVA hot film under different conditions. (a) cotton fabric (b) untreated EVA film (c) treated EVA film (d) treated EVA film on cotton fabric (e) treated EVA film with small size of pattern (f) treated EVA film with XS size of pattern

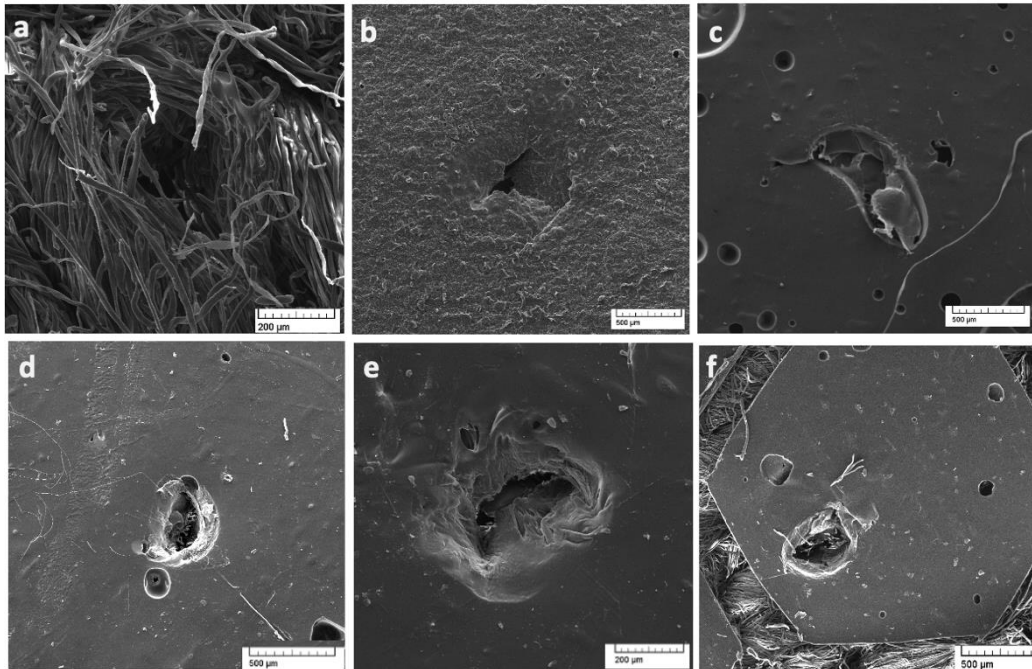


Figure 5.5: SEM images of samples under 5N needle stick penetration force. (a) cotton fabric, (b) untreated EVA film, (c) treated EVA film, (d) treated EVA film on cotton fabric (e) treated EVA film with small size of pattern, (f) treated EVA film with xs size of pattern

3.2 Effect of EVA coverage on penetration and flexibility performance

The needle resistance and flexibility test results (bending angle and bending force) for the different samples are plotted in Figure 5.6. The area coverage of the hot film for the hexagon pattern and the combined triangle and hexagon pattern are 73% and 63%, respectively. The needle resistance of the two-layer EVA hot film was nearly twice that of the single layer EVA hot-film. Having two layers, however, decreased the flexibility where the BA was decreased by 29%. With the patterned EVA hot film, the needle resistance increased without compromising the flexibility. Coating the fabric on both sides with patterned hot film ensures that most of the gaps within the patterns is covered by the pattern coated on the opposite side and the ratio of the surface area of cotton covered by at least one layer of hot film to that of the entire cotton fabric is the effective coverage. The effective coverage of the hexagon pattern on cotton samples coated on both sides for the four different sizes is 98.7% , and 98.4% for the hexagon and triangle combinations,. The needle resistance increased from 2.0 ± 0.1 N for the 1 layer cotton coated with plain hot film to 6.0 ± 1.0 N for the 3 layer hexagon/triangle patterned fabric and is consistent with the increase in coverage from 100% to 189%. The needle resistance for a two-layer hot film (200% coverage) is 4.3 ± 0.7 N. This is lower than the value for the hexagon/triangle three-layer pattern with 189 % coverage. When a three-layer fabric stack with hexagon (L) pattern of 219% effective coverage was used, the needle resistance force increased to 6.8 ± 1.3 N. The flexibility is characterized using both the Bending Angle (BA) and the Bending Force (BF). The BA value drops from 69.8 ± 5.3 degree for the plain hot film to 56.4 ± 2.0 degree and then experiences fluctuations with different coverage areas and 50.0 ± 1.9 degree is associated with the largest coverage. The BF increases from 39.5 ± 7.2 N to 96.6 ± 0.4 N and drops to 85.7 ± 6.9 N for the 3 layer cotton with hexagon (L) patterns as the coverage increases.

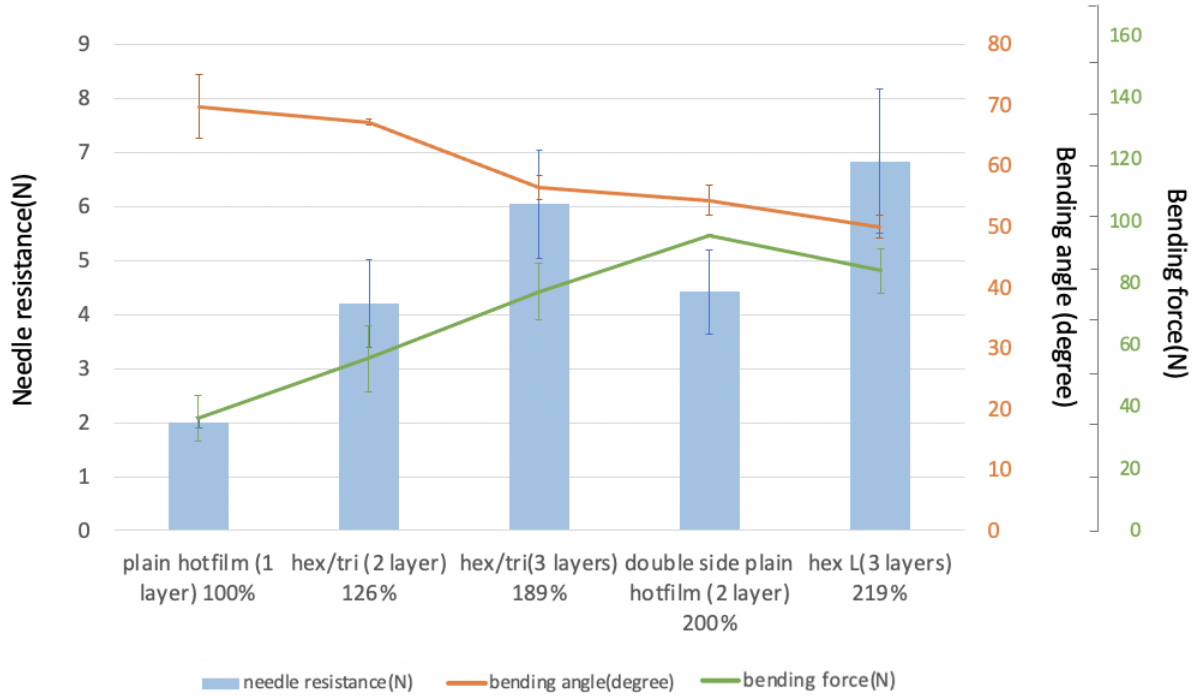


Figure 5.6: Needle resistance, bending angle and bending force for the different fabric samples.

Although a 2-layer plain hot film sample has a larger coverage area compared with hexagon and triangle patterned samples with same number of layers, the patterned samples provide a similar needle penetration resistance but with a greater flexibility evidenced by a lower value of bending force and larger bending angle. In comparison to the 2-layer of plain hot film, the 3-layer hexagon and triangle patterned sample has a better performance on both penetration protection and flexibility with similar coverage area of hot film on fabric. The reason for this is likely due to the higher areal density of the 3-layer patterned sample compared to the 2-layer hot film on a single sheet of cotton fabric. The three-layer patterned sample has 3 cotton layers with one layer of hot film for each fabric layer leading to an increase of thickness by 33% compared to a 2 cotton layer sample with the same composition. The higher flexibility evaluated from both the BA and BF value of the 126%, 189%, 219% coverage samples in Figure 5.6 can be attributed to the gaps between the hot film patterns on the cotton fabric compared with 200% coverage

sample without a pattern. The SEM images in Figure 5.4 show the exposed gaps of the patterned samples which directly contribute to an increase in the freedom of bending in different directions compared with the fully covered cotton fabric by EVA hot film.

The effect of EVA hot film is clearer when the needle penetration force, BA and BF are normalized to the areal density as shown in Figure 5.7, where the specific penetration resistance (SPR), specific bending angle (SBA) and specific bending force (SBF) are plotted. It can be seen that the SPR of the different coverage area samples are not very significantly different, and within the range $3-5.8 \times 10^{-3} \text{ N}/(\text{g}/\text{m}^2)$. Thus, the change in the needle penetration resistance of the samples can be attributed to the difference in the areal density or mass. The trend of SBA of 2-layer of hexagon and triangle patterned hot film samples, however, shows the superior performance of the patterned design compared to the 1-layer of un-patterned hot film with respect to the flexibility. The SBF values are in the same range for all patterned samples and lower than the two un-patterned samples which are also within a similar range. This is an indication that patterning of the hot film has a more significant influence on the flexibility of the samples than the mass of the samples.

The bending force of the 200% coverage without pattern sample increased compared with 189% coverage sample. One of the probable reason is the bending force recorded is influenced by friction coefficient and flexibility [17] and the bending angle is a result of the flexibility. Therefore, the friction between the surface of samples during the deformation by the stiffness plunger is slightly higher for the plain hot film than the patterned samples.

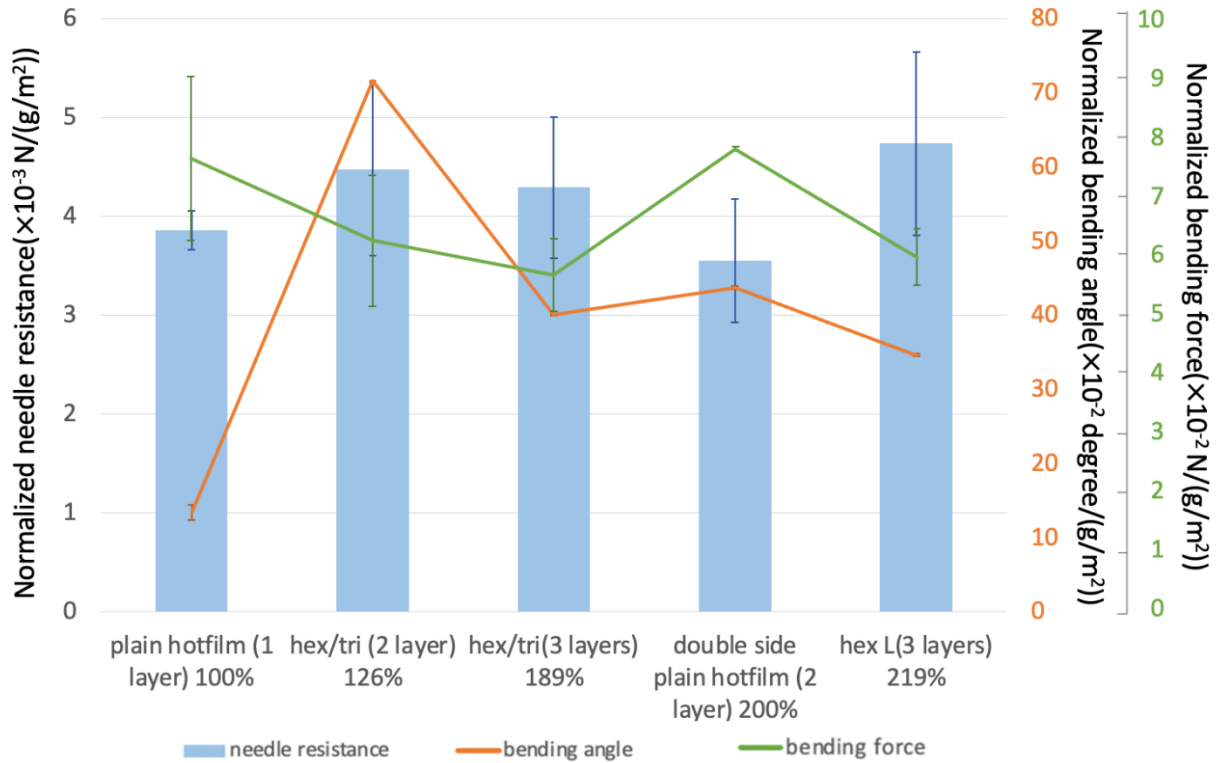


Figure 5.7: Normalized needle resistance and flexibility parameters (bending angle and bending force) by areal density for samples with different coverage area on cotton fabric

In order to quantify the change in needle resistance relative to the flexibility, two factors, namely the Flexibility Factor (FF) and Stiffness Factor (SF) are defined. These are defined as the ratio of the bending angle and bending force to the needle penetration resistance force, respectively. These two ratios for samples with different coverage area are plotted in Figure 5.9. A higher FF and lower SF means a higher flexibility relative to the needle resistant force. From Figure 5.8, the patterned samples do not improve the FF value and are within similar levels except for the 189% and 219% coverage samples which have slightly better performance. Patterned samples with various percentage of coverage all have lower SF values compared with the un-patterned sample, which shows advantages of the patterned design.

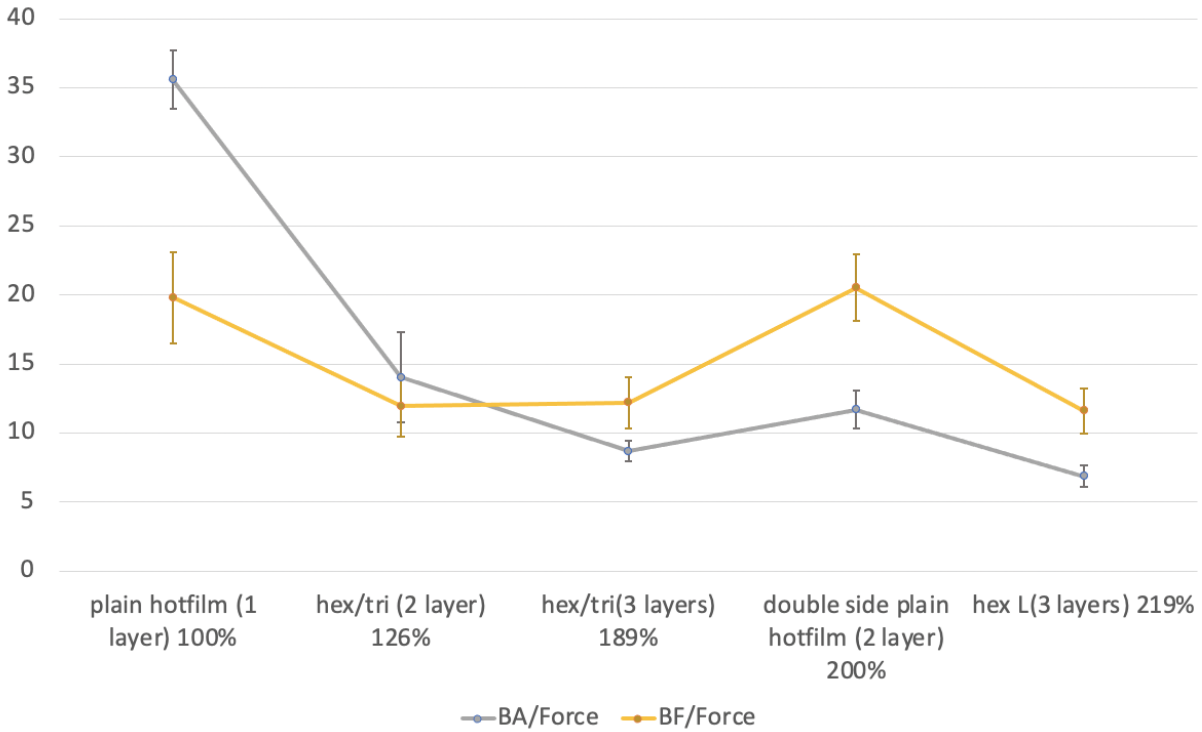


Figure 5.8: Normalized flexibility parameters (bending angle and bending force) by needle penetration force for samples with different coverage area on cotton fabric

5.3.3 Effect of patterned size of EVA on penetration and flexibility performance

Four different sizes of the hexagon patterned samples with 3 layers were tested, and the results are shown in Figure 5.9. The needle-stick penetration resistances of the four samples are 5.9 ± 0.6 N, 6.8 ± 1.3 N, 5.5 ± 1.0 N and 7.2 ± 1.61 N. As shown before, a three-layer patterned fabric provides sufficient coverage to ensure the gaps between the patterns in any layer are overlapped by another layer with the patterned hot film. The coverage by the three layers is not uniform, which can result in some variation of the needle resistance force over different locations on the fabric sample. The non-uniformity is also caused to some extent by the uneven distribution of EVA hot film as seen in the SEM images. The needle resistances for all four

samples are in a range of 5.9 ± 0.6 N to 7.2 ± 1.6 N, and shows the change in the size does significantly affect the needle penetration resistance force. This is expected since the effective coverage area (219%) and thickness of samples are similar for all four pattern sizes.

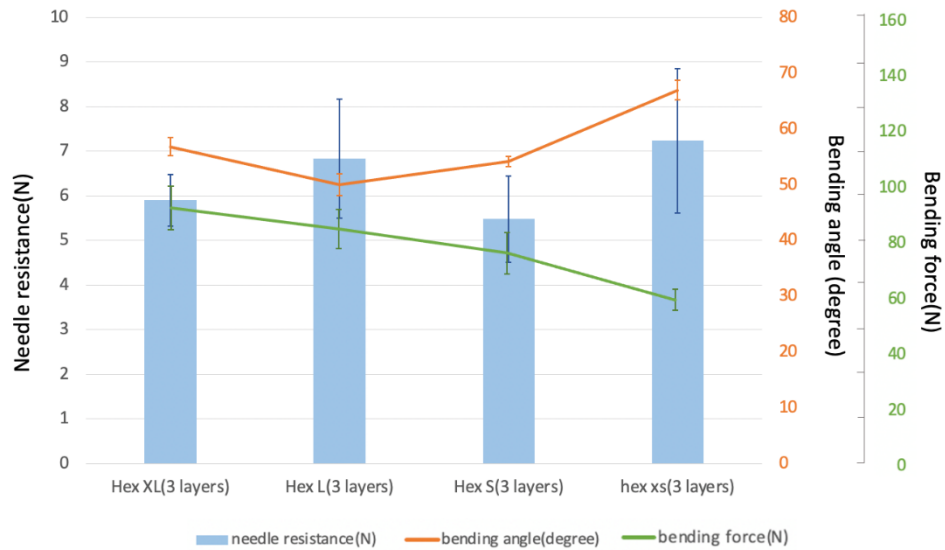


Figure 5.9: Needle penetration force and flexibility parameters of different size of hexagon pattern

The flexibility performance of the samples, however, depends on the size of the pattern as seen in Figure 5.9. The BA value changes from 56.8 ± 1.6 degree for the largest pattern to 66.9 ± 1.7 for the XS size patterned sample. The BF decreases from 93.1 ± 7.6 N to 60.8 ± 3.7 N as the pattern size is reduced. From the results above, the smaller size pattern leads to better flexibility performance, while providing similar needle resistance protection. The flexibility of bending angle improves around 30% by shrinking the pattern size six times compared with the largest pattern size. The larger number of gaps in the smaller pattern size over the same area increases the freedom of bending. The largest pattern size still shows better flexibility and higher needle resistance compared with the plain hot film sample. The results of FF and SF for the four

samples are presented in Figure 5.10. The FF values are in a similar range and it is difficult to evaluate the quality of the design by this parameter since the needle resistance and bending angle changes similarly. Since the FF values appear to be within the same range of values for all the pattern sizes, the metric cannot be used independently to evaluate flexibility. The SF value is more informative than the FF in this case where the first three sizes have similar values while that for the smallest size of hexagon is lowest. This reflects the better flexibility and stiffness of the smallest size while having a similar needle resistance.

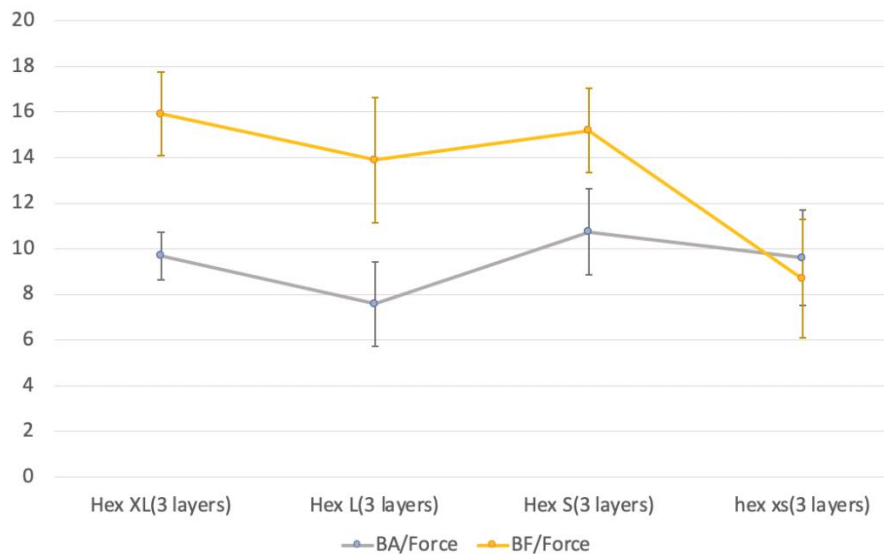


Figure 5.10: Normalized flexibility parameters (bending angle and bending force) by needle penetration force for samples with different size of hexagon pattern on cotton fabric

5.3.4 Effect of multiple layers of stacked fabrics on penetration and flexibility performance

The effect of using multiple layers on the needle resistance and flexibility was tested on different patterns/sizes with 1, 2 and 3 layers. The various combinations of double-sided coated designs with different sizes of patterns are provided in Table 5.2. The results of the penetration and flexibility tests for these samples are plotted in Figure 5.11. In all cases, the needle resistance force increases with an increase in the number of layers. The needle resistance force

increases by about 55-73% when the number of layers are doubled and a further increase of about 113-158% when a third layer is attached. This is 305 to 478 percent higher than a single plain layer of hot film on cotton fabric sample. The 3-layer of double sided xs patterned sample had the highest needle stick resistance force of 11.6 ± 1.6 N. The flexibility, however, decreases with an increase in the number of layers. Here, the bending angle decreased by about 12% to 26% when the number of layers was increased to two and three, respectively. The smallest size has the best performance in all the situation and improved around 29% of needle resistance for 3-layer samples and 30% flexibility compared with the biggest size. Interestingly, it shows almost linear relationship of BA of hexagon and triangle design which is different from others. It might be because the degrees of freedom are slightly different between the two designs. By stacking 3 layer of patterned EVA hot film on double sides of cotton fabric, the needle resistance can achieve more than 10 N which is an increment of over 5 times compared with 3-layer of neat cotton fabric.

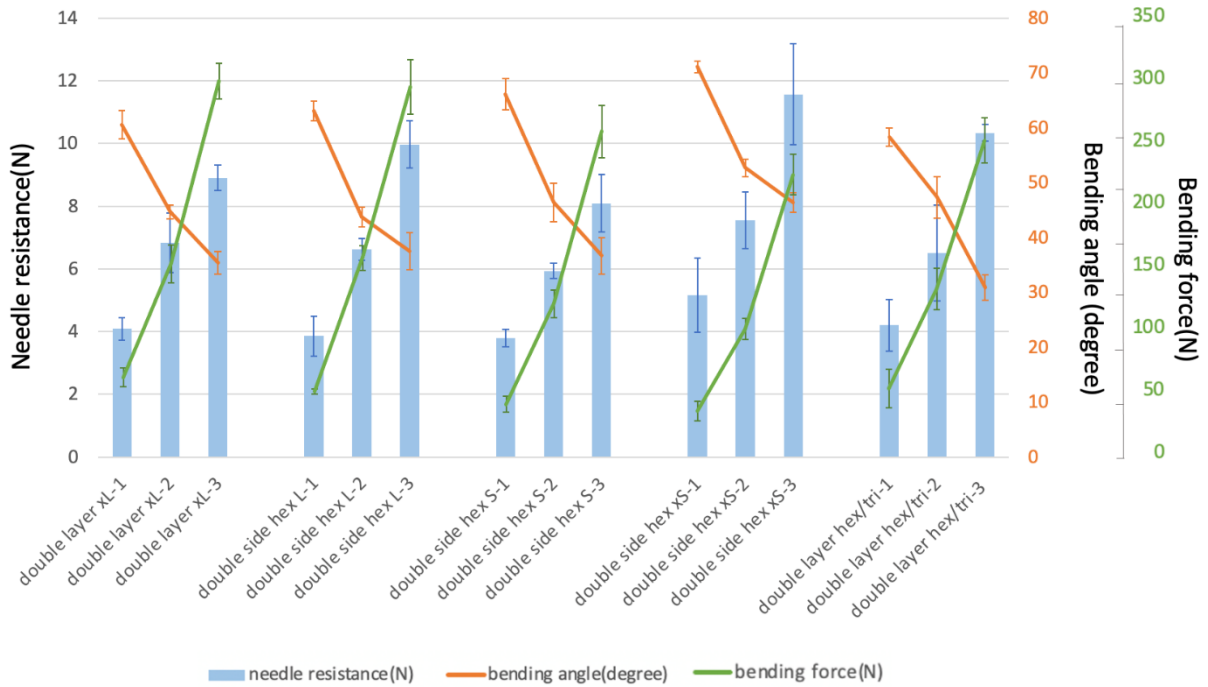


Figure 5.11: Needle penetration force and flexibility parameters of different size of hexagon pattern with different layer of stack.

The results of BA and BF are also normalized by force and shown in Figure 5.12. The normalized values show that although the needle resistance increases manyfold, it compromises the flexibility leading to higher magnitudes of the two ratios (FF and SF). From the final product perspective, the flexibility performance of one layer samples is the most attractive while samples with more stacked layer provide higher level of needle-stick protection with slightly lower flexibility.

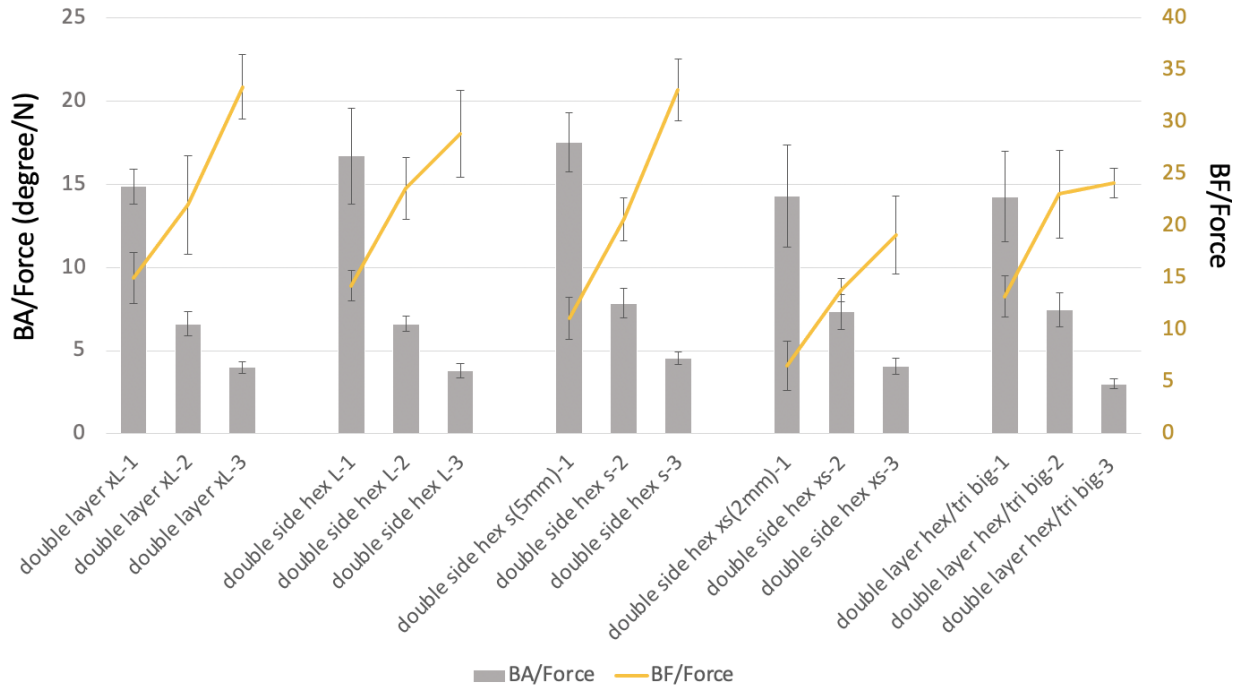


Figure 5.12: Normalized flexibility parameters (bending angle and bending force) by needle penetration force for samples with different size of hexagon pattern with different layer of stack

5.4. Conclusions

A novel needle stick penetration resistant fabric is developed using multiple layers of patterned EVA hot film coated on cotton fabric. The patterns consisted of hexagonal and triangular shapes of different sizes. The EVA film was patterned using HTV sheets and heat press bonded on the fabric followed by cooling in an air flow. Having similar needle resistance force, the patterned EVA hot film covered cotton fabric had at least a 28% of improvement in the flexibility performance compared with un-patterned combination of hot film and cotton. The needle resistance force of 3 layer cotton fabric covered each side (per cotton layer) with patterned EVA hot film increased by 478% from that of a single plain layer of hot film on cotton fabric. Increasing the number of fabric layers was found to increase the needle penetration

resistance but resulted in a decrease in the flexibility. However, in comparison to just one layer, the flexibility decreased by about 12% to 26% for two and three layers, respectively. Reducing the sizes of the patterns was observed to improve the flexibility of the samples by up to 30% without compromising the needle penetration resistance force. Therefore, patterned hot film lamination is an attractive fabric treatment technique that can be used in the development of flexible needle resistant PPE.

5.5 References

- [1] L. F. Leslie, J. A. Woods, J. G. Thacker, R. F. Morgan, W. McGregor, and R. F. Edlich, “Needle puncture resistance of surgical gloves, finger guards, and glove liners,” *J. Biomed. Mater. Res.*, vol. 33, no. 1, pp. 41–46, 1996.
- [2] U.S. Department of Justice, “Stab resistance of personal body armor: NIJ standard-0115.00,” *Body Armor Ballist. Stab Resist. Stand. with a Guid. to Sel.*, pp. 63–100, 2012.
- [3] A. Bleetman, C. H. Watson, I. Horsfall, and S. M. Champion, “Wounding patterns and human performance in knife attacks: Optimising the protection provided by knife-resistant body armour,” *J. Clin. Forensic Med.*, vol. 10, no. 4, pp. 243–248, 2003.
- [4] D. P. Kalman, R. L. Merrill, N. J. Wagner, and E. D. Wetzel, “Effect of particle hardness on the penetration behavior of fabrics intercalated with dry particles and concentrated particle-fluid suspensions,” *ACS Appl. Mater. Interfaces*, 2009.
- [5] D. Firouzi, M. K. Russel, S. N. Rizvi, C. Y. Ching, and P. R. Selvaganapathy, “Development of flexible particle-laden elastomeric textiles with improved penetration resistance to hypodermic needles,” *Mater. Des.*, vol. 156, pp. 419–428, 2018.
- [6] C. T. Nguyen, P. I. Dolez, T. Vu-Khanh, C. Gauvin, & J. Lara, and J. Lara, “Effect of protective glove use conditions on their resistance to needle puncture,” *Plast. Rubber Compos.*, vol. 42, no. 5, pp. 187–193, 2013.
- [7] D. Firouzi *et al.*, “A new technique to improve the mechanical and biological performance of ultra high molecular weight polyethylene using a nylon coating,” *J. Mech. Behav. Biomed. Mater.*, 2014.
- [8] J. B. Mayo, E. D. Wetzel, M. V. Hosur, and S. Jeelani, “Stab and puncture characterization of thermoplastic-impregnated aramid fabrics,” *Int. J. Impact Eng.*, vol. 36, no. 9, pp. 1095–1105, 2009.
- [9] J. B. Mayo, E. D. Wetzel, M. V. Hosur, and S. Jeelani, “Stab and puncture characterization of thermoplastic-impregnated aramid fabrics,” *Int. J. Impact Eng.*, 2009.
- [10] D. Firouzi, D. A. Foucher, and H. Bougherara, “Nylon-coated ultra high molecular weight polyethylene fabric for enhanced penetration resistance,” *J. Appl. Polym. Sci.*, 2014.
- [11] N. Hassim, M. R. Ahmad, W. Y. W. Ahmad, A. Samsuri, and M. H. M. Yahya, “Puncture resistance of natural rubber latex unidirectional coated fabrics,” *J. Ind. Text.*, vol. 42,

no. 2, pp. 118–131, 2012.

[12] L. E. Gates, “Ulm~ EVALUATION AND DEVELOPMENT OF FLUID ARMOR SYSTEAIS.”

[13] Y. Xu, X. Chen, Y. Wang, and Z. Yuan, “Stabbing resistance of body armour panels impregnated with shear thickening fluid,” *Compos. Struct.*, vol. 163, pp. 465–473, Mar. 2017.

[14] H. Mahfuz, F. Clements, V. Rangari, V. Dhanak, and G. Beamson, “Enhanced stab resistance of armor composites with functionalized silica nanoparticles,” *J. Appl. Phys.*, vol. 105, no. 6, p. 064307, Mar. 2009.

[15] N. J. Wagner and Y. S. Lee, “Molecular Simulations of the Amorphous Polymers View project Modelling the rheology of complex suspensions View project.”

[16] H. M. Rao, M. V. Hosur, and S. Jeelani, “Stab characterization of STF and thermoplastic-impregnated ballistic fabric composites,” *Adv. Fibrous Compos. Mater. Ballist. Prot.*, pp. 363–387, Jan. 2016.

[17] D. Firouzi, C. Y. Ching, S. N. Rizvi, and P. R. Selvaganapathy, “Development of oxygen-plasma-surface-treated UHMWPE fabric coated with a mixture of SiC/polyurethane for protection against puncture and needle threats,” *Fibers*, 2019.

[18] R. Gadow and K. von Niessen, “Lightweight Ballistic Structures Made of Ceramic and Cermet / Aramide Composites,” *Ceram. Trans.*, vol. 151, pp. 1–18, 2003.

[19] Kim, “Application Data (63) Continuation-in-part of application No. 09/610,” *Int. Cl.*, vol. 748, no. 6, p. 739, 2000.

[20] S. Kim and B. Llp, “United States US 20080206526A1 (12) Patent Application Publication (10) Pub,” no. 43, 2008.

[21] N. J. Wagner, J. M. Houghton, B. A. Schiffman, D. P. Kalman, E. D. Wetzel, and N. J. Wagner, “Hypodermic needle puncture of shear thickening fluid (STF)-treated fabrics Molecular Simulations of the Amorphous Polymers View project Modelling the rheology of complex suspensions View project HYPODERMIC NEEDLE PUNCTURE OF SHEAR THICKENING FLUID (STF)-TREATED FABRICS,” pp. 3–7, 2007.

[22] M. Takemoto, M. Kajiyama, H. Mizumachi, A. Takemura, and H. Ono, “Miscibility and adhesive properties of ethylene vinyl acetate copolymer (EVA)-based hot-melt adhesives. I. Adhesive tensile strength,” *J. Appl. Polym. Sci.*, vol. 83, no. 4, pp. 719–725, 2001.

[23] A. M. Henderson, “Ethylene-Vinyl Acetate (EVA) Copolymers: A General Review,” no.

1, 1993.

[24] S. P. Tambe, S. K. Singh, M. Patri, and D. Kumar, "Ethylene vinyl acetate and ethylene vinyl alcohol copolymer for thermal spray coating application," *Prog. Org. Coatings*, vol. 62, no. 4, pp. 382–386, 2008.

[25] N. Kumar, P. K. Jain, P. Tandon, and P. M. Pandey, "The effect of process parameters on tensile behavior of 3D printed flexible parts of ethylene vinyl acetate (EVA)," *J. Manuf. Process.*, vol. 35, pp. 317–326, Oct. 2018.

[26] P. R. Selvaganapathy, K. Chan Yu Ching, Russel, S. N. H. R. Iqbal, and D. Firouzi, "FLEXIBLE PARTICLE - LADEN ELASTOMERIC TEXTILES WITH PENETRATION RESISTANCE," *United States Pat. Appl. Publ.*, vol. 2021, no. US 2021/0002438 A1, 2021.

[27] T. A. Hassan, V. K. Rangari, and S. Jeelani, "Synthesis, processing and characterization of shear thickening fluid (STF) impregnated fabric composites," *Mater. Sci. Eng. A*, 2010.

[28] Y. S. Lee, E. D. Wetzel, and N. J. Wagner, "The ballistic impact characteristics of Kevlar® woven fabrics impregnated with a colloidal shear thickening fluid," *J. Mater. Sci.*, 2003.

[29] A. Bhatnagar, *Lightweight Ballistic Composites: Military and Law-Enforcement Applications: Second Edition*. 2016.

[30] R. Of and U. Medical, "SOFT BALLISTIC RESISTANT ARMOR," 2017.

[31] E. G. Koricho, E. Verna, G. Belingardi, B. Martorana, and V. Brunella, "Parametric study of hot-melt adhesive under accelerated ageing for automotive applications," *Int. J. Adhes. Adhes.*, vol. 68, pp. 169–181, Jul. 2016.

Chapter 6: Conclusions

Two novel techniques are introduced to produce ballistic composite laminates: (i) hot press compression of plain weave UHMWPE using patterned hot film and (ii) cold-press compression of plain weave UHMWPE using pressure sensitive adhesive. Laminated composite panels consisting of 22 and 25 layers of UHMWPE were cold pressed at 0.1, 4 and 8 MPa in addition to 40 and 45 layers of UHMWPE neat fabric which were stacked together in order to compare their ballistic performance with the laminated panels when tested by shooting 9 mm ammunition at ~347 m/s. For the hot press compression technique, the samples were prepared by hot-pressing the plain weave UHMPWE with thermoplastic hot film which was either patterned into distinct uniform hardened hexagonal regions (nominal diameter of 27.9 mm with a 1 mm gap between each region) or applied without any patterning and tested with a 0.357 magnum ammunition at ~435 m/s. The tested laminate samples were analyzed using X-Ray Computed Tomography (CT) scans to investigate their failure mechanism under the ballistic impact and metrics such as backface signature (BFS) and backface volume (BFV) were calculated.

For the cold lamination technique, an increase in compression pressure resulted in a significant improvement in bullet penetration resistance and energy absorption of the panels laminated with PSA as shown by the decrease in BFS, BFV. It also resulted in an increase in the percentage of unperforated layers. The energy of impact was found to be transferred through fiber straining and delamination at the backface, formation of a permanent deformation on the backface (BFS) and an upward flow of the material forming a plug at the strikeface. An increase in energy dissipation upon impact through an extensive delamination mechanism which propagated to the sides of the panel was observed as a result of increasing the processing pressure from 0.1 to 4 and 8 MPa. The 45 layer stack of unlaminated layers showed lower

ballistic performance compared to the partially-perforated 22- and 25-layer laminated samples at 8 MPa. An increase in applied pressure was found to increase the inter-ply bond strength which also resulted in increased stiffness due to the PSA spreading more effectively into the depth of fabric layers when processing pressure is increased. However, only a small increase in bending stiffness was observed when processing pressure was increased from 4 to 8 MPa.

The use of patterned hot film resulted in an increase in ballistic performance against the 0.357 mag FMJ ammunition as shown by the decrease in BFS, BFV, height to full width at half height ratio (Height:FWHH) and increase in area at half height (AHH). Specifically, the 25 layer panel laminated with HF had the least BFS, BFV and Height:FWHH. Ballistic test results showed that patterning did not affect the ballistic performance whilst increasing the flexibility of the laminated panels as compared to using plain (not patterned) hot film. Patterning of HF was found to increase the bending angle of the composite panel by 20.9 % and significantly reduced the bending length of the laminated ply by 8 mm making it more flexible. The percentage of the unperforated depth of 25-layer panels laminated with PSA increased from about 32 to 43 and 53%, when processing pressure increase from 0.1 to 4 and 8 MPa, respectively, which demonstrates a higher energy absorption of the laminates manufactured at higher pressure. However, the panels laminated with 25 layers of HF had the highest energy absorbed per areal density making them the most superior among the tested configurations. The main impact energy absorption mechanisms observed were fiber fracture at the strikeface and fiber straining and delamination at the backface of the panels. These two lamination techniques are robust and relatively easy to implement in the manufacturing of ballistic soft body armor.

In addition to the above, the technique of using patterned hot film was extended to develop needle resistant fabric using woven cotton. Here, a number of different patterns using

hexagon and triangle shapes with nominal diameters ranging from 2.6 to 13.5 mm and different gaps between the patterns ranging from 0.3 to 1.8 mm. The samples were tested for both the flexibility and needle penetration resistance. The flexibility tests were performed using two methods: (i) overhanging method similar to ASTM D1388 standard and (ii) tensile tester using a plunger similar to ASTM D4032-08 standard, while the needle penetration tests were performed according to ASTM F2878-10 standard. The needle resistance of the 3 layer hexagon/triangle patterned fabric increased from 2.0 ± 0.1 N for the plain hot film layer to 6.0 ± 1.0 N and is consistent with the increase in coverage from 100% to 189%. The results showed that coating the cotton with the patterned hot film significantly improved the needle penetration resistance of the fabric whilst remaining flexible. The lamination techniques introduced have proven to be highly efficient and practically adaptable from the conventional lamination techniques currently widely used.

6.1 Recommendations for future work

Although the methods introduced produced attractive results, there still exist some improvements that can be investigated further. The following recommendations are made for future studies.

1. Investigate the infusion of nanoparticles to further improve the ballistic penetration resistance.
2. Investigate the effects of additional compounds to further increase the hardness of the hot film.
3. Investigate alternative thermoplastic hot films that require shorter heating times whilst producing good ballistic results.

4. Investigate how the lamination techniques perform with other high strength fabrics such as Kevlar.